Report No. FAA-RD-74-160

COPY 1

FAA WJH Technical Center
00090690

RESPONSES OF SMALL RIGID AIRCRAFT TO DISCRETE AND CONTINUOUS GUST ANALYSIS

PHASE I

John Petrakis, SRDS

Nelson Miller, NAFEC

NAFEC
LIBRARY
JAN 29 '76

DECEMBER 1975

FINAL REPORT

Document is available to the public through the
National Technical Information Service,
Springfield, Virginia 22151

Prepared for

U. S. DEPARTMENT OF TRANSPORTATION
FEDERAL AVIATION ADMINISTRATION
Systems Research & Development Service
Washington, D. C. 20590

NOTICE

This document is disseminated under the sponsorship of the Department of Transportation in the interest of information exchange. The United States Government assumes no liability for its contents or use thereof.

Technical Report Documentation Page

1. Report No.	2. Government Accession No.	3. Recipient's Catalog No.
FAA-RD-74-160		

4. Title and Subtitle	5. Report Date
RESPONSES OF SMALL RIGID AIRCRAFT TO DISCRETE AND CONTINUOUS GUST ANALYSIS - PHASE I	December 1975
	6. Performing Organization Code
7. Author(s) John Petrakis, SRDS, and Nelson Miller, NAFEC	8. Performing Organization Report No. FAA-NA-74-44
9. Performing Organization Name and Address Federal Aviation Administration National Aviation Facilities Experimental Center Atlantic City, New Jersey 08405	10. Work Unit No. (TRAIS)
	11. Contract or Grant No. 184-520-020
12. Sponsoring Agency Name and Address U.S. Department of Transportation Federal Aviation Administration Systems Research and Development Service Washington, D.C. 20590	13. Type of Report and Period Covered Final November 1972-November 1974
	14. Sponsoring Agency Code ARD-520

15. Supplementary Notes

16. Abstract

An evaluation is made of methods developed for estimating longitudinal and lateral rigid-body responses of airplanes to random atmospheric turbulence (reference 2). A computer program has evolved from this study which calculates general aviation aircraft stability derivatives from known geometric properties to be used as inputs to the calculation of aircraft response (also a developed part of the computer program). It was found that the two degrees-of-freedom rigid-body power spectral density analysis produced lower normal load factor responses than a similar single degree-of-freedom analysis for aircraft of gross weight from 3,000 to 17,500 pounds. Also to produce an equivalent discrete load factor for the two degrees-of-freedom analysis, a higher spectral velocity value must be used compared to that of the single degree-of-freedom approach of reference 1.

17. Key Words	18. Distribution Statement
General Aviation Aircraft, Gust Loads Turbulence Power Spectral Density Application Stability Derivatives	Document is available to the public through the National Technical Information Service, Springfield, Virginia 22151

19. Security Classif. (of this report)	20. Security Classif. (of this page)	21. No. of Pages	22. Price
Unclassified	Unclassified	120	

Form DOT F 1700.7 (8-72) Reproduction of completed page authorized

PREFACE

The work presented in this report was jointly prepared by personnel of the National Aviation Facilities Experimental Center (NAFEC) and Systems Research and Development Service (SRDS) for the Federal Aviation Administration (FAA). The authors wish to acknowledge original work pertaining to a simplified method of calculating gust tail load responses for rigid aircraft performed by Mr. E. Peele of NASA, Langely Research Center, and the cooperation afforded FAA on this project. Appreciation is also extended to the General Aviation Manufacturers Association (GAMA) and its associated members who willingly furnished the necessary aircraft parameters used in the numerical computations. The authors especially wish to recognize the following individuals for their extended cooperation:

Mr. Stanley J. Green	General Aviation Manufacturers Association
Mr. R. D. Christian	Commander Aircraft Division, Rockwell International
Mr. King/Mr. Shields	Sabreliner Division, Rockwell International
Mr. Donald P. Zurfluh	Piper Aircraft Corporation
Mr. Mike H. Abla	Gates Learjet Corporation
Dr. Gary L. Thompson/ Mr. Chester A. Rembleske	Beech Aircraft Corporation
Mr. A. Pickens	Swearingen Aviation Corporation

TABLE OF CONTENTS

	Page
INTRODUCTION	1
Purpose	1
Background	1
APPROACH	2
General	2
Stability Derivatives Estimation	2
Simplified PSD Analysis	3
Basic Statistical Response Relations	3
Center of Gravity Response	4
Tail Load Responses	5
Design Manual Analysis	6
FAR, Parts 23 and 25, Analysis	7
Design Procedures	7
Computer Program	8
AIRPLANE DESCRIPTIONS	8
DISCUSSION AND RESULTS	8
Stability Derivatives	8
Center of Gravity Response Comparison	17
Tail Load Response Comparison	31
CONCLUSIONS	36
PHASE II	41
REFERENCES	42
APPENDIXES	
A General Aviation Aircraft Stability Derivatives	
B Computer Program User's Guide	
C Aircraft Response to Continuous Atmospheric Turbulence	
D Federal Aviation Regulations, Parts 23 and 25	
E General Aviation Airplane Description and Characteristics	
GLOSSARY OF TERMS	

LIST OF ILLUSTRATIONS

Figure		Page
1	Gust Spectrum Function	3
2	Effect of Stability Derivatives on Airplane Center of Gravity Response Factor	11
3	Change in C_{L_α} With Mach Number	11
4	Gust-Alleviation Factor, K_ϕ	18
5	Zero-Crossing Values, K_o	19
6	Spectral "Velocities" Equivalent to the Discrete Gust Velocity for One Degree-of-Freedom Analysis	30
7	Effect of Altitude on Spectral Velocity for Airplanes I and II	37
8	Effect of Altitude on Spectral Velocity for Airplanes III, IV, and V	38
9	Effect of Altitude on Spectral Velocity for Airplane VI	39
10	Effect of Altitude on Spectral Velocity for Airplane VII	40

LIST OF TABLES

Table		Page
1	Summary of Stability Derivative Calculations	10
2	Summary of Limitations for Stability Derivative Calculations	12
3	Stability Derivatives for Airplane II	14
4	Stability Derivatives for Airplanes III, IV, and VII	15
5	Stability Derivatives for Airplanes I, V, and VI	16
6	Comparison of Aircraft Center of Gravity Responses Using NASA CR-1975 Estimated Derivatives for L = 750 Feet (2 Pages)	21
7	Comparison of Aircraft Center of Gravity Responses Using Manufacturer's Estimated Derivatives for L = 750 Feet (2 Pages)	23
8	Comparison of Aircraft Center of Gravity Responses Using NASA CR-1975 Estimated Derivatives for L = 2,500 Feet (2 Pages)	25
9	Comparison of Aircraft Center of Gravity Responses Using Manufacturer's Derivatives for L = 2,500 Feet (2 Pages)	27
10	Comparison of Aircraft Tail Load Responses Using NASA CR-1975 Estimated Derivatives for L = 750 Feet	32
11	Comparison of Aircraft Tail Load Responses Using Manufacturer's Estimated Derivatives for L = 750 Feet	33
12	Comparison of Aircraft Tail Load Responses Using NASA CR-1975 Estimated Derivatives for L = 2,500 Feet	34
13	Comparison of Aircraft Tail Load Responses Using Manufacturer's Estimated Derivatives for L = 2,500 Feet	35

INTRODUCTION

PURPOSE.

The identification of relative spectral velocity values $\eta_d \sigma_{w_g}$ is presented for several typical general aviation aircraft utilizing discrete gust and simplified power spectral density (PSD) techniques. A computer program has been developed to estimate the required stability derivatives and analyze the discrete gust and PSD responses. A user's guide is provided, explaining the programs' use on a computer time-sharing system along with sample calculations.

The objectives of the work reported herein are as follows:

1. Provide an engineering evaluation of the simplified methods of estimating longitudinal and lateral responses of small rigid aircraft to continuous atmospheric turbulence.

2. Provide a comparison between wing (i.e., center of gravity load factor responses) and tail load responses which would create equivalent spectral velocities when calculated by the simplified continuous turbulence methods of reference 2 which is a two degrees-of-freedom analysis, and the design manual which is a single degree-of-freedom analysis, of reference 1, as related to the discrete method outlined in the Federal Aviation Regulations (FAR), Parts 23 and 25. This comparison is made to establish reasonable relative equivalent spectral velocity values for the range of aircraft and conditions considered

3. Establish procedures for calculation and/or selection from test data of those stability derivatives required as inputs to the calculation of gust loads using the simplified power spectral technique.

BACKGROUND.

Earlier FAR, Parts 23 and 25, prescribed airworthiness design requirements based on a discrete gust concept. Subsequent FAR amendments to FAR, Part 25, now require assessment of aircraft dynamic loads during flight through continuous turbulence. The use of PSD techniques to assess the continuous turbulence dynamic loading has been studied for large transport-type aircraft. The application of power spectral techniques involves aircraft rigid body as well as elastic structural modes, thus making the technique directly applicable to the large flexible transport-type airplanes where the elastic response contributes significantly to the structural loads.

The application of these techniques to small rigid airplanes would involve unnecessarily complex and lengthy computations to obtain their dynamic response. Simplified approaches toward the calculations of center-of-gravity (c.g.) responses of small rigid aircraft have been thus developed (reference 2) along with tail loading associated with gust penetration. However, the applicability of these approaches has not been fully determined.

It is assumed that the reader of this report is familiar with the concept of stationary random processes and PSD techniques. One reference worthy of mention here for classical background is the "AGARD Flight Test Manual, Volume IV; The Application of Power Spectral Techniques to Airplane Dynamic Response Investigations," December 1963.

APPROACH

GENERAL.

In order to determine the aforementioned relative spectral velocity values, the first step was to obtain some basic aerodynamic derivatives. The necessary stability derivatives were estimated by several methods and these derivatives in turn, were utilized to generate the frequency response functions which relate directly to the response parameters and the number of positive zero crossings for the two simplified PSD methods. Discrete gust load factors were then calculated. A relationship between PSD responses and the discrete load factor was established to yield the relative spectral velocities of interest.

STABILITY DERIVATIVES ESTIMATION.

The frequency response functions required to determine the output power spectrums and ultimately the airplane's response parameters are obtained by solving the equations of motion of the airplane for independently applied gust forces resulting from unit sinusoidal vertical and lateral gust velocities as developed in reference 2. Thus, the formulation of the response equations involves grouping of some terms into the familiar aircraft stability form. Therefore, a necessary ingredient for the response calculation involves the determination of certain stability derivatives.

The sources of stability derivative determination include analytical (theoretical, empirical, semiempirical), flight-test, and wind-tunnel data. Certain combinations of basic methods have been used such as those presented in references 3 through 6, along with aircraft manufacturers in-house developed methods. The work presented in reference 7 addresses the calculation of riding and handling qualities as they specifically apply to light aircraft. In that work, stability derivative information is presented pertaining to design of future light aircraft, along with detailed methods of calculation regarded as most reasonable for such aircraft.

The stability derivative data and methods of reference 7 were utilized in this report (appendix A). These stabiliity derivative calculations were also incorporated into a computer program. The computer program (fully described in appendix B) allows the calculation of the required stability derivatives by inputting known aircraft geometric characteristics. A discussion of the assumptions and limitations of the calculations is presented in a later section of this report.

SIMPLIFIED PSD ANALYSIS.

BASIC STATISTICAL RESPONSE RELATIONS. Procedures for determining airplane responses to atmospheric turbulence involve the use of two basic quantities; $\bar{A}$, the response parameter which relates the rms input gust velocity, σ_{w_g}, to the output rms quantity, $\sigma_{\Delta n}$, and N_o, the average number of zero crossings which is essentially the airplanes characteristic frequency of response. These dynamic response parameters are applicable to fatigue design and limit load calculations. Furthermore, the basic quantities are used in the development of the c.g. and tail load responses in the two simplified PSD methods described in the following sections. As an illustration, $\bar{A}$ and N_o are presented for the normal load factor as follows:

$$\bar{A}_{\Delta n} = \frac{\sigma_{\Delta n}}{\sigma_{w_g}} = \frac{1}{\sigma_{w_g}}\left[\int_0^\infty \Phi_{\Delta n}(\omega)\, d\omega\right]^{1/2} \tag{1}$$

$$N_o(\Delta n) = \frac{\sigma_{\dot{\Delta n}}}{2\pi\sigma_{\Delta n}} = \frac{1}{2\pi\sigma_{\Delta n}}\left[\int_0^\infty \omega^2\, \Phi_{\Delta n}(\omega)\, d\omega\right]^{1/2} \tag{2}$$

Equations (1) and (2) contain the function, $\Phi_{\Delta n}(\omega)$, which is the PSD dynamic frequency response function of the particular response quantity being investigated (in this case it is the normal load factor). The function is found from the input-output relation,

$$\Phi_{\Delta n}(\omega) = \Phi_{w_g}(\omega)\left|H^{\Delta n}_{w_g}(\omega)\right|^2 \tag{3}$$

where, $H^{\Delta n}_{w_g}(\omega)$, is the normal load factor frequency response function due to unit sinusoidal gusts, and the power spectrum for the gust input, $\Phi_{w_g}(\omega)$, is the recommended spectrum for isotropic homogeneous turbulence, known as the Von Karman spectrum. This particular spectrum best represents the vertical and lateral atmospheric turbulence. The Von Karman spectrum is shown in figure 1 and is given by the equation,

$$\Phi_{w_g}(L\Omega) = \frac{\sigma_{w_g}^2}{\pi}\,\frac{1 + 8/3\,(1.339\,L\Omega)^2}{\left[1 + (1.339\,L\Omega)^2\right]^{11/6}} \tag{4}$$

where, $\Omega = \omega/U$ and $\Phi_{w_g}(\omega) = \frac{L}{U}\Phi_{w_g}(L\Omega)$

L is the scale of turbulence

When calculating $\bar{A}_{\Delta n}$ and N_o from equations (1) and (2), a finite upper limit on the integral is employed since the response power spectrum typically tends to decrease rapidly with frequency. Conversely, the zero crossings integral is quite sensitive to cutoff frequency because the circular frequency is squared within the integrand of equation (2). Consequently, as discussed in reference 1, at high frequencies the response power spectrum critically affects the number of zero crossings. While its contribution to the response parameter is negligible. Therefore, cutoff frequencies are customarily critical in the determination of N_o where the so called top of the knee approach applies to $\bar{A}_{\Delta n}$.

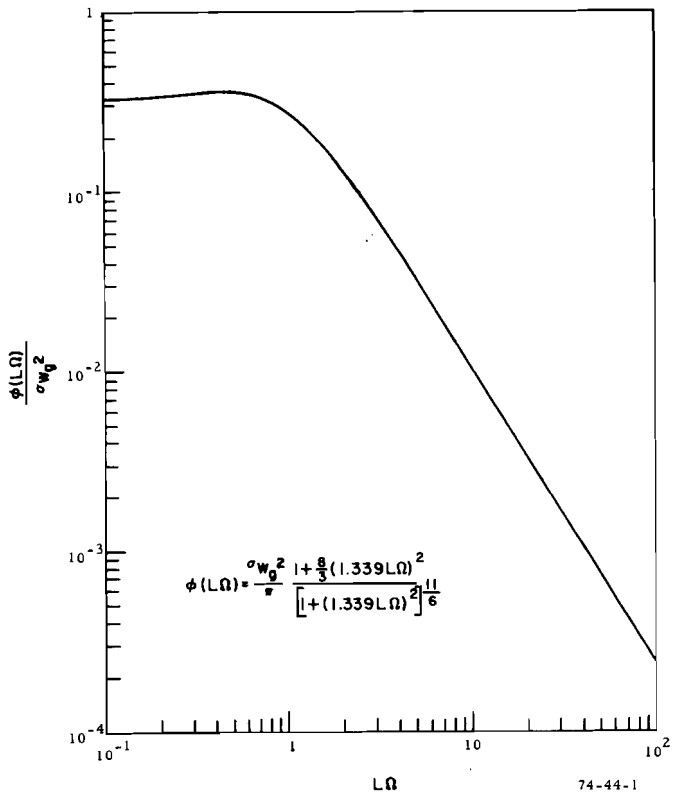

FIGURE 1. GUST SPECTRUM FUNCTION

CENTER OF GRAVITY RESPONSES. The estimation of longitudinal and lateral rigid body responses to continuous atmospheric turbulence employed herein utilizes the methods developed in reference 2. In that analysis, the lateral and longitudinal responses, due to independently applied lateral and vertical gust forces, are described in terms of two degree-of-freedom systems. The responses are expressed in terms of stability characteristics which are functions of the stability derivatives previously mentioned and certain definite integrals (response integrals) that appear in both the lateral and longitudinal formulas for normal load factor, pitch-angle rate, pitch acceleration, lateral load factor, yaw angle, and yaw-angle root mean square (rms) responses as indicated in appendix C equations (C-17) through (C-28). Numerical values of the response integrals are expressed in chart form for simplification in reference 2 and then entered into the appropriate response formulae presented in appendix C.

In order to simplify the procedures for PSD gust load calculations, a computer program described in appendix B, employing the above methods outlined in appendix C were utilized. Numerical integration techniques were used to eliminate the use of charts in the computation of rms response quantities.

Assumptions associated with the simplified PSD method are as follows:

1. The motion of the airplane consists of rigid-body plunge and pitch in the longitudinal mode and of sideslip and yaw in the lateral mode.

2. The dynamic analysis considers a plane of symmetry, neglecting longitudinal and lateral motion coupling with linearized equations of motion.

3. The effects of spanwise variations in gust velocity are not considered.

4. The unsteady lift function representing lift forces is approximated with a single attenuation function.

5. The treatment of homogeneous isotropic atmospheric turbulence allows the use of identical power spectra for vertical and lateral gusts.

6. The turbulence scale is large compared to size of the airplane. (This allows the use of a point correlation function in determining the gust power spectra.)

7. Turbulence response calculations consider small rigid airplanes with lowest elastic frequencies three to five times higher than the rigid body short period or dutch roll frequencies (i.e., elastic deformation shapes and frequencies have very small affect on the dynamic response of the airplane).

8. Tail lag is not considered in the gust forces.

TAIL LOAD RESPONSES. The development of tail load responses was done in a similar manner as that described in the previous sections. The same basic assumptions outlined in the preceding section also apply to the tail load responses.

A complete derivation of the tail load responses is presented in appendix C. A similar derivation was also performed by Mr. Ellwood L. Peele of NASA Langley Research Center in work done in conjunction with reference 2.

The response of the horizontal tail surface to atmospheric turbulence is:

$$\bar{A}_{z_t} = \left| Z_s \right| \left[C_1^2 R_4 + C_2^2 R_2 \right]^{1/2} \tag{5}$$

$$N_o(Z_t) = \frac{\omega_{o\alpha}}{2\pi} \left[\frac{C_1^2 R_6 + C_2^2 R_4}{C_1^2 R_4 + C_2^2 R_2} \right]^{1/2} \tag{6}$$

where,

$$Z_s = qS_w C_{L_{\alpha_t}}/U$$

$$C_1 = -\frac{S_t}{S_w} + \frac{2C_{L_{\dot{\alpha}_t}} K_{\alpha} \zeta_{\alpha}}{C_{L_{\alpha_t}} \gamma_{\alpha}} + \frac{4U^2 K_{\alpha} W_t}{qS_w \bar{c}_w C_{L_{\alpha_t}}} \left(\frac{\zeta_{\alpha}}{\gamma_{\alpha}} - \frac{K_{\alpha} l_t}{\bar{c}_w} \left[4 \frac{\zeta_{\alpha}^2}{\gamma_{\alpha}} \left(1 - \frac{1}{\gamma_{\alpha}} \right) - 1 \right] \right)$$

$$C_2 = 2\zeta_{\alpha} \frac{S_t}{S_w} \left(1 - \frac{1}{\gamma_{\alpha}} \right) - K_{\alpha} \frac{C_{L_{\dot{\alpha}_t}}}{C_{L_{\alpha_t}}} + K_{\alpha} \frac{C_{L_{q_t}}}{C_{L_{\alpha_t}}} \left(4 \frac{\zeta_{\alpha}^2}{\gamma_{\alpha}} \left(1 - \frac{1}{\gamma_{\alpha}} \right) - 1 \right) - \frac{2K_{\alpha} W_t U^2}{\bar{c}_w q S_w C_{L_{\alpha_t}}} \left(4 \frac{\zeta_{\alpha}^2}{\gamma_{\alpha}} \left(1 - \frac{1}{\gamma_{\alpha}} \right) \right)$$

The response of the vertical tail surface to atmospheric turbulence is:

$$\bar{A}_{Y_v} = \left| Y_s \right| \left[C_3^2 R_{4_\beta} + C_4^2 R_{2_\beta} \right] \tag{7}$$

$$N_o(Y_v) = \frac{\omega_{o_\beta}}{2\pi} \left[\frac{C_3^2 R_{6_\beta} + C_4^2 R_{4_\beta}}{C_3^2 R_{4_\beta} + C_4^2 R_{2_\beta}} \right]^{1/2} \tag{8}$$

where,

$$Y_s = qS_w C_{Y_{\beta_v}}/U$$

$$C_3 = 1$$

$$C_4 = -2\zeta_{\beta} \left(1 - \frac{1}{\gamma_{\beta}} \right) + K_{o_\beta} \frac{C_{Y_{r_v}}}{C_{Y_{\beta_v}}} \left[4 \frac{\zeta_{\beta}}{\gamma_{\beta}} \left(1 - \frac{1}{\gamma_{\beta}} \right) - 1 \right]$$

DESIGN MANUAL ANALYSIS.

A rigid airplane in vertical translation forms the basis for the single-degree-of-freedom analysis of reference 1. The same basic response relations apply in this method as in the previous simplified PSD approach.

In this analysis, the frequency response function used to determine the normal load-factor response is a function of the reduced frequency, Theodorsen's and a corresponding sinusoidal gust encounter function and will yield a normal load-factor response given by the following equations,

$$\overline{A}_r = \frac{\sigma_{\Delta n}}{\sigma_{wg}} = \frac{C_{L_w} \rho S_w U K_\phi}{2 W_{to}} \; ; \; N_o = \frac{U K_o}{\pi \overline{c}_w}$$

where K_ϕ is the spectral gust alleviation factor, and K_o is the zero crossing value.

FAR, PARTS 23 AND 25, ANALYSIS.

A discussion of gust design is presented in reference 8, tracing the evolution of developments from consideration of wing loading and alleviation curves through the use of the mass parameter, μ_g. For this analysis it should suffice to summarize the discrete gust method as follows:

1. Rigid aircraft.
2. Aircraft are similar in mission profile.
3. Assumes aircraft have similar response characteristics.
4. Discrete gust of (1-cosine) type.
5. Assumes prior distribution of derived gust velocity with altitude.
6. Gust is symmetrical with respect to airplane in a vertical sense.
7. Relative loads for a single isolated gust are a measure of relative loads in a sequence of gusts.
8. Gust load is applied to wings and horizontal tail surfaces simultaneously or separately depending upon C_n or C_L used.

The design considers a (1-cosine) discrete gust with a gradient distance of 12.5 chords. The equations used in the calculation of gust loads by the method of FAR, used in Parts 23 and 25, are given in appendix D.

DESIGN PROCEDURES.

The design level for any given response can be determined from the following relationship

$$\Delta n \text{ design} = \overline{A}\, \eta_d \sigma_{wg}$$

Response design levels utilize a quantity $\eta_d \sigma_{wg}$ termed as the spectral velocity value where η_d is the ratio of design load to rms load. Discrete gust delta load factors were used as a basis for establishing design levels in this report. Consequently, for response parameters using the two-degrees-of-freedom spectral analysis, a spectral velocity is obtained equivalent to the derived gust velocity of the discrete method. This commonly accepted method has been similarly employed in the analysis presented in reference 1 and in the FAA ADS-53 report.

COMPUTER PROGRAM.

The computer program referred to in previous sections is fully described in appendix B and was developed as a general analysis tool which could assist the general-aviation manufacturer in predicting low speed airplane stability derivatives and gust responses. The program allows the user to assess the relative effectiveness of an airplane to withstand continuous turbulence compared to that of discrete gusts.

Appendix B is presented to provide the user with an understanding of the computer program and its execution on a Control Data Corporation (CDC) 6400 computer time-sharing system. Input and output quantities and a program listing are included. Program execution time is approximately 160 system seconds.

AIRPLANE DESCRIPTIONS

In order to span the range of aircraft in the general-aviation fleet and to provide a good base for analyzing the simplified power spectral technique, seven representative aircraft were selected.

All but one of the representative airplanes are in the 12,500 pounds or less category specified by FAR, Part 23. Represented are a light single- and twin-engine general-aviation airplane, three light passenger twin-turboprop transports, and two twin-jet light executive transports. The general description and characteristics of these airplanes are listed in appendix E.

DISCUSSION AND RESULTS

STABILITY DERIVATIVES.

In the development of stability derivative determination for light aircraft as reported in reference 7, the following limitations apply:

1. Aircraft is considered as a rigid structure.
2. Little or no wing sweep.
3. Aspect ratio greater than 5.0.
4. Maximum Mach number 0.4.
5. Maximum indicated airspeed 300 miles per hour (mi/h).
6. Maximum wing loading 40 pounds per square foot (lb/ft^2).
7. Maximum gross weight 10,000 pounds (lb).

As was discussed in the data of references 7, 9, and 10, the stability derivative calculations are also limited in other ways when their results are applied to the calculation of small aircraft response to continuous atmospheric turbulence. Frequency effects on lift and moment due to aircraft motion

are not adequately accounted for in the stability derivative approach to calculation of aircraft gust load responses. Nonsteady effects are only partially considered when stability derivatives are used. Intermediate and high-frequency effects on the oscillating lift forces due to airplane motion are not treated adequately.

Highlights of the stability derivative prediction method presented in reference 7 and used primarily as an input source for the analysis are as follows:

1. C_{L_α} : Considers wing contribution to be 85 to 90 percent of total. Approximation given for aircraft with partial span flaps.

2. $C_{L_{\dot{\alpha}}}$: Neglects aeroelastic effects.

3. C_{L_q} : Neglects fuselage contribution, assumes center of gravity (c.g.) located very near aerodynamic center (a.c.).

4. C_{m_α} : Neglects aeroelastic effects.

5. $C_{m_{\dot{\alpha}}}$: Neglects aeroelastic effects and fuselage terms.

6. C_{m_q} : Neglects fuselage contribution.

7. C_{y_β}, C_{y_r}, C_{n_β} : Considers wing contribution small.

8. C_{n_r} : Considers vertical tail to be 70 to 90 percent of derivative total.

A summary of the required stability derivatives and suggested sources for their determination and use in the gust load calculations (as reported in reference 9) are shown in table 1.

The dependence of the stability derivatives upon the aircraft response calculations vary greatly as evidenced in figure 2. For example, ΔC_{L_α} bears an almost direct linear variation with $\overline{A}_{\Delta n}$, while ΔC_{m_α} may be varied as much as 100 percent while only changing $\overline{A}_{\Delta n}$ 4 percent. Thus, requiring an accurate determination of C_{L_α}.

A comparison of the stability derivative limitations with respect to the seven general aviation aircraft studied in this report is found in table 2. As can be seen from this table, airplanes I through IV are within the limitations of reference 7. The high performance airplanes, V through VII, have swept wings and operate at Mach numbers >0.4, thus exceeding the limitations of the calculation procedures. In addition, the weight used for gust analysis of airplanes V and VII exceeds the allowable 10,000 lbs. These items are to be considered when evaluating the stability derivatives thus calculated using the methods presented herein. Typical effects of Mach number on C_{L_α} may be seen in figure 3. Calculations using the incompressible theory may well underestimate the derivative.

TABLE 1. SUMMARY OF STABILITY DERIVATIVE CALCULATIONS

Stability Derivative	Applicability to Light Aircraft	Limitations	Recommended Reference
C_{l_α}	Adequate for single-engine aircraft.	Sweep, compressibility, aeroelasticity	References 5, 6, and 11 Structural analysis
C_{m_α}	Adequate for wing/fuselage. Inadequate for tail contribution and downwash factor.	Wing aerodynamic center estimation, compressibility, aeroelasticity	References 5 and 6 Structural analysis
$C_{m_{\dot{\alpha}}}$	Adequate because insignificant. Inadequate for tail contribution.	Compressibility, sweep, aeroelasticity	
C_{m_q}	Inadequate for tail lift curve.	Sweep, compressibility	
C_{y_β}	Inadequate vertical tail slope, aspect ratio (AR). Inadequate sidewash factor.		References 3, 6, 12, and 13 Wind tunnel
C_{n_β}	Inadequate wing contribution. Adequate fuselage contribution, sidewash factor.	Aeroelasticity	Structural analysis
C_{n_r}	Vertical tail terms.		

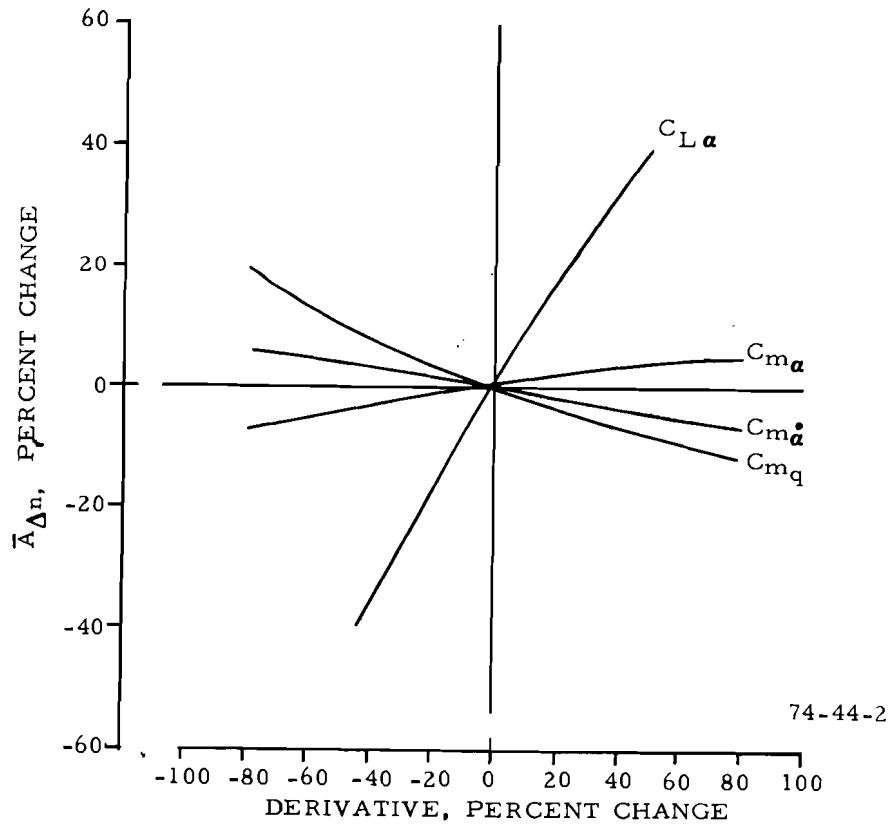

FIGURE 2. EFFECT OF STABILITY DERIVATIVES ON AIRPLANE CENTER OF GRAVITY RESPONSE FACTOR

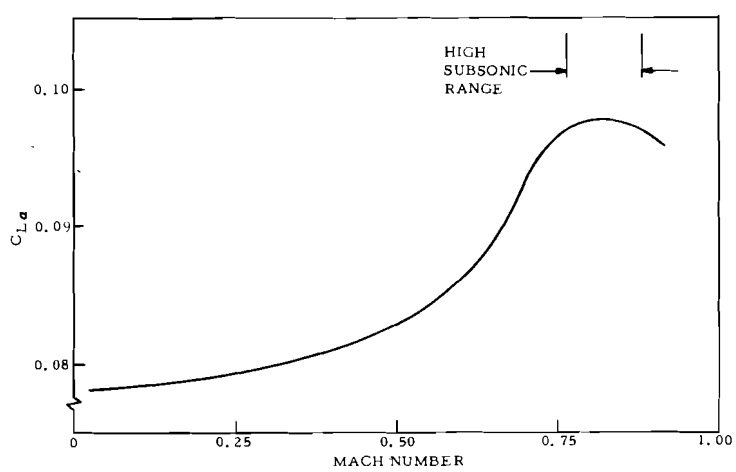

FIGURE 3. CHANGE IN C_{L_α} WITH MACH NUMBER

TABLE 2. SUMMARY OF LIMITATIONS FOR STABILITY DERIVATIVE CALCULATIONS

Parameter	Reference 7 CR-1975	AIRPLANE I	II	III	IV	V	VI	VII
Λ	Small	0	0	0	0	4	16	32
AR_w	$\gtrsim 5$	7.4	7.3	7.5	8.2	7.7	5.0	5.8
U(mi/h)	300	149	195	285	278	254	599	636
$W/S(lb/ft^2)$	<40	17	20.2	36.5	38.5	45	38.8	50.8
W_{to}	<10,000	2,950	3,600	10,200	10,250	12,500	9,000(1)	17,375
ω_e	Rigid	Rigid	Rigid	(2)	(2)	(2)	(2)	(2)
M	< .4	.2	.2	.3	.4	.4	.8	.8

NOTES: (1) Weight used in calculation = 9,000 lb., weight max. = 12,800 pounds, $W/S = 55.4\ lb/ft^2$.

(2) May require structural analysis to determine rigidity.

The geometric data for the seven aircraft from appendix E were used as inputs to the computer program in appendix B from which the stability derivatives were calculated. The results of these calculations may be found in tables 3 through 5. The first column of numbers are the result of the computer program and the subsequent columns are self-explanatory. It is to be noted that although the references are given for the source calculation, in reality, this data was supplied by the manufacturers of their aircraft using the indicated sources. The derivatives for airplane II (table 3) were presented first since it represents the most complete data of the aircraft used in this study.

The most important derivative in the calculation of $\bar{A}_{\Delta n}$ is C_{L_α}. The lift curve slope is seen to have a value which is consistent with all of the methods presented in table 3.

The DATCOM (reference 6) method shows a higher value as compared to CR-1975 (reference 7). Similarly, C_{m_α}, is shown to be consistent with all of the methods. Large differences are noted on the calculation of C_{n_β}, however, inconsistencies are seen between wind tunnel and flight-test data. Large differences are also seen between references 5 and 7; however, the important factor to keep in mind herein is that although large differences exist, they are not significant enough to affect gust load calculations for this aircraft.

Similar comparison of the remaining six airplanes may be found in tables 4 and 5. The differences in derivatives for airplanes III through VII are partially due to exceeding the limitations of M, ,W_{to}, etc., as seen in table 2. In some cases, as noted, the actual derivative was input rather than calculated since limitations were greatly exceeded. Other differences in the derivatives were due to calculation of effects of wing and body only and neglecting other terms.

As was pointed out in the data of reference 10, discrepancies in stability derivatives calculations for the airplane II could be due to the following considerations:

C_{n_β} : Tail contribution needs empirical data.
Estimates fuselage contribution.
Inability to determine sidewash factor.
Judgment required for S_v, AR_v.

C_{n_r} : Sidewash term difficult to determine.
Tail contribution uncertain.

C_{y_β} : Difficult to estimate propeller, fuselage and wing contributions.

C_{L_α} : Need to include other than wing terms.

C_{m_α} : Need to accurately determine elevator terms.

NOTE: The above discrepancies may very well apply to airplanes I through V.

TABLE 3. STABILITY DERIVATIVES FOR AIRPLANE II

DERIV.	NASA CR-1975 (REF 7)	NASA TN D -6800 (REF 14)	SECKEL[1] (REF 5)	USAF[1] DATCOM (REF 6)	WIND[1] TUNNEL	FLIGHT[1] TEST
C_{L_α}	4.372	4.350	4.500	4.990	4.730	4.200
$C_{L_{\dot\alpha}}$	1.726	3.649[2]	—	—	—	—
C_{L_q}	4.399	8.579[3]	—	—	—	—
C_{m_α}	-.976	-1.120	-1.240	-1.705	-1.000	-1.210
$C_{m_{\dot\alpha}}$	-4.976	-6.380[4]	—	—	—	—
C_{m_q}	-11.316	-13.760[5]	—	—	—	—
C_{y_β}	-.288	—	—	—	—	—
C_{y_r}	.169	—	—	—	—	—
C_{n_β}	.047	—	.073	.053	.088	.057
C_{n_r}	-.072	—	—	—	—	—

NOTES:

(1) Derivatives were furnished by the manufacturer of the airplane.
(2) Includes fuselage and nacelles.
(3) Includes fuselage, nacelles, and wing fuselage interference terms.
(4) Wing/fuselage interaction, tail/fuselage interaction.
(5) Includes fuselage, nacelles, and mutual interference effects.

TABLE 4. STABILITY DERIVATIVES FOR AIRPLANES III, IV, AND VII

	AIRPLANE IV		AIRPLANE III		AIRPLANE VII	
DERIV.	NASA CR-1975 (REF 7)	DATCOM(1) (REF 6)	NASA CR-1975 (REF 7)	PERKINS(1) & HAGE (REF 3)	NASA CR-1975 (REF 7)	PERKINS(1) & HAGE (REF 3)
C_{L_α}	4.932	5.203	4.744	5.200	4.345	6.300
$C_{L_{\dot\alpha}}$	3.146	3.192	3.358	2.700	2.171	—
C_{L_q}	6.393	3.948(2)	5.425	8.100	3.046	—
C_{m_α}	-.933	-.545(2)	-.386	-1.719	-.571	-1.100
$C_{m_{\dot\alpha}}$	-10.842	-7.818	-11.064	-9.100	-4.433	-3.600
C_{m_q}	-21.262	-23.688	-21.740	-34.000	-6.660	-8.050
C_{Y_β}	-.526	—	-.523	-.590	-.374	-.808
C_{Y_r}	.391	—	.365	.394	.218	—
C_{n_β}	.082	.086	.059	.082	.122(3)	.122
C_{n_r}	-.173	—	-.139	-.194	-.092	-.140

NOTES:

(1) Derivatives were furnished by the manufacturer of the airplane.
(2) Wing and body only.
(3) Airplane VII exceeds the limitations of NASA CR-1975, therefore, derivative was input in order to get realistic lateral derivatives.

FAA WJH Technical Center
00090690

TABLE 5. STABILITY DERIVATIVES FOR AIRPLANES I, V, AND VI

	AIRPLANE I		AIRPLANE V		AIRPLANE VI	
DERIV.	NASA CR-1975 (REF 7)		NASA CR-1975 (REF 7)		NASA CR-1975 (REF 7)	DATCOM(1) (REF 5)
C_{L_α}	4.610		5.058		4.169	5.840
$C_{L_{\dot\alpha}}$	1.822		3.685		2.553	—
C_{L_q}	4.164		9.399		4.910	—
C_{m_α}	-.955		-1.599		-.552	—
$C_{m_{\dot\alpha}}$	-5.822		-16.382		-7.064	—
C_{m_q}	-14.055		-35.274		-12.658	—
C_{Y_β}	-.306		-.834		-.449	—
C_{Y_r}	.210		.923		.355	—
C_{n_β}	.067		.297		.122(2)	—
C_{n_r}	-.097		-.603		-.171	—

NOTES:

(1) Derivatives were furnished by the manufacturer of the airplane.
(2) Airplane VI exceeds the limitations of NASA CR-1975, therefore, derivative was input in order to get realistic lateral derivatives.

CENTER OF GRAVITY RESPONSE COMPARISON.

Some limitations in the use of the abbreviated PSD method are noted in reference 9 and are summarized as follows:

1. Frequency effects on lift and moment developed due to aircraft motion are only partially considered when using this "stability analyses" approach.

2. The method utilizes the same nonsteady lift function for lift and moment to account for nonsteady lift effects due to gust penetration. The phase lag between the wing and tail is not considered.

At present, the effects of these items upon the calculation of gust loading have not been fully determined. Quantitative values will depend upon the specific configuration under investigation. Further studies aimed at determining the magnitude of these limitations are outlined Section Phase II of this report.

Since FAR, Parts 23 and 25, address only the symmetrical vertical gust loading conditions, the comparison to follow will be restricted solely to the longitudinal load factor responses.

Keep in mind that the major stability derivative, C_{L_α}, is shown to have a pronounced effect on $\bar{A}_{\Delta n}$. Data presented in references 3 and 10 show some variations in the C_{L_α} derivative depending upon whether analytical, wind tunnel or flight-test data is used.

Furthermore, the flight conditions, in the following comparison, may not be entirely realistic to those used by a manufacturer in a gust analysis. But the analysis is intended only to be a basis for comparison of the methods utilized. The comparison is between the one degree-of-freedom analysis from the "Design Manual for Vertical Gusts Based on Power Spectral Techniques," reference 1 and the two degress-of-freedom approach of reference 2 outlined within. This is done to determine a spectral velocity value, $\eta_d \sigma_{wg}$ suitable for the range of airplanes investigated and to note differences between the two methods.

Calculation of spectral velocity values for the single degree-of-freedom analysis requires the use of figures 4 and 5 to determine the spectral gust alleviation factors, K_ϕ, and the zero crossing values, K_o, for substitution into the equations presented with those figures. The one degree-of-freedom normal load factor response $\bar{A}_r$ calculated in this manner can produce a spectral velocity which is equivalent to the discrete derived gust velocity. Figure 6 depicts equivalent spectral velocities, $\eta_d \sigma_{wg}$ solely as a function of the mass parameter, μg, and the relative gust scale, s at sea level. Spectral velocity values for other altitudes have been adjusted as shown by the following equations,

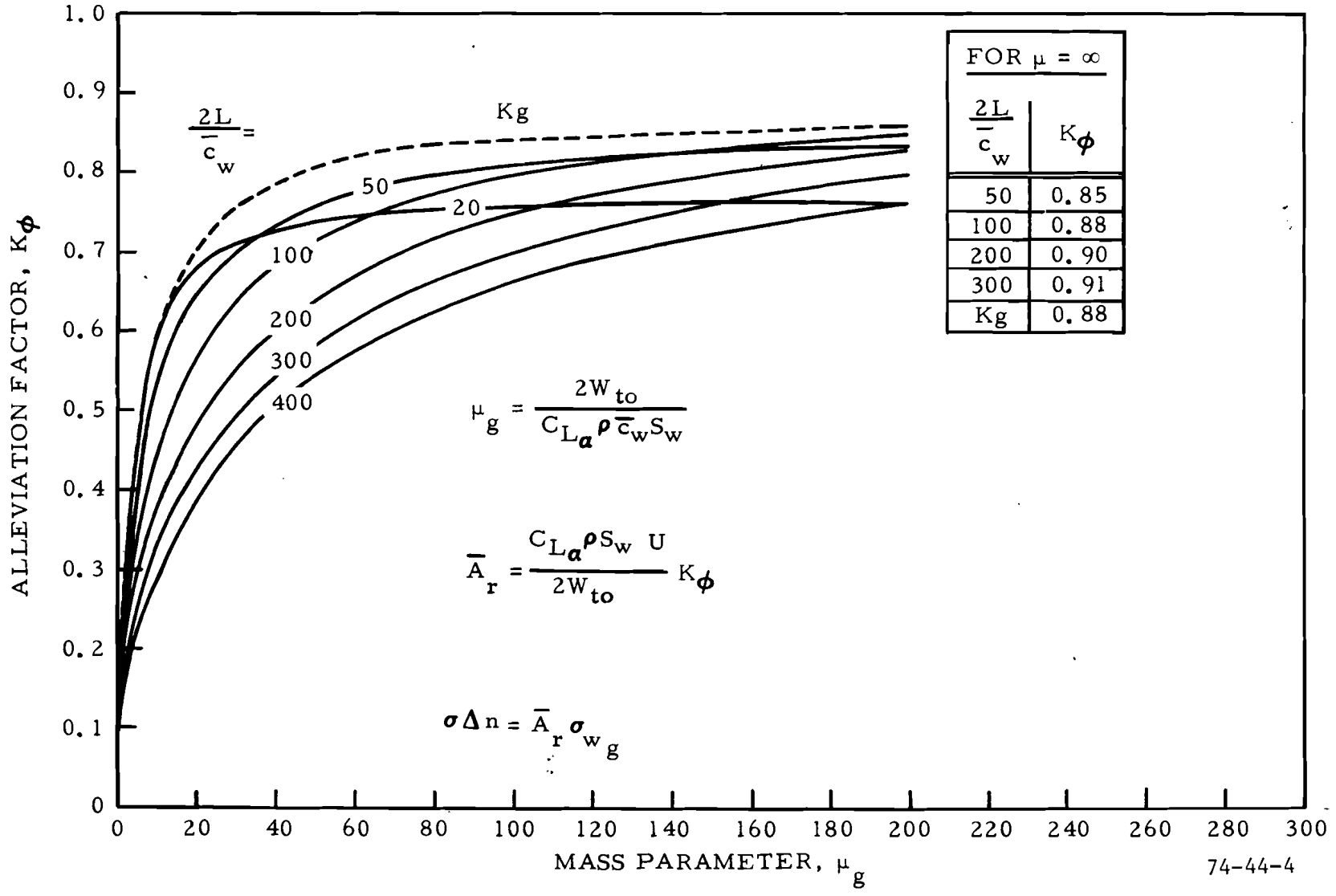

FOR $\mu = \infty$	
$\frac{2L}{\bar{c}_w}$	K_ϕ
50	0.85
100	0.88
200	0.90
300	0.91
Kg	0.88

FIGURE 4. GUST-ALLEVIATION FACTOR, K_ϕ

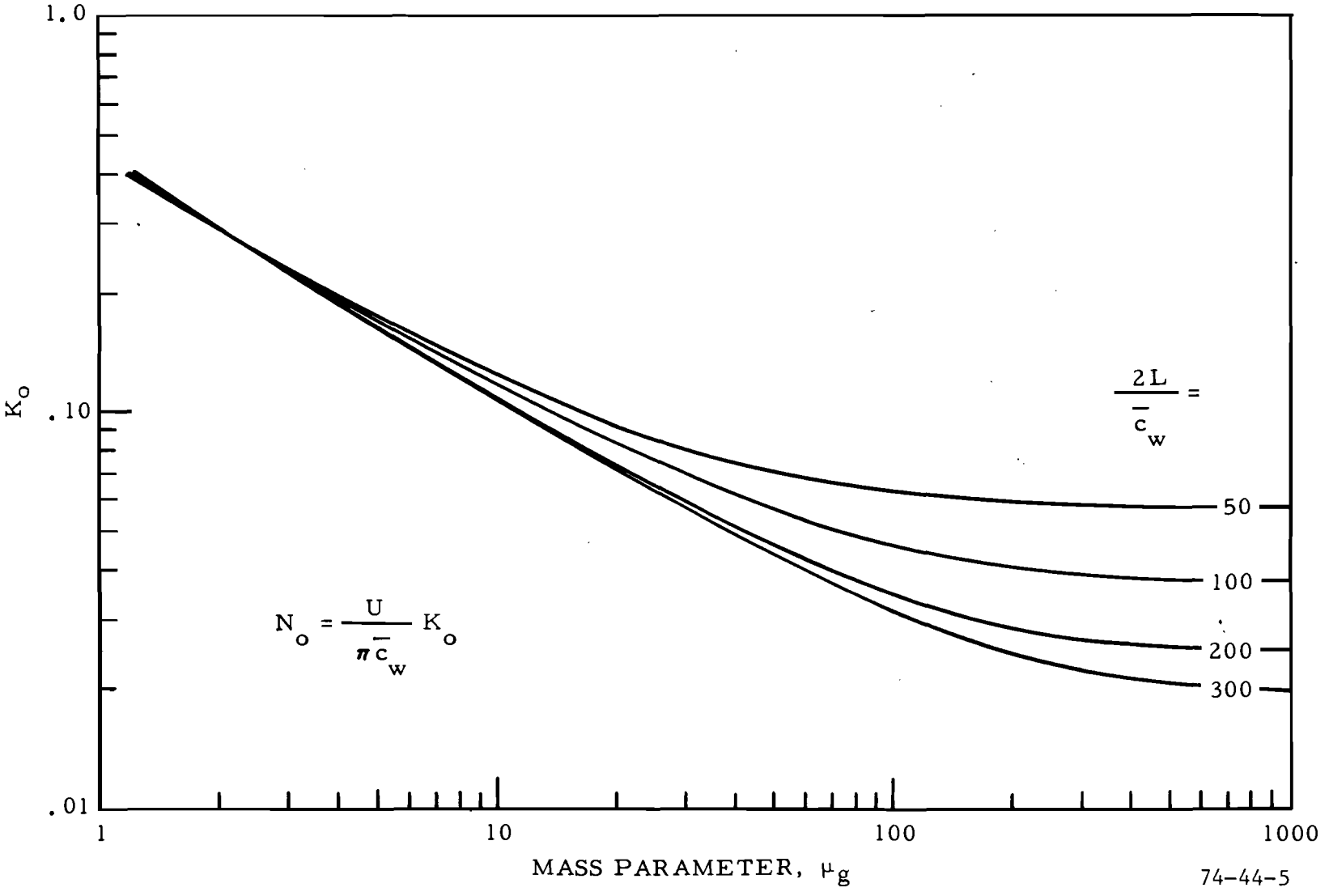

FIGURE 5. ZERO-CROSSING VALUES, K_o

where $$\Delta n = \frac{C_{L\alpha}}{2W_{to}} \rho S_w U K_g U_{de} \sqrt{\frac{\rho_o}{\rho}}$$

$$= \frac{C_{L\alpha} \rho S_w}{2W_{to}} U K_\phi \eta_d \sigma_{wg}$$

$$= \bar{A}_r \eta_d \sigma_{wg}$$

and $$\eta_d \sigma_{wg} = \sqrt{\rho_o/\rho} \left(50\right)\left(\frac{K_g}{K_\phi}\right)$$

To accomplish the comparison of the PSD approach of reference 2, which is a two degrees-of-freedom analysis to the one degree-of-freedom analysis, the normal load factor responses, $\bar{A}_{\Delta n}$, created by the rms gust input is equated to the FAR discrete-gust incremental normal load factor from appendix D by the equation $\Delta n = \bar{A}_{\Delta n} \eta_d \sigma_{wg}$ and from this $\eta_d \sigma_{wg}$ can again be determined such that it may be considered to play an equivalent role in the spectral approach as does the derived gust velocity, U_{de}, in the discrete-gust approach.

A compilation of rigid body airplane normal load factor responses and spectral velocities for both PSD methods and FAR, Parts 23 and 25, discrete-gust analysis is presented in tables 6 through 9. Seven representative aircraft in a cruise configuration were analyzed from sea level up to the aircraft service ceiling in 5,000 foot increments using a scale of turbulence, L, of 750 and 2,500 feet.

Airplanes I and V, as can be seen from table 5, have no manufacturer's derivatives, thus they are omitted from tables 7 and 9.

A scale of turbulence of L=750 feet was selected for this analysis as recommended in reference 1 for all altitudes. Tables 8 and 9 present only the two degrees-of-freedom responses at L=2,500 feet, for comparison with the responses at the recommended value of 750 feet, because the relative gust scales, s, are out of range in figures 4 and 5 for the one degree-of-freedom analysis.

In reviewing tables 6 and 7, it becomes immediately obvious that the responses of the two degrees-of-freedom analysis are consistently smaller than those produced by the one degree-of-freedom analysis. The only difference between table 6 and 7 is the origin of stability derivatives used in the analyses. The differences between the single and two degrees-of-freedom responses of tables 6 and 7, are due to the additional consideration of pitch rotation used in the analysis of reference 2, the pitch rotation tends to alleviate some of the normal load factor response.

Any increases in normal load factor responses, A_r, in table 7 over those of table 6 are due to primarily the increase in the lift curve slope used in the analysis. These increases are due to what could be called the improved derivatives (i.e., derivatives calculated by alternative methods) furnished by the manufacturers as opposed to those predicted by reference 7.

TABLE 6. COMPARISON OF AIRCRAFT CENTER OF GRAVITY RESPONSES USING NASA CR-1975 ESTIMATED DERIVATIVES FOR L = 750 FEET

				One Degree-of-Freedom Reference 1			Two Degrees-of-Freedom Reference 2			Discrete FAR 23/25
Airplane	Altitude $X\text{-}10^{-3}$	s_α	μ_g	$\bar{A}_r$ (1)	N_o (1)	$\eta_d \sigma_{wg}$ (2)	$\bar{A}_{\Delta n}$ (1)	$N_{o(\Delta n)}$ (1)	$\eta_d \sigma_{wg}$	Δn
	0		21.02	.0298	1.038	83.56	.0253	3.079	98.23	2.49
I	5		24.40	.0269	.931	88.48	.0228	2.882	104.33	2.38
	10	328.4	28.25	.0242	.885	93.39	.0205	2.695	110.32	2.26
	15		33.55	.0213	.824	100.00	.0182	2.484	117.30	2.13
	20		39.28	.0197	.748	102.03	.0162	2.300	123.62	2.01
	0		24.25	.0322	1.184	81.99	.0278	3.501	95.15	2.64
II	5		28.14	.0303	1.093	84.00	.0251	3.275	100.41	2.52
	10	301.10	32.59	.0273	1.002	87.55	.0227	3.053	105.51	2.39
	15		38.70	.0243	.911	92.18	.0201	2.804	111.36	2.24
	20		45.30	.0220	.838	95.91	.0181	2.588	116.59	2.11
	0		31.22	.0343	1.200	70.85	.0337	2.174	72.20	2.43
III	5		36.23	.0306	1.097	75.16	.0302	1.987	76.31	2.30
	10	233.29	41.94	.0279	1.035	78.14	.0271	1.819	80.43	2.18
	15		49.81	.0247	.931	82.59	.0239	1.640	85.35	2.04
	20		58.31	.0222	.848	86.04	.0212	1.492	89.95	1.91
	25		70.32	.0192	.724	84.38	.0185	1.333	87.55	1.62
	0		32.85	.0335	1.150	70.15	.0293	2.947	80.178	2.35
IV	5		38.13	.0305	1.067	73.11	.0263	2.738	84.64	2.23
	10	241.59	44.15	.0273	1.004	76.92	.0236	2.542	89.03	2.10
	15		52.43	.0241	.920	81.33	.0209	2.327	94.17	1.96
	20		61.38	.0216	.858	85.19	.0186	2.142	98.85	1.84
	25		74.02	.0187	.753	83.42	.0163	1.937	95.67	1.56

NOTE: (1) Stability derivatives required for these responses were calculated from reference 7 methods (tables 3, 4, and 5).

(2) $\eta_d \sigma_{wg}$ spectral velocities from figure 6 have been adjusted for altitude.

TABLE 6. COMPARISON OF AIRCRAFT CENTER OF GRAVITY RESPONSES USING NASA CR-1975 ESTIMATED DERIVATIVES FOR L = 750 FEET (continued)

				One Degree-of-Freedom Reference 1			Two Degrees-of-Freedom Reference 2			Discrete FAR 23/25
Airplane	Altitude X-10^{-3}	s_α	μ_g	$\bar{A}_r$ (1)	N_o (1)	$\eta_d \sigma_{wg}$ (2)	$\bar{A}_{\Delta n}$ (1)	$N_{o(\Delta n)}$ (1)	$\eta_d \sigma_{wg}$	Δn
	0		36.50	.0273	.985	69.96	.0244	2.482	78.09	1.91
V	5		42.37	.0248	.929	72.58	.0219	2.298	82.16	1.80
	10	235.49	49.06	.0226	.892	75.22	.0198	2.127	86.14	1.70
	15		58.26	.0199	.781	79.90	.0175	1.940	90.77	1.59
	20		68.20	.0178	.725	83.15	.0156	1.780	94.97	1.48
	25		82.24	.0154	.669	81.17	.0137	1.604	91.58	1.25
	0		34.53	.0617	2.167	69.37	.0575	4.566	74.38	4.28
	5		40.08	.0570	2.064	70.88	.0518	4.222	78.09	4.04
	10		46.40	.0509	1.905	75.05	.0467	3.904	81.73	3.82
VI	15		55.10	.0450	1.746	79.11	.0414	3.555	85.95	3.56
	20	212.99	64.51	.0396	1.627	84.09	.0371	3.258	89.79	3.33
	25		77.79	.0343	1.508	82.22	.0326	2.932	86.44	2.82
	30		91.20	.0306	1.389	78.10	.0292	2.678	81.75	2.39
	35		110.21	.0263	1.270	75.29	.0257	2.401	76.95	1.98
	40		139.21	.0217	1.190	72.81	.0219	2.095	72.09	1.58
	45		176.33	.0178	1.111	69.66	.0186	1.822	66.39	1.24
	0		36.43	.0569	2.018	63.97	.0514	4.106	70.89	3.64
	5		42.28	.0515	1.912	66.80	.0466	3.800	73.81	3.44
	10		48.95	.0459	1.770	70.81	.0424	3.515	76.61	3.25
	15		58.13	.0404	1.629	75.00	.0379	3.201	79.82	3.03
VII	20	179.02	68.06	.0355	1.487	79.72	.0342	2.934	82.69	2.83
	25		82.07	.0307	1.416	77.85	.0303	2.640	78.87	2.39
	30		96.22	.0269	1.345	75.46	.0274	2.410	74.03	2.03
	35		116.26	.0232	1.275	71.98	.0242	2.160	69.11	1.67
	40		146.86	.0191	1.168	70.16	.0208	1.883	64.17	1.34
	45		186.02	.0154	1.098	68.18	.0179	1.638	58.63	1.05

TABLE 7. COMPARISON OF AIRCRAFT CENTER OF GRAVITY RESPONSES USING MANUFACTURER's ESTIMATED DERIVATIVES FOR L = 750 FEET

				One Degree-of-Freedom Reference 1			Two Degree-of-Freedom Reference 2			Discrete FAR 23/25
Airplane	Altitude X 10^{-3}	s_α	μ_g	$\bar{A}_r$(1)	N_o(1)	$\eta_d \sigma_{wg}$(2)	$\bar{A}_{\Delta n}$(1)	$N_o(\Delta n)$(1)	$\eta_d \sigma_{wg}$	Δn
	0		24.37	.0321	1.184	81.93	.0271	3.645	97.03	2.63
II	5		28.28	.0302	1.093	83.11	.0244	3.417	102.71	2.51
	10	301.10	32.75	.0277	1.002	85.92	.0220	3.1996	108.24	2.38
	15		38.89	.0242	.911	92.15	.0195	2.954	114.63	2.23
	20		45.53	.0219	.838	95.89	.0175	2.737	120.34	2.10
	0		28.47	.0376	1.242	69.95	.0321	3.253	81.80	2.63
III	5		33.05	.0330	1.138	75.45	.0290	3.013	86.13	2.49
	10	233.29	38.26	.0296	1.076	79.73	.0262	2.790	90.36	2.36
	15		45.44	.0257	.993	82.77	.0232	2.545	95.25	2.21
	20		53.20	.0235	.890	88.51	.0208	2.335	99.67	2.08
	25		64.15	.0208	.848	84.62	.0183	2.104	96.08	1.76
	0		31.14	.0354	1.234	69.49	.0321	2.652	76.78	2.46
IV	5		36.14	.0311	1.109	74.92	.0287	2.444	81.12	2.33
	10	241.59	41.85	.0283	1.046	77.74	.0258	2.255	85.55	2.20
	15		49.70	.0250	.920	82.40	.0227	2.050	90.77	2.06
	20		58.19	.0224	.899	86.16	.0202	1.877	95.62	1.93
	25		70.16	.0195	.795	84.10	.0176	1.689	92.99	1.64

NOTE: (1) Stability derivatives required for these responses were supplied by the manufacturers. except airplane II which used derivatives from reference 14 in table 3.

(2) $\eta_d \sigma_{wg}$ spectral velocities from figure 6 have been adjusted for altitude.

(3) Derivatives not supplied were calculated from reference 7 methods.

TABLE 7. COMPARISON OF AIRCRAFT CENTER OF GRAVITY RESPONSES USING MANUFACTURER'S ESTIMATED DERIVATIVES FOR L = 750 FEET (continued)

				One Degree-of-Freedom Reference 1			Two Degrees-of-Freedom Reference 2			Discrete FAR 23/25
Airplane	Altitude X 10^{-3}	s_α	μ_g	$\bar{A}_r$ (1)	N_o (1)	$\eta_d \sigma_{wg}$ (2)	$\bar{A}_{\Delta n}$ (1)	$N_o(\Delta n)$ (1)	$\eta_d \sigma_{wg}$	Δn
	0		24.65	.0801	2.698	71.04	.0862	3.726	69.31	5.69
	5		28.61	.0717	2.460	75.45	.0736	3.383	73.55	5.41
	10		33.12	.0655	2.262	78.47	.0660	3.075	77.87	5.14
	15		39.33	.0581	2.103	82.96	.0580	2.750	83.11	4.82
	20	212.99	46.05	.0521	1.944	86.95	.0514	2.484	88.11	4.53
VI	25		55.53	.0453	1.746	84.99	.0446	2.204	86.45	3.85
	30		65.10	.0404	1.627	81.19	.0394	1.993	83.16	3.28
	35		78.67	.0349	1.508	77.94	.0340	1.772	79.98	2.72
	40		99.37	.0288	1.349	75.69	.0283	1.536	77.06	2.18
	45		125.87	.0240	1.270	71.25	.0234	1.334	73.11	1.71
	0		25.13	.0742	2.408	67.25	.0669	5.003	74.66	4.99
	5		29.16	.0675	2.231	70.37	.0611	4.633	77.77	4.75
	10		33.76	.0604	2.089	74.67	.0559	4.289	80.72	4.51
	15		40.10	.0534	1.912	79.21	.0503	3.909	84.06	4.23
	20	179.02	46.94	.0478	1.806	83.26	.0457	3.585	87.02	3.98
	25		56.61	.0415	1.664	81.45	.0407	3.227	82.88	3.38
VII	30		66.37	.0364	1.522	78.85	.0370	2.947	77.68	2.87
	35		80.19	.0314	1.416	75.80	.0329	2.642	72.36	2.38
	40		101.29	.0259	1.310	73.75	.0285	2.304	66.95	1.91
	45		128.31	.0213	1.204	70.42	.0246	2.002	60.91	1.50

TABLE 8. AIRCRAFT CENTER OF GRAVITY RESPONSES USING NASA CR-1975 ESTIMATED DERIVATIVES FOR L = 2,500 FEET

Airplane	Altitude X 10^{-3}	s_α	μ_g	Two Degrees-of-Freedom Reference 2 $\bar{A}_{\Delta n}$ (1)	N_o (Δn) (1)	$\eta_d \sigma_{wg}$	Discrete FAR 23/25 Δn
	0		21.02	.0170	3.062	145.96	2.49
I	5		24.40	.0153	2.866	155.01	2.38
	10	1094.7	28.25	.0138	2.630	163.92	2.26
	15		33.55	.0122	2.471	174.28	2.13
	20		39.28	.0109	2.288	183.67	2.01
	0		24.25	.0187	3.494	141.48	2.64
II	5		28.14	.0169	3.261	149.31	2.52
	10	1003.7	32.59	.0152	3.040	156.89	2.39
	15		38.70	.0136	2.792	165.58	2.24
	20		45.30	.0122	2.576	173.34	2.11
	0		31.22	.0233	2.108	104.52	2.43
	5		36.23	.0209	1.923	110.25	2.30
	10	777.64	41.94	.0188	1.757	115.97	2.18
III	15		49.81	.0166	1.581	122.77	2.04
	20		58.31	.0148	1.435	129.08	1.91
	25		70.32	.0129	1.279	125.27	1.62
	0		32.85	.0199	2.906	118.05	2.35
	5		38.13	.0179	2.699	124.58	2.23
	10	805.30	44.15	.0161	2.506	131.00	2.10
IV	15		52.43	.0142	2.292	138.50	1.96
	20		61.38	.0127	2.109	145.33	1.84
	25		74.02	.0111	1.906	140.56	1.56

NOTE: (1) Stability derivatives required for these responses were calculated from reference 7 methods (tables 3, 4, and 5).

TABLE 8. AIRCRAFT CENTER OF GRAVITY RESPONSES USING NASA CR-1975 ESTIMATED DERIVATIVES FOR L = 2,500 FEET (continued)

				Two Degrees-of-Freedom Reference 2			Discrete FAR 23/25
Airplane	Altitude X 10^{-3}	s_α	μ_g	$\bar{A}_{\Delta n}$ (1)	No (Δn) (1)	$\eta_d \sigma_{wg}$	Δn
	0		36.50	.0166	2.448	115.04	1.91
	5		42.37	.0149	2.266	120.98	1.80
	10	784.95	49.06	.0134	2.097	126.79	1.70
V	15		58.26	.0119	1.912	133.54	1.59
	20		68.20	.0106	1.753	139.64	1.48
	25		82.24	.0093	1.579	134.53	1.25
	0		34.53	.0392	4.485	109.07	4.28
	5		40.08	.0353	4.145	114.45	4.04
	10		46.40	.0319	3.830	119.69	3.82
	15		55.10	.0283	3.485	125.74	3.56
	20	709.96	64.51	.0254	3.191	131.20	3.33
VI	25		77.79	.0224	2.868	126.08	2.82
	30		91.20	.0201	2.615	119.01	2.39
	35		110.21	.0177	2.338	111.69	1.98
	40		139.21	.0151	2.032	104.15	1.58
	45		176.33	.0130	1.757	95.29	1.24
	0		36.43	.0349	4.054	104.47	3.64
	5		42.28	.0317	3.794	108.69	3.44
	10		48.95	.0288	3.466	112.71	3.25
VII	15		58.13	.0258	3.153	117.27	3.03
	20	596.74	68.06	.0233	2.886	121.29	2.83
	25		82.07	.0207	2.591	115.40	2.39
	30		96.22	.0188	2.361	108.05	2.03
	35		116.26	.0167	2.109	100.49	1.67
	40		146.86	.0144	1.830	92.75	1.34
	45		186.02	.0125	1.581	84.08	1.05

TABLE 9. AIRCRAFT CENTER OF GRAVITY RESPONSES USING MANUFACTURER'S DERIVATIVES FOR L = 2,500 FEET

Airplane	Altitude X 10^{-3}	s_α	μ_g	Two Degrees-of-Freedom Reference 2 $\bar{A}_{\Delta n}$ (1)	N_o (Δn) (1)	$\eta_d \sigma_{wg}$	Discrete FAR 23/25 Δn
	0		24.37	.0183	3.626	144.20	2.63
II	5		28.28	.0164	3.400	152.63	2.51
	10	1003.7	32.75	.0148	3.184	160.86	2.38
	15		38.89	.0131	2.939	170.36	2.23
	20		45.53	.0117	2.724	178.90	2.10
	0		28.47	.0217	3.222	120.99	2.63
	5		33.05	.0196	2.984	127.37	2.49
	10	777.64	38.26	.0177	2.762	133.57	2.36
III	15		45.44	.0157	2.518	140.74	2.21
	20		53.20	.0141	2.310	147.21	2.08
	25		64.15	.0124	2.080	141.82	1.76
	0		31.14	.0219	2.597	112.28	2.46
	5		36.14	.0197	2.391	118.56	2.33
	10	805.30	41.85	.0177	2.204	124.83	2.20
IV	15		49.70	.0156	2.001	132.29	2.06
	20		58.19	.0139	1.830	139.19	1.93
	25		70.16	.0121	1.645	135.16	1.64

NOTE: (1) Stability derivatives required for these responses were supplied by the manufacturers, except airplane II which used derivatives from reference 14 in table 3.

(2) Derivatives not supplied were calculated from reference 7 methods.

TABLE 9. AIRCRAFT CENTER OF GRAVITY RESPONSES USING MANUFACTURER'S DERIVATIVES FOR L = 2,500 FEET (continued)

				Two Degrees-of-Freedom Reference 2			Discrete FAR 23/25
Airplane	Altitude X 10^{-3}	S_α	μ_g	$\bar{A}\Delta n^{(1)}$	$N_o\ (\Delta n)^{(1)}$	$\eta_d \sigma_{wg}$	Δn
	0		24.65	.0580	3.535	98.11	5.69
	5		28.61	.0522	3.193	103.60	5.41
	10		33.12	.0471	2.889	109.13	5.14
	15		39.33	.0416	2.569	115.78	4.82
	20	709.96	46.05	.0371	2.308	122.05	4.53
VI	25		55.53	.0321	2.035	118.90	3.85
	30		65.10	.0288	1.830	113.67	3.28
	35		78.67	.0251	1.615	108.44	2.72
	40		99.37	.0211	1.387	103.35	2.18
	45		125.87	.0177	1.191	96.79	1.71
	0		25.13	.0451	4.969	110.72	4.99
	5		29.16	.0412	4.600	115.26	4.75
	10		33.76	.0377	4.256	119.57	4.51
	15		40.10	.0340	3.877	124.41	4.23
	20	596.74	46.94	.0309	3.552	128.66	3.98
VII	25		56.61	.0276	3.194	122.35	3.38
	30		66.37	.0251	2.913	114.49	2.87
	35		80.19	.0224	2.606	106.40	2.38
	40		101.29	.0195	2.265	98.08	1.91
	45		128.31	.0169	1.961	88.79	1.50

Looking at the differences in the two degrees-of-freedom responses due to effects of alternative derivatives (see tables 6 and 7, and tables 8 and 9), it can be seen that the changes are not uniform. The $\bar{A}_{\Delta n}$ for airplanes II and III decreased with the increased lift curve slope, signifying that other derivative changes are affecting the response in an adverse manner discussed previously and as shown in figure 2.

A noticeable deviation in the number of positive zero crossings between the two PSD methods can be seen in tables 6 and 7. The discrepancies noted in N_o, specifically the larger zero crossings created by the two degrees-of-freedom PSD analysis, are due to the choice of a cutoff frequency. As discussed previously, the cutoff frequency is critical in the determination of N_o because it eliminates the high frequency components which do not contribute to the response $\bar{A}_{\Delta n}$ but affect N_o, markedly. Cutoff frequencies normally can be expected to be in the area of $.99\sigma$ for the zero crossing rate. However, as can be seen in appendix C both $\bar{A}$ and N_o utilize what are termed a response integrals (see equations C29 and C30) which are functions of the frequency ratio $\bar{\beta} = \omega/\omega_o$. These integrals do not lend themselves easily to the selection of a cutoff frequency for each N_o. Therefore, a finite interval was used for all responses, thus producing arbitrary cutoff frequencies which ranged from approximately 0.4 to 15 where values in the neighborhood of 0.3 for the aircraft considered would have been more realistic. The fact large cutoff frequencies were utilized created larger values of N_o than anticipated for all of the cases studied compared to those of the single degree-of-freedom approach.

The relationship between the spectral velocity values and the relative gust scale can be seen in figure 6 and tables 6 through 9. Generally, the spectral velocity values decrease consistently with relative gust scale for both estimated and manufactures derivatives at all altitudes.

From the airplanes analyzed in tables 6 through 9, it can be seen that both PSD approaches would require a spectral velocity value $\eta_d \sigma_{wg}$ which would be significantly larger than the normally recommended values of 54 ft/sec from reference 1 or 57.5 ft/sec from reference 15 for a single-degree-of-freedom analysis at sea level. These recommended These values are adequate for the size and type of aircraft used in those studies. That is to say, the spectral velocities apply to large civil or military transport aircraft with a small relative gust scale, $s=2L/\bar{c}_w$, due to the larger mean aerodynamic chords involved, "s" values on the range of 50 to 100 are appropriate which puts $\eta_d \sigma_{wg}$ for these aircraft in the range of 54 to 57.7 ft/sec as shown in figure 6, where the recommended scale of turbulence is L=750 feet.

Spectral velocities using estimated derivatives for all seven of the representative aircraft at sea level for L=750 feet are plotted on figure 6. The trend towards higher spectral velocities than those recommended in references 1 and 15 is evident. $\eta_d \sigma_{wg}$ values ranged from 64.0 to 83.6 ft/sec for the single degree-of-freedom analysis. For the two degrees-of-freedom analysis the velocities varied from 69.3 to 98.2 ft/sec as depicted in tables 6 and 7. Similarly from tables 8 and 9 for L=2500 feet at sea level spectral velocity values ranged from 98.1 ft/sec to 146.0 ft/sec for the two degrees-of-freedom analysis. These velocities generally increase with altitude for both PSD methods as expected.

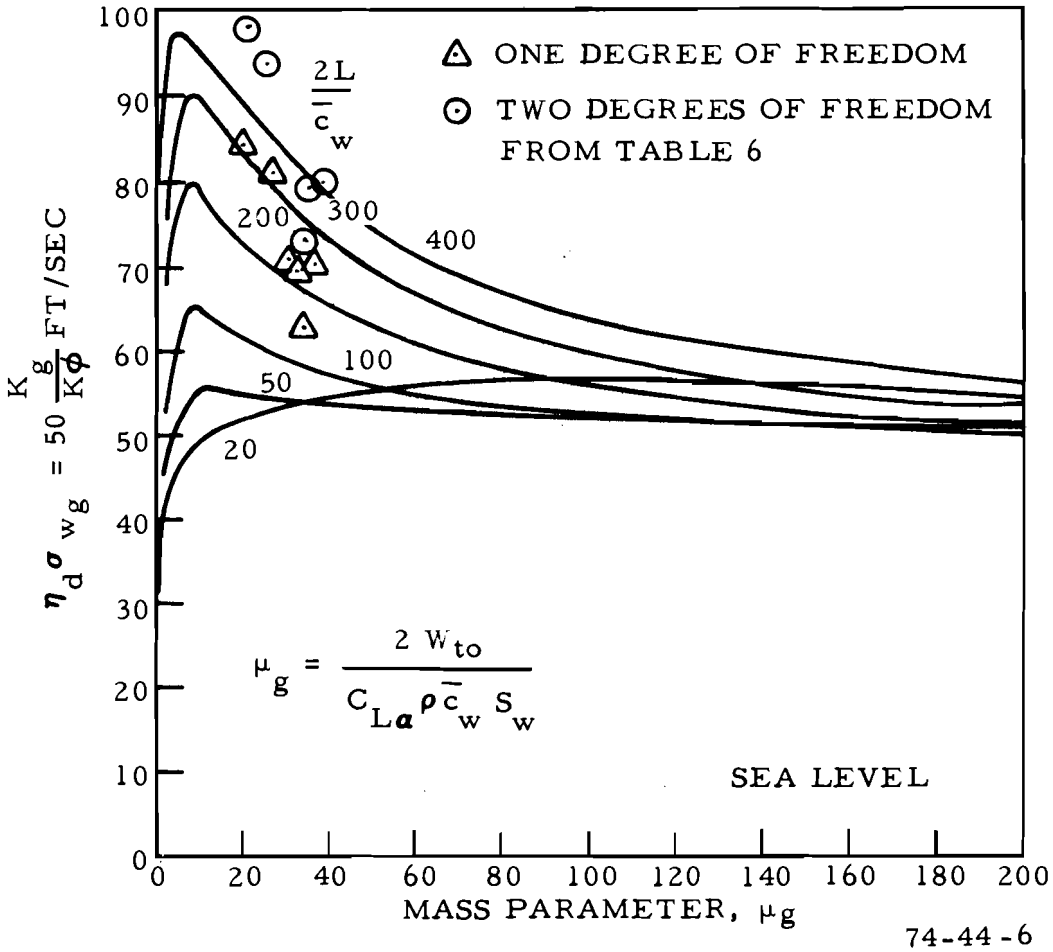

FIGURE 6. SPECTRAL "VELOCITIES" EQUIVALENT TO THE DISCRETE GUST VELOCITY FOR ONE DEGREE-OF-FREEDOM ANALYSIS

TAIL LOAD RESPONSE COMPARISON.

Tail load responses derived from the two degrees-of-freedom analysis, as in the previous section are compared to the discrete-gust tail load. The objective again is to derive a spectral velocity value, $\eta_d \sigma_{wg}$, which would yield equivalent results.

Tabulation of horizontal and vertical tail load responses for the two degrees-of-freedom and discrete-gust approaches are presented in tables 10 through 13. Where tables 11 and 13 again differ from tables 10 and 12 only in the use of improved stability derivatives in the analyses. Also, the discrete-gust horizontal tail loads, are based on the determination of a (1-g) balancing tail load which in this study was only approximate and produced interminate results.

The number of positive zero crossings, N_o (Z_t), for the two degrees-of-freedom horizontal tail load responses, as in the center of gravity responses, are somewhat inflated as shown in tables 10 through 13. Again, this increase is due to the arbitrary selection of a cutoff frequency to give realistic results.

It was hoped that some correlation would be evident between the center of gravity normal load factor and horizontal tail load response spectral velocity values, however, from tables 6 through 13, it appears that there is no general relationship between the two spectral velocities except in the case of airplanes I and II. The tail load spectral velocities for airplanes III, IV, and V using NASA estimated derivatives as shown in tables 10 and 12 were approximately 30 percent less than the c.g. spectral velocities shown in tables 6 and 8 at sea level. The comparison is compounded by the fact that the aircraft center of gravity location greatly affects the balancing tail load and center of gravity travel can vary as much as 30 percent over the mean aerodynamic chord, depending on the aircraft. Under the extremes of center of gravity travel it can be expected that at some point the $\eta_d \sigma_{wg}$ values would coincide.

Tables 10 through 13, in general, indicate that the vertical tail load spectral velocity values are less than the horizontal tail load velocity values. Spectral velocity values for the vertical tail load responses ranged from 35.2 to 94.4 ft/sec for L=750 feet from 51.8 to 140.6 ft/sec for L=2,500 feet.

TABLE 10. COMPARISON OF AIRCRAFT TAIL LOAD RESPONSES USING NASA CR-1975 ESTIMATED DERIVATIVES FOR L = 750 FEET

	Horizontal Tail Two Degrees-of-Freedom				Vertical Tail Two Degrees-of-Freedom			Discrete FAR 23/25
Airplane	$\bar{A}_{z_t}$ (2)	$N_o(Z_t)$ (2)	$\eta_d \sigma_{wg}$	L_t	$\bar{A}_{y_v}$ (2)	$N_o(Y_v)$ (2)	$\eta_d \sigma_{wg}$	L_v
I	9.359	3.493	98.6	923.2	6.109	.989	94.4	576.7
II	13.699	3.953	82.6	1131.3	11.411	.774	50.7	578.9
III	72.973	2.224	50.5	3683.8	55.988	.768	43.6	2438.7
IV	50.382	3.202	53.1	2677.0	40.818	1.055	65.9	2691.0
V	46.219	2.745	52.9	2442.7	54.636	1.157	56.1	3063.4
VI	98.823	4.810	----	(3)	95.840	1.935	36.6	3505.0
VII	165.884	4.310	----	(3)	152.172	1.535	35.2	5350.9

NOTES: (1) Comparisons are at sea level altitude.

(2) Stability derivatives required for these responses were calculated from reference 7 methods (tables 3, 4, and 5).

(3) Insufficient data to determine load for balanced flight.

TABLE 11. COMPARISON OF AIRCRAFT TAIL LOAD RESPONSES USING MANUFACTURER'S ESTIMATED DERIVATIVES FOR L = 750 FEET

Airplane	Horizontal Tail Two Degrees-of-Freedom			Discrete	Vertical Tail Two Degrees-of-Freedom			Discrete FAR 23/25
	$\bar{A}_{z_t}$ (2)	$N_o(Z_t)$ (2)	$\eta_d \sigma_{wg}$	L_t	$\bar{A}_{y_v}$ (2)	$N_o(Y_v)$ (2)	$\eta_d \sigma_{wg}$	L_v
II	13.204	4.143	86.0	1136.0	11.411	.774	50.7	578.9
III	54.165	3.601	61.9	3353.7	50.122	.892	48.7	2438.7
IV	54.351	2.796	46.3	2514.2	40.806	1.063	65.9	2691.0
VI	103.317	3.665	----	(3)	95.840	1.935	36.6	3505.0
VII	135.476	5.330	----	(3)	117.130	1.820	45.7	5350.9

NOTES: (1) Comparison are sea level altitude.

(2) Stability derivatives required for these responses were supplied by the manufacturers (tables 3, 4, and 5).

(3) Insufficient data to determine load for balanced flight.

(4) Derivatives not supplied were calculated from reference 7 methods, except airplane II which used derivatives from reference 14 in table 3.

TABLE 12. COMPARISON OF AIRCRAFT TAIL LOAD RESPONSES USING NASA CR-1975 ESTIMATED DERIVATIVES FOR L = 2,500 FEET

Airplane	Horizontal Tail Two Degrees-of-Freedom			Discrete	Vertical Tail Two Degrees-of-Freedom			Discrete FAR 23/25
	$\bar{A}_{z_t}$ (2)	$N_o(Z_t)$ (2)	$\eta_d \sigma_{wg}$	L_t	$\bar{A}_{y_v}$ (2)	$N_o(Y_v)$ (2)	$\eta_d \sigma_{wg}$	L_v
I	6.287	3.481	146.8	923.2	4.101	.987	140.6	576.7
II	9.195	3.942	123.0	1131.3	7.697	.769	75.2	578.9
III	50.332	2.160	73.2	3683.8	38.331	.754	63.6	2438.7
IV	34.118	3.166	78.5	2677.0	27.609	1.046	97.5	2691.0
V	31.248	2.719	78.2	2442.7	36.832	1.151	83.2	3063.4
VI	67.188	4.739	----	(3)	64.875	1.920	54.0	3505.0
VII	112.246	4.267	----	(3)	103.346	1.522	51.8	5350.9

NOTES: (1) Comparisons are at sea level altitude.

(2) Stability derivatives required for these responses were calculated from reference 7 methods (tables 3, 4, and 5).

(3) Insufficient data to determine load for balanced flight.

TABLE 13. COMPARISON OF AIRCRAFT TAIL LOAD RESPONSES USING MANUFACTURER'S ESTIMATED DERIVATIVES FOR L = 2,500 FEET

Airplane	Horizontal Tail Two Degrees-of-Freedom			Discrete	Vertical Tail Two Degrees-of-Freedom			Discrete FAR 23/25
	$\bar{A}_{z_t}$ (2)	$N_o(Z_t)$ (2)	$\eta_d \sigma_{wg}$	L_t	$\bar{A}_{y_v}$ (2)	$N_o(Y_v)$ (2)	$\eta_d \sigma_{wg}$	L_v
II	8.868	4.130	128.1	1136.0	7.697	.769	75.2	578.9
III	36.501	3.578	91.9	3353.7	34.118	.881	71.5	2438.7
IV	37.086	2.744	67.8	2514.2	27.587	1.055	97.5	2691.0
VI	73,099	3.471	----	(3)	64.875	1.920	54.0	3505.0
VII	91.110	5.308	____	(3)	79.507	1.802	67.3	5350.9

NOTES: (1) Comparison are sea level altitude.

(2) Stability derivatives required for these responses were supplied by the manufacturers (tables 3, 4, and 5).

(3) Insufficient data to determine load for balanced flight.

(4) Derivatives not supplied were calculated from reference 7 methods, except airplane II which used derivatives from reference 14 in table 3.

CONCLUSIONS

A computer program has been developed to predict aerodynamic stability derivatives and both power spectral density and discrete-gust responses. The following conclusions are thus drawn:

1. The methods of reference 7 for estimating low-speed stability derivatives are adequate for the power spectral density gust analysis investigated.

2. The two degrees-of-freedom rigid body power spectral density analysis of reference 2 for airplanes in the 3,000 to 12,500 pound range produced lower normal load factor responses than a similar one degree-of-freedom analysis of reference 1. Consequently, to produce an equivalent discrete-gust load factor for the two degrees-of-freedom analysis of reference 2, a higher spectral velocity value must be used compared to that of the single-degree-of-freedom approach of reference 1. Spectral velocity values $\eta_d \sigma_{wg}$ for both power spectral gust analyses are summarized in figures 7 through 10, for L=750 feet.

3. For the seven aircraft considered, the spectral velocity values were inconsistent for the vertical tail load response, but generally tended to be less than the horizontal tail load response spectral velocities.

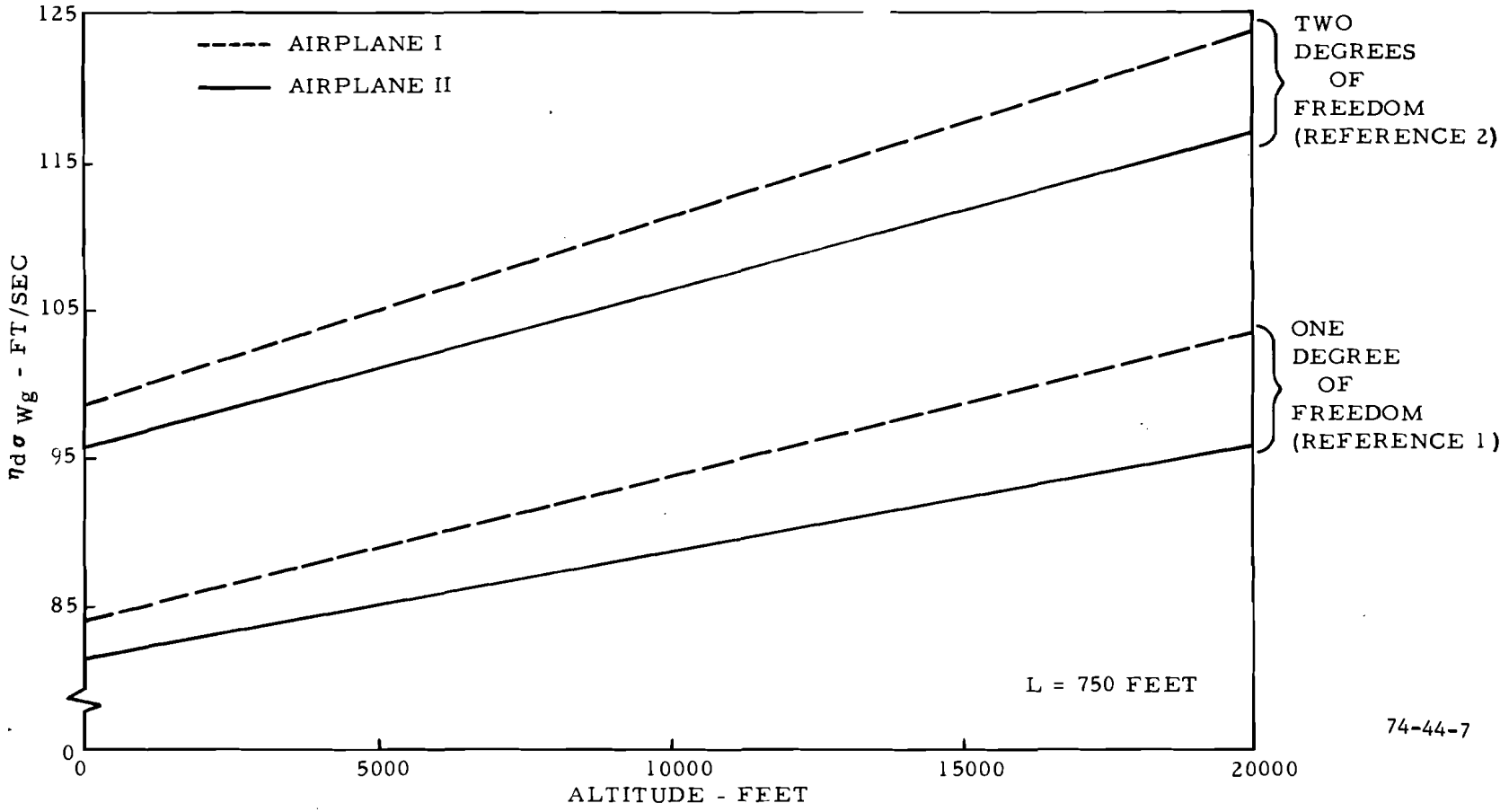

FIGURE 7. EFFECT OF ALTITUDE ON SPECTRAL VELOCITY FOR AIRPLANES I AND II

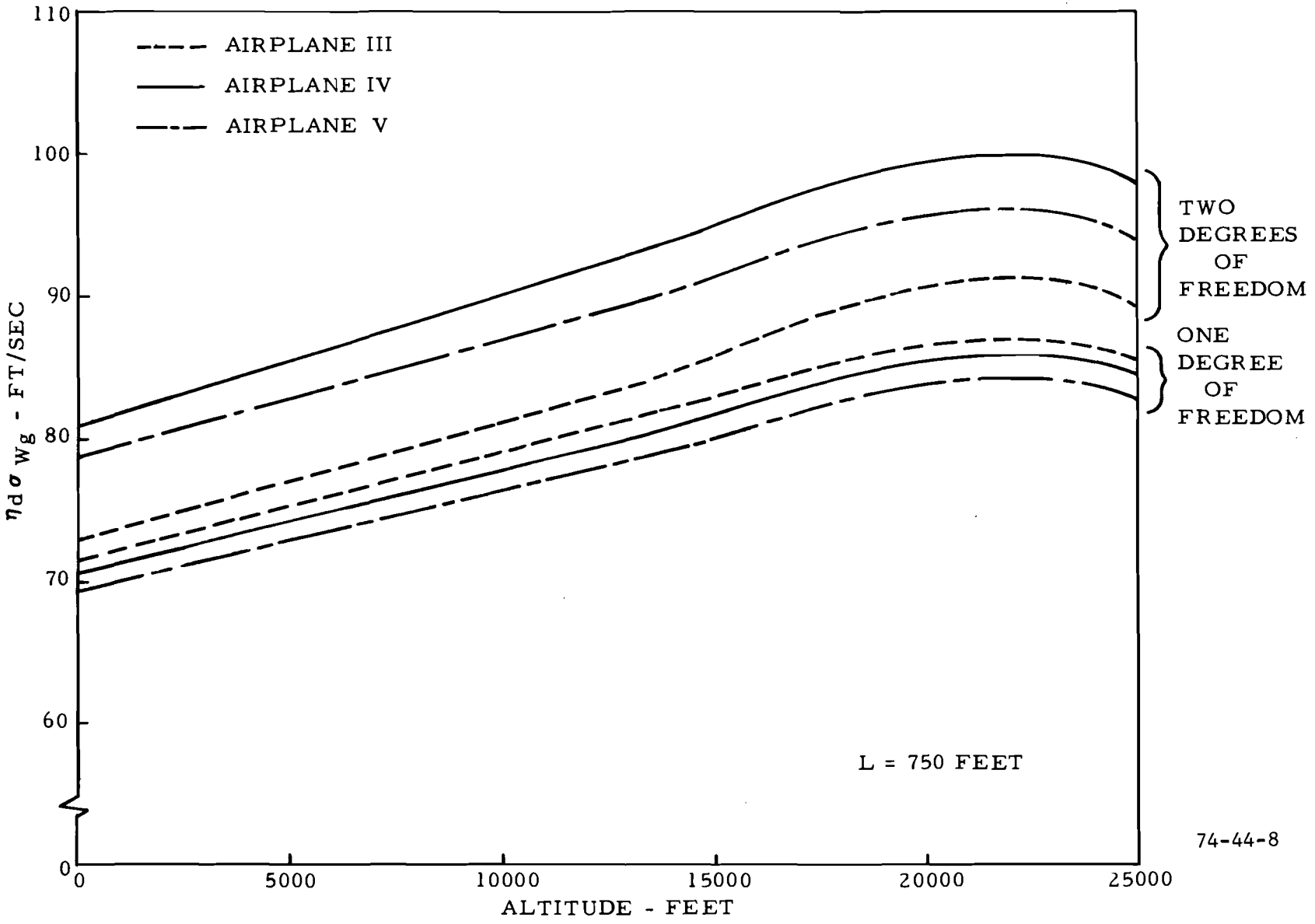

FIGURE 8. EFFECT OF ALTITUDE ON SPECTRAL VELOCITY FOR AIRPLANES III, IV, AND V

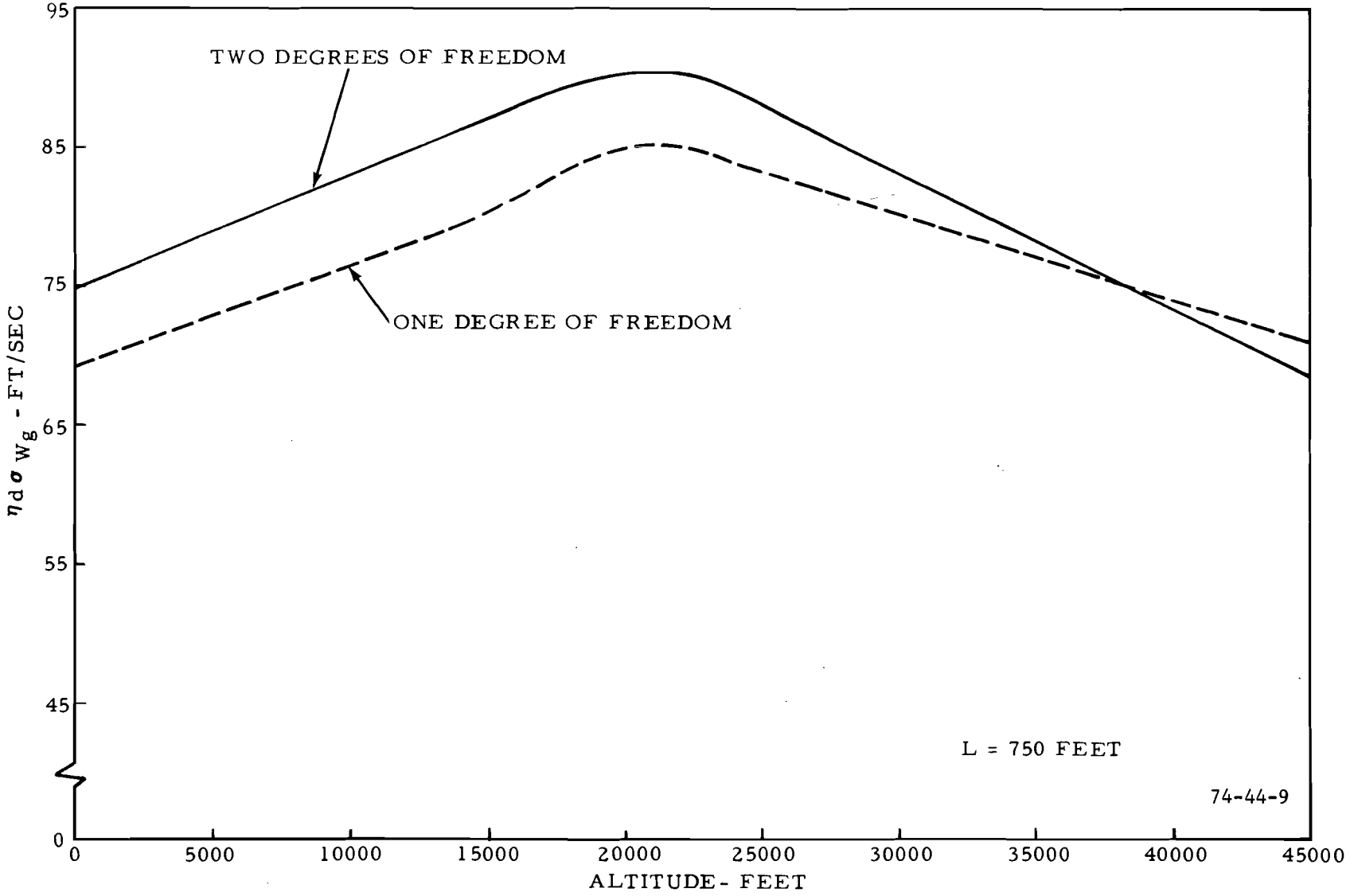

FIGURE 9. EFFECT OF ALTITUDE ON SPECTRAL VELOCITY FOR AIRPLANE VI

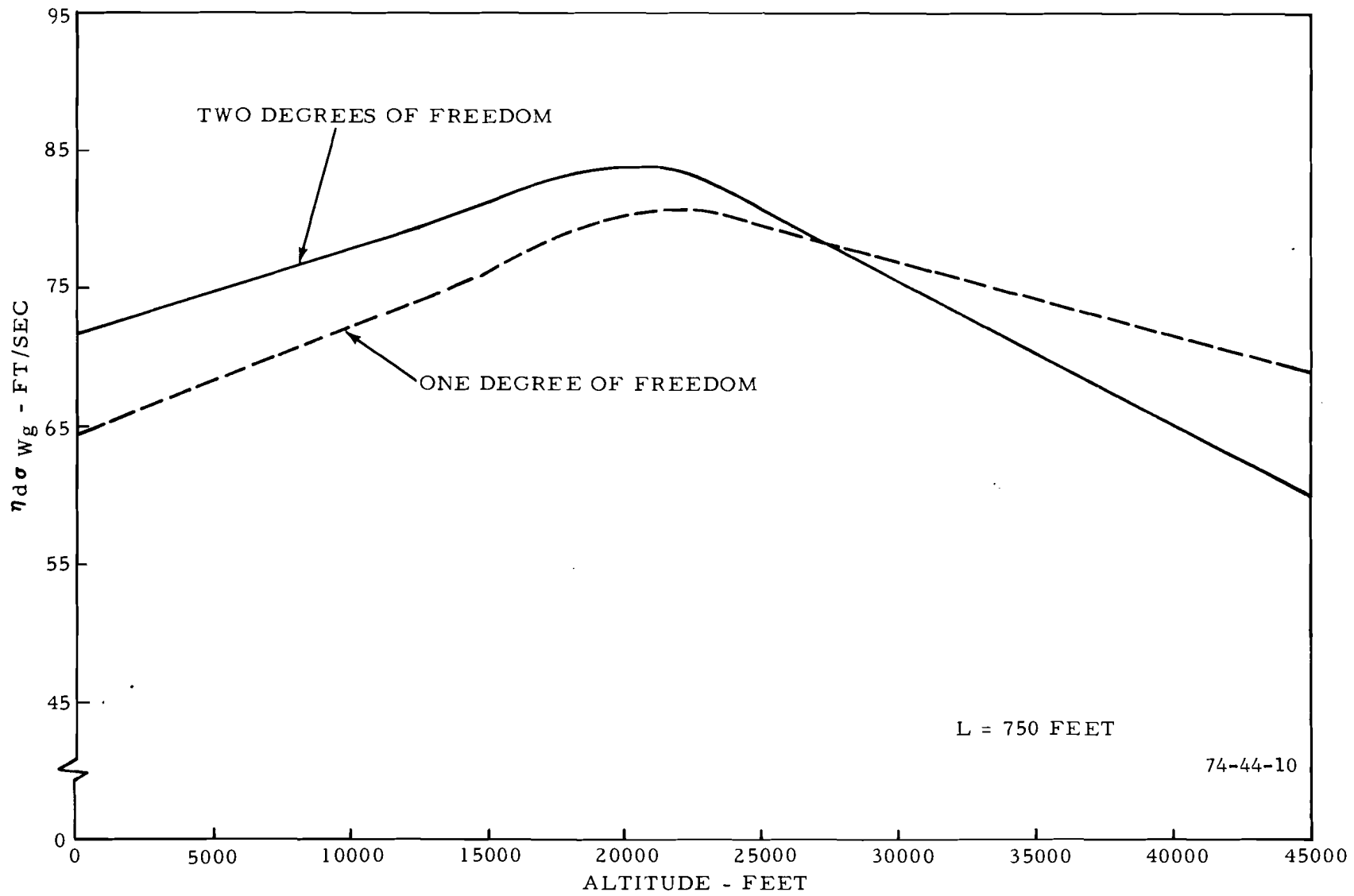

FIGURE 10. EFFECT OF ALTITUDE ON SPECTRAL VELOCITY FOR AIRPLANE VII

Phase II

Based on the results of the work performed in phase I, items to be performed in phase II are as follows:

1. A study to determine if the PSD analysis method presented in this report can be further simplified.

2. Develop longitudinal and lateral two degrees-of-freedom aircraft response analyses along aeroelastic lines, including the effects of gust penetration, wing and tail interaction, and downwash effects. This development will eliminate the need for the calculation of aircraft stability derivatives.

REFERENCES

1. Houbolt, John C., Design Manual for Vertical Gusts Based on Power Spectral Techniques, Technical Report AFFDL-TR-70-106, December 1970.

2. Peele, Ellwood L., A Method for Estimating Some Longitudinal and Lateral Rigid-Body Responses of Airplanes to Continuous Atmospheric Turbulence, NASA TN D-6273, August 1971.

3. Perkins, C. D., and Hage, R. E., Airplane Performance Stability and Control, John Wiley and Sons, 1958.

4. Etkin, Bernard, Dynamics of Flight, Stability and Control, John Wiley and Sons, May 1967.

5. Seckel, E., Stability and Control of Airplanes and Helicopters, Academic Press, 1964.

6. Hoak, O. E., and Ellison D. E., USAF Stability and Control Handbook, (DATCOM), Wright-Patterson AFB, Ohio, Revised August 1968.

7. Smetana, Frederick O., and Summey, Robert C., Riding and Handling Qualities of Light Aircraft - A Review and Analysis, NASA CR-1975, March 1972.

8. Houbolt, J. C., Steiner, R., and Pratt, K. G., Dynamic Response of Airplanes to Atmospheric Turbulence Including Flight Data on Input and Response, NACA TR-R-199, June 1964.

9. Houbolt, John C., and Seckel, Edward, Evaluation of Methods Which Estimate the Response of Small Ridgid Aircraft to Continuous Atmospheric Turbulence, ARAP Report No. 223, July 1974.

10. Seckel, E. and Morris, J. J., The Stability Derivatives of the Navion Aircraft Estimated by Various Methods and Derived from Flight Test Data, SRDS FAA Report RD-71-6, January 1971.

11. Weissinger, J., The Lift Distribution of Swept-Back Wings, NACA TM 1120, 1947.

12. Campbell,J. P., and McKinney, M. O., Summary of Methods for Calculating Dynamic Lateral Stability and Response and for Estimating Lateral Stability Derivatives, NACA Report 1098, 1952.

13. Fisher, L. R., and Fletcher, H. S., Effect of Lag of Sidewash on the Vertical-Tail Contribution to Oscillatory Damping in Yaw of Airplane Models, NACA TN 3356, 1955.

14. Wolowicz, Chester H. and Yancey, Roxanah B., Longitudinal Aerondynamic Characteristics of Light Twin-Engine, Propeller-Driven Airplanes, NASA TN D-6800, June 1972.

15. Houbolt, John C., Updated Gust Design Values for Use With AFFDL-70-106, Technical Report AFFDL TR-73-148, November 1973.

GLOSSARY OF TERMS

Nomenclature	Computer Equivalent	
$\bar{A}$	--	Airplane response parameter relating root-mean-square (rms) input and output values (subscript refers to response quantity)
$\bar{A}_{y_v}$	AYVT	Vertical tail load response, lb/ft/sec
$\bar{A}_{z_t}$	AZHT	Horizontal tail load response, lb/ft/sec
$\bar{A}_{\Delta_n}$	ADN	Normal load factor response, g/ft/sec
$\bar{A}_{\dot{\theta}}$	ATHD	Pitch angle rate response, rad/sec/ft/sec
$\bar{A}_{\ddot{\theta}}$	ATDD	Pitch angle acceleration response, rad/sec^2/ft/sec
$\bar{A}_{\ddot{\gamma}/g}$	ADL	Lateral load factor response, g/ft/sec
$\bar{A}_{\psi}$	ASI	Yaw angle response, rad/ft/sec
$\bar{A}_{\dot{\psi}}$	ASID	Yaw angle rate response, rad/sec/ft/sec
$\bar{A}_r$	--	Normal load factor response for one-dimensional analysis, g/ft/sec
A_e	--	Effective aspect ratio
AR_t	ART	Aspect ratio of horizontal tail
AR_w	ARW	Aspect ratio of wing
--	ALT	Altitude, ft
--	ALTC	Service ceiling, ft
$\tilde{a}_\alpha$	ABA	Unsteady lift force attenuation factor, longitudinal
$\tilde{a}_\beta$	ABB	Unsteady lift force attenuation factor, lateral
a.c.	--	Aerodynamic center
b_t	BT	Horizontal tail span, ft
b_v	BV	Vertical tail span, ft
b_w	B	Wing span, ft
C_D	CDP	Drag coefficient, $\frac{\text{Drag}}{q S_w}$

C_{D_e}	CDE	Drag coefficient of empennage
C_{D_f}	CDF	Drag coefficient of fuselage
$C_{D_{f_p}}$	CDFP	Parasite drag
$C_{D_{nac}}$	CDNAC	Drag coefficient, nacelle
$C_{D_{ng}}$	CDNG	Drag coefficient, nose gear
$C_{D_{ttk}}$	CDTTK	Drag coefficient, tiptank
C_{D_w}	CDW	Drag coefficient, wing
C_{D_o}	CDO	Three-dimensional drag coefficient
C_L	CLP	Lift coefficient, $\frac{\text{Lift}}{q S_w}$
C_{L_t}	CLT	Lift coefficient, tail
C_{L_w}	CLW	Lift coefficient, wing
C_{L_α}	CLAP	Lift curve slope, $\partial C_L/\partial \alpha$, per rad
$C_{L_{\alpha_f}}$	CLAF	Lift curve slope, $\left(\partial C_L/\partial \alpha\right)_f$, fuselage per rad
$C_{L_{\alpha_t}}$	CLAT	Lift curve slope, $\partial C_{L_t}/\partial \alpha_t$, horizontal tail, per rad
$C_{L_{\alpha_v}}$	CLAV	Lift curve slope, $\partial C_{L_v}/\partial \alpha_v$, vertical tail, per rad
$C_{L_{\alpha_w}}$	CLAW	Lift curve slope, $\partial C_{L_w}/\partial \alpha_w$, wing, per rad
$C_{L_{\dot{\alpha}}}$	CLADP	$\partial C_L/\partial(\dot{\alpha}\bar{c}_w/2U)$, per rad
$C_{L_{\dot{\alpha}_t}}$	CLADT	$\partial C_{L_t}/\partial(\dot{\alpha}\bar{c}_w/2U)_t$, horizontal tail, per rad
C_{L_q}	CLQP	$\partial C_L/\partial(q\bar{c}_w/2U)$, per rad
$C_{L_{qt}}$	CLQT	$\partial C_{L_t}/\partial(q\bar{c}_w/2U)_t$, horizontal tail, per rad
$C_{L_{qw}}$	CLQW	$\partial C_{L_w}/\partial(q\bar{c}_w/2U)_w$, wing, per rad
C_{l_s}	CLS	Section lift coefficient
$C_{l_{\alpha_t}}$	CLATD	Section lift curve slope of the horizontal tail, per deg
$C_{l_{\alpha_w}}$	CLA2D	Section lift curve slope of the wing, per deg

C_m	--	Pitching moment coefficient, $\frac{\text{Pitching Moment}}{q S_w \bar{c}_w}$
$C_{m_{o_w}}$	CMOWS	Wing section pitching moment coefficient at zero lift
C_{m_q}	CMQP	Pitch rate damping, $\partial C_m / \partial (q \bar{c}_w / 2U)$, per rad
C_{m_α}	CMAP	Static stability derivative, $\partial C_m / \partial \alpha$, per rad
$C_{m_{\alpha f}}$	CMAF	Static stability derivative, $\partial C_{m_f} / \partial \alpha_f$, fuselage, per rad
$C_{m_{\alpha t}}$	CMAT	Static stability derivative, $\partial C_{m_t} / \partial \alpha_t$, horizontal tail per rad
$C_{m_{\alpha w}}$	CMAW	Static stability derivative, $\partial C_{m_w} / \partial \alpha_w$, wing, per rad
$C_{m_{\dot{\alpha}}}$	CMADP	Angle-of-attack damping derivative, $\partial C_m / \partial (\dot{\alpha} \bar{c}_w / 2U)$, per rad
C_n	--	Yawing moment coefficient, $\frac{\text{Yawing Moment}}{q S_w b_w}$
C_{n_r}	CNRP	Yawing damping derivative, $\partial C_n / \partial (r b_w / 2U)$, per rad
$C_{n_{r_t}}$	CNRT	Yawing damping derivative, $\partial C_{n_t} / \partial (r b_w / 2U)_t$, horizontal tail, per rad
$C_{n_{r_w}}$	CNRW	Yawing damping derivative, $\partial C_{n_w} / \partial (r b_w / 2U)$, wing, per rad
C_{n_β}	CNBP	Directional stability derivative, $\partial C_n / \partial \beta$, per rad
C_y	--	Side force coefficient, $\frac{\text{Side Force}}{q S_w}$
C_{y_r}	CYRP	$\partial C_y / \partial (r b_w / 2U)$, per rad
$C_{y_{r_v}}$	CYRVT	$\partial C_{y_v} / \partial (r b_w / 2U)_v$, vertical tail, per rad
$C_{y_{r_w}}$	CYRW	$\partial C_{y_w} / \partial (r b_w / 2U)_w$, wing, per rad
C_{y_β}	CYBP	Side force derivative, $\partial C_y / \partial \beta$, per rad
$C_{y_{\beta f}}$	CYBF	Side force derivative, $\partial C_{y_f} / \partial \beta_f$, fuselage, per rad
$C_{y_{\beta t}}$	CYBT	Side force derivative, $\partial C_{y_t} / \partial \beta_t$ horizontal tail, per rad
$C_{y_{\beta w}}$	CYBW	Side force derivative, $\partial C_{y_w} / \partial \beta_w$, wing, per rad
$\bar{c}_t$	CT	Horizontal tail mean aerodynamic chord, ft
$\bar{c}_v$	CV	Vertical tail mean aerodynamic chord, ft

$\bar{c}_w$	CW	Wing mean aerodynamic chord, ft
c_r	CWRT	Wing root chord, ft
c_t	CWTP	Wing tip chord, ft
c.g.	--	Airplane center of gravity
e	E	Oswald's span efficiency factor
e_1	E1	Induced angle span efficiency factor of the wing
e_2	E2	Induced angle span efficiency factor of the horizontal tail
f_{mg}	FCDMG	Main gear equivalent parasite area, ft^2
FH	FH	Fuselage height, ft
FW	FW	Fuselage width, ft
g	--	Acceleration due to gravity, 32.2 ft/sec^2
$H(\omega)$	--	Frequency response function
HBCY	HBCY	Fuselage height at back of canopy, ft
HFCY	HFCY	Fuselage height at front of canopy, ft
HNOSE	HNOSE	Fuselage height at nose, ft
I_{yy}	IYY	Mass moment of inertial about lateral axis, lb_m-ft^2
Izz	IZZ	Mass moment of inertia about vertical axis; lb_m-ft^2
i_w	IW	Incidence angle, deg
K	K	Emperical factor
K_f	KF	Emperical factor of fuselage or nacelle contributions to C_{m_α}
K_g	KG	Gust alleviation factor
K_i	KI	Wing fuselage interference factor
K_n	KN	Interference factor

K_α	--	Reduced frequency, $\bar{c}_w \omega / 2U$, longitudinal
K_β	--	Reduced frequency, $b_w \omega / 2U$, lateral
K_ϕ	--	Spectral gust alleviation factor
K_{o_α}	KOA	Undamped natural reduced frequency, $\bar{c}_w \omega_o / 2U$, longitudinal
K_{o_β}	KOB	Undamped natural reduced frequency, $b_w \omega_o / 2U$, lateral
L	LGUST	Scale of turbulence, ft
L_t	HTL	Horizontal balancing tail load, lb
L_v	DLVT	Vertical tail load, lb
LBCY	LBCY	Length from nose to back of canopy, ft
LFCY	LFCY	Length from nose to front of canopy, ft
LMH	LMH	Length from nose to maximum fuselage height, ft
l_b	LB	Length of fuselage or body, ft
l_t	LT	Length from c.g. to tail quarter chord, ft
l_t'	LTP	Length from wing quarter chord to tail quarter chord, ft
l_v	LV	Length from c.g. to vertical tail a.c. , ft
$N_o(\ )$	--	Average number of peaks per unit time which exceed a given level of response and average number of zero crossings per (cross/) unit time with positive slope (symbol in parenthesis refers to response quantity)
$N_o(Z_t)$	NOHT	Horizontal tail load zero crossings, cross/sec
$N_o(Y_{yv})$	NOVT	Vertical tail load zero crossings, cross/sec
$N_o(\Delta n)$	NODN	Normal load factor zero crossings, cross/sec
$N_o(\dot{\theta})$	NOTHD	Pitch angle rate zero crossings, cross/sec
$N_o(\ddot{\theta})$	NOTHDD	Pitch angle acceleration zero crossings, cross/sec
$N_o(\ddot{y}/g)$	NODL	Lateral load factor zero crossings cross/sec

$N_o(\psi)$	NOSI	Yaw angle zero crossings, cross/sec
$N_o(\dot{\psi})$	NOSID	Yaw angle rate zero crossings, cross/sec
n	N	Center of gravity normal load factor, g
q	Q	Dynamic pressure ($1/2\ \rho\ U^2$), lb/ft^2 or pitching velocity, $\dot{\theta}$, ft/sec
q_t	--	Dynamic pressure at the horizontal tail, lb/ft^2
q_v	--	Dynamic pressure at the vertical tail, lb/ft^2
R_j	RJ	Longitudinal response integrals (j = 0, 2, 4, 6)
R_{j_β}	RJB	Lateral response integrals (j = 0, 2, 4, 6)
R_n	--	Reynolds number
R_1	R1	Height of fuselage in area of the tail, ft
RNAC	RNAC	Nacelle radius, ft
RTTK	RTTK	Tiptank radius, ft
r	--	Yaw velocity, $\dot{\psi}$, ft/sec
r_x	RX	Radius of gyration about pitch axis, $\left[\frac{I_{yy}}{W_{to}}\right]^{1/2}$, ft
r_y	RY	Radius of gyration about yaw axis, $\left(\frac{I_{zz}}{W_{to}}\right)^{1/2}$, ft
$S_{\beta s}$	SBS	Body side area, ft^2
S_t	ST	Horizontal tail area, ft^2
S_v	SV	Vertical tail area, ft^2
S_w	SW	Wing area, ft^2
s_α	SAGUST	Relative gust scale, $2L/\bar{c}_w$, longitudinal
s_β	SBGUST	Relative gust scale, $2L/b_w$, lateral
U	U	Airplane speed, ft/sec
U_{de}	--	Derived gust velocity, ft/sec
v	--	Perturbation velocity along z-axis
v_g	--	Lateral component of turbulence velocities, ft/sec

WBCY	WBCY	Fuselage width at back of canopy, ft
WD	WD	Nose wheel width, ft
WFCY	WFCY	Fuselage width at front of canopy, ft
WH	WH	Nose wheel height, ft
w_t	WHT	Mass of the horizontal tail, lb_m
WNOSE	WNOSE	Fuselage width at nose, ft
W_{to}	WTO	Airplane mass, lb_m
w	--	Perturbation velocity along z-axis
w_g	--	Vertical component of true turbulence velocities ft/sec
x'	XP	Distance from c.g. to wing quarter chord (positive for c.g. ahead of quarter chord), ft
x_a	XA	Distance parallel to relative wind from the wing a.c. to the c.g. (positive for a.c. ahead of the c.g.), ft
$\ddot{y}$	--	Absolute lateral acceleration, ft/sec^2
z_a	ZAA	Vertical distance from wing a.c. to c.g. (positive for a.c. above c.g.), ft
z_{ww}	ZWW	Distance from body centerline to quarter chord point of exposed wing root chord (positive for the quarter chord point below the body centerline), ft
$\ddot{z}$	--	Absolute vertical acceleration, ft/sec^2
α	A	Angle-of-attack, $\approx w/U$, deg
$\dot{\alpha}$	--	Rate of change of angle-of-attack, deg/sec
β	--	Angle of sideslip, $\approx v/U$, deg
$\bar{\beta}$	BETA	Frequency ratio, ω/ω_0
Γ	L	Dihedral angle, deg

γ_α	GA	Dimensionless damping parameter for short period
γ_β	GB	Dimensionless damping parameter for dutch roll
ΔL_t	DLHT	Incremental horizontal tail load, lb
δ	D	Correction factor for induced drag
ϵ	--	Downwash angle, deg
$\delta\epsilon/\delta\alpha$	DEDA	Change in downwash angle due to change in angle-of-attack
ζ_α	ZA	Damping ratio for short period
ζ_β	ZB	Damping ratio for dutch roll
η_d	--	Multiplier denoting number of standard deviations
η_t	NT	Efficiency factor for tail, qt/q, or the propeller efficiency
θ	--	Angle-of-pitch, deg
$\dot{\theta}$	--	Rate-of-change of pitch angle, deg/sec
K_α	KA	Mass parameter, longitudinal
K_β	KB	Mass parameter, lateral
λ_w	TRW	Taper ratio of the wing
μ_g	UG	Airplane mass ratio
μ_{g_t}	UGT	Lateral mass ratio
ρ	RHO	Mass density of air, lb_m/ft^3
ρ_o	RHOO	Mass density of air at sea level, lb_m/ft^3
σ	--	Root mean square (subscript refers to rms quantity)
τ	T	Correction factor for induced angle
τ'	TT	Elevator effectiveness factor
$\Phi(\omega)$	--	Von Karman spectrum

$\phi(\omega)$	--	Unsteady lift function
$\Psi(\omega)$	--	Unsteady side force function
ψ	--	Angle-of-yaw, degrees
$\dot{\psi}$	--	Rate-of-change of yaw angle, deg/sec
ω	--	Circular frequency
$\omega_{o\alpha}$	WOA	Undamped natural circular frequency, longitudinal
$\omega_{o\beta}$	WOB	Undamped natural circular frequency, lateral

SUBSCRIPTS

f	Fuselage
t	Horizontal tail
v	Vertical tail
w	Wing
m	mass
n	yawing
s	side
y	side force

APPENDIX A

GENERAL AVIATION AIRCRAFT STABILITY DERIVATIVES

LIST OF ILLUSTRATIONS

Figure		Page
A-1	Variation of γ and δ With Taper Ratios at Aspect Ratio of 6.28	A-9
A-2	Variation of $1 + \gamma$ and $1 + \delta$ With Aspect Ratios at Taper Ratio of 1.0	A-9
A-3	Empirical Factor For Fuselage or Nacelle Contribution To $C_{m_{\dot{\alpha}}}$	A-10
A-4	Values for K as a Function of the Ratio of Vertical Tail Span to Fuselage Diameter in the Tail Region	A-10
A-5	Values of a_v as a Function of Vertical Tail Aspect Ratio	A-11
A-6	Values for Wing-Fuselage Interference Factor	A-11
A-7	Dimensions Required to Estimate Body Side Area and Fuselage Volume	A-12
A-8	Empirical Interference Factor, K_n, as a Function of Aircraft Geometry and Reynold's Number	A-13

LIST OF TABLES

Table		Page
A-1	Fuselage Drag Where S_c = Maximum Cross Sectional Area and l_b = Fuselage Length	A-5
A-2	Empennage Drag	A-5
A-3	Landing Gear Drag	A-6
A-4	Airplane Components	A-7
A-5	Attenuation Factors $\tilde{a}$	A-8

APPENDIX A

GENERAL AVIATION AIRCRAFT STABILITY DERIVATIVES

The following equations offer a simplistic estimation of the stability derivatives of general aviation aircraft. The applicable equations were extracted from NASA report titled, "Riding and Handling Qualities of Light Aircraft - A Review and Analysis" (reference 7 of this report).

The nondimensional stability derivatives contained in the rigid body equations of motion, which are pertinent to light plane performance, are outlined herein. Derivatives and related materials are included to facilitate usage of the computer program listed in appendix B. These equations are listed in the order as they appear in the program listing.

LONGITUDINAL DERIVATIVES.

Lift Curve Slope:

$$AR_w = b_w^2 / S_w \tag{A-1}$$

$$\bar{c}_t = S_t / b_t \tag{A-2}$$

$$\lambda_w = c_t / c_r \tag{A-3}$$

$$\bar{c}_w = \frac{2}{3} c_r \frac{1 + \lambda_w + \lambda_w^2}{1 + \lambda_w} \tag{A-4}$$

$e_1 = 1/1+\tau$ (Obtain τ from figure A-1 or A-2)

$$C_{L_\alpha} = C_{L_{\alpha_w}} = \frac{C_{l_{\alpha_w}}}{1 + (C_{l_{\alpha_w}} / (\pi e_1 AR_w))} \tag{A-5}$$

Change in lift coefficient due to time rate-of-change in angle-of-attack:

$$\frac{\delta \epsilon}{\delta \alpha} = 20\, C_{L_{\alpha_w}} \frac{(1/\lambda_w)^{.3}}{57.3 (AR_w)^{.725}} \left(\frac{3\, \bar{c}_w}{l_t'} \right)^{.25} \tag{A-6}$$

$e_2 = 1/(1+\tau')$ (Obtain τ' from figure A-1 or A-2)

$$C_{L_{\alpha_t}} = \frac{C_{l_{\alpha_t}}}{1 + (C_{l_{\alpha_t}} / (\pi e_2 AR_t))} \tag{A-7}$$

$$C_{L_{\dot{\alpha}}} = C_{L_{\dot{\alpha}_t}} = 2 C_{L_{\alpha_t}} \frac{\delta \epsilon}{\delta \alpha} \left(\frac{l_t'}{\bar{c}_w} \right) \left(\frac{S_t}{S_w} \right) \eta_t \tag{A-8}$$

Change in lift coefficient due to change in pitching velocity:

$$C_{L_{q_t}} = 2 \left(\frac{l_t}{\bar{c}_w} \right) C_{L_{\alpha_t}} \left(\frac{S_t}{S_w} \right) \eta_t \tag{A-9}$$

$$C_{Lq_w} = 2\left(\frac{x'}{\bar{c}_w}\right) C_{L_\alpha} \tag{A-10}$$

$$C_{Lq} = C_{Lq_w} + C_{Lq_t}$$

Change in pitching moment coefficient due to change in angle of attack:

$e = 1/(1+\delta)$ (Obtain δ from figure A-1 or A-2)

$$C_{L_w} = \frac{C_{l_s}}{1+(2/AR_w)} \tag{A-11}$$

$$C_{L_t} = C_{L_w}\left(\frac{x_a}{l_t}\right)\frac{S_w}{S_t}\left(\frac{1}{\eta_t}\right) \tag{A-12}$$

$$C_L = C_{L_w} + \left(C_{L_t}\frac{S_t}{S_w}\eta_t\right) \tag{A-13}$$

$$C_{D_{f_p}} = \left(C_{D_w}S_w + 1.2\,C_{D_f}A_f + f_{mg} + C_{D_{ng}}A_{ng} + C_{D_e}S_t + C_{D_{nac}}A_{nac} + C_{D_{ttk}}A_{ttk}\right)1.15/S_w \tag{A-14}$$

(Obtain C_{D_f}, C_{D_e}, f_{mg} & $C_{D_{ng}}, C_{D_{nac}}$ & $C_{D_{ttk}}$ from tables A-1, A-2, A-3, and A-4, respectively)

$$C_D = C_{D_{fp}} + \frac{C_{L_w}}{\pi e AR_w} \tag{A-15}$$

$$C_{m_{\alpha_w}} = \left[\left(1 + \frac{2C_L(\alpha - i_w)}{\pi e AR_w 57.3} + \frac{C_D}{C_{L_\alpha}}\right)\frac{x_a}{\bar{c}_w} + \left(\frac{2C_L}{\pi e AR_w} - \frac{(\alpha - i_w)}{57.3} - \frac{C_L}{C_{L_\alpha}}\right)\frac{z_a}{\bar{c}_w}\right]C_{L_\alpha} \tag{A-16}$$

$$C_{m_{\alpha_t}} = C_{L_{\alpha_t}}(1 - \delta\epsilon/\delta\alpha)\frac{S_t}{S_w}\left(\frac{l_t}{\bar{c}_w}\right)\eta_t \tag{A-17}$$

$$C_{m_{\alpha_f}} = K_f FW^2 l_b / S_w \bar{c}_w \quad \text{(Obtain } K_f \text{ from figure A-3)} \tag{A-18}$$

$$C_{m_\alpha} = C_{m_{\alpha_w}} - C_{m_{\alpha_t}} + C_{m_{\alpha_f}}$$

Change in pitching moment coefficient due to time rate-of-change in angle-of-attack:

$$C_{m_{\dot{\alpha}}} = -2C_{L_{\alpha_t}}\frac{\delta\epsilon}{\delta\alpha}\left(\frac{l_t}{\bar{c}_w}\right)\frac{l_t'}{\bar{c}_w}\left(\frac{S_t}{S_w}\right)\eta_t \tag{A-19}$$

Change in pitching moment coefficient due to change in pitching velocity:

$$C_{m_q} = -\frac{2x'|x'|}{\bar{c}_w^2}C_{L_\alpha} - 2\frac{l_t^2}{\bar{c}_w^2}C_{L_{\alpha_t}}\frac{S_t}{S_w}\eta_t \tag{A-20}$$

LATERAL DERIVATIVES

Change in side force due to change in sideslip angle:

$$\left(1+\frac{\delta\sigma}{\delta\beta}\right)\frac{q_v}{q} = .724 + 1.53\frac{S_v}{S_w} + .4\frac{z_{ww}}{FH} + .009\,AR_w \tag{A-21}$$

$$C_{Y_{\beta_t}} = -K C_{L_{\alpha_v}}\left(1+\frac{\delta\sigma}{\delta\beta}\right)\frac{q_v}{q}\frac{S_v}{S_w}$$ (Obtain K and $C_{L_{\alpha_v}}$ from figures A-4 and A-5, respectively) (A-22)

The fuselage volume is determined using four prismoids as an estimate. See figure A-8 for dimensions.

V1=LFCY[2(HNOSE(WNOSE) + HFCY(WFCY) + HFCY(WNOSE) + HNOSE(WFCY)] (A-23)

V2=(LMH - LFCY)[2(HFCY(WFCY) + FH(FW)) + FH(WFCY) + HFCY(FW)] (A-24)

V3=(LBCY - LMH)[2(HBCY(WBCY) + FH(FW)) + FH(WBCY) + FW(HBCY)] (A-25)

V4=(l_b - LBCY)[2(HBCY(WBCY + R_1^2) + HBCY(R_1) + WBCY(R_1)] (A-26)

FUSV=(V1 + V2 + V3 + V4)/6 (A-27)

BRA=(FUSV)$^{2/3}$ (A-28)

$$C_{Y_{\beta_f}} = -K_i C_{L_{\alpha_f}} BRA/S_w$$ (Obtain K_i from figure A-6) (A-29)

$$C_{Y_{\beta_w}} = -.0001|\Gamma|$$ (A-30)

$$C_{Y_\beta} = C_{Y_{\beta_w}} + C_{Y_{\beta_f}} + C_{Y_{\beta_t}}$$

Change in side force due to change in yawing velocity:

$$C_{Y_{r_v}} = -2\frac{l_v}{b_w}C_{Y_{\beta_t}} \tag{A-31}$$

$$C_{Y_{r_w}} = .143\,C_{L_w} - .05$$

$$C_{Y_r} = C_{Y_{r_w}} + C_{Y_{r_v}} \tag{A-32}$$

Change in yawing moment coefficient due to change in sideslip angle "weathercock:"

BODSA=[(HNOSE + HFCY)LFCY + (FH + HFCY)(LMH - LFCY)
+ (FH + HBCY)(LBCY - LMH) + (HBCY + R_1)(l_b - LBCY)]/2 (A-33)

$$C_{n_\beta} = -\frac{K_n\,BODSA\,l_b}{S_w b_w} - C_{Y_{\beta_t}}\frac{l_v}{b_w}$$ (Obtain K_n from figure A-7) (A-34)

Change in yawing moment coeffient due to change in yawing velocity "yaw damping derivative:"

$$C_{D_o} = C_{D_{f_p}}$$

$$C_{n_{r_w}} = -.33\left(\frac{1+3\lambda_w}{2+2\lambda_w}\right)C_{D_o} - .02\left[1-\frac{(AR_w-6)}{13}-\frac{(1-\lambda_w)}{2.5}\right]C_{L_w}^2 \qquad \text{(A-35)}$$

$$C_{n_{r_t}} = 2\left(\frac{l_v}{b_w}\right)^2 C_{y_{\beta_t}}$$

$$C_{n_r} = C_{n_{r_t}} + C_{n_{r_w}} \qquad \text{(A-36)}$$

TABLE A-1. FUSELAGE DRAG WHERE S_c = MAXIMUM CROSS SECTIONAL AREA AND l_b = FUSELAGE LENGTH

	Ref. Area	C_{D_f}
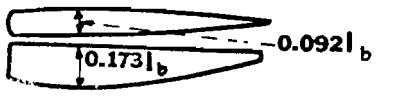	S_c	0.266
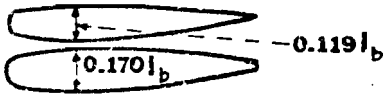	S_c	0.062
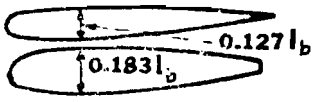	S_c	0.071
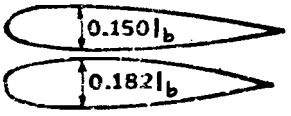	S_c	0.063
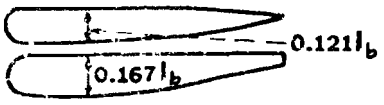	S_c	0.116

TABLE A-2. EMPENNAGE DRAG

Tail Arrangement	Description	Area	C_{D_e}
	Tapered fillets, vertical and horizontal tapered surfaces $i_t = 0^\circ$ $i_t = -4^\circ$	S_t	.0043 .0063
	Tapered fillets, tail surfaces with end plates $i_t = 0^\circ$ $i_t = -4^\circ$	S_t	.0058 .0063
	Symmetrical tapered fillets $i_t = 0^\circ$	S_t	.0059
	Vertical and horizontal tail surfaces $i_t = 0^\circ$ $i_t = -4^\circ$	S_t	.0070 .0058
	Tail surfaces with end plates $i_t = 0^\circ$	S_t	.0058
	Tapered fillets, horizontal tail surfaces $i_t = 0^\circ$ $i_t = -4^\circ$ $i_t = 4^\circ$	S_t	.0039 .0083 .0061

TABLE A-3. LANDING GEAR DRAG

Configuration	Remarks	$f_{mg} = C_{D_{mg}} A_{mg}$
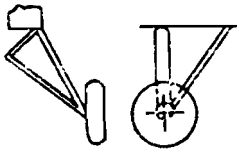	8.50-10 wheels, not faired . . . . . . 8.50-10 wheels, faired . . . . . . 8.50-10 wheels, no streamline members . .	1.67 1.50 3.83
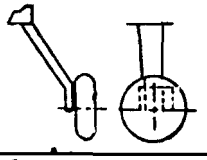	8.50-10 wheels, faired . . . . . . 27-in. streamlined wheels, not faired	0.74 0.98
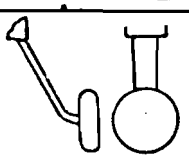	27-in. streamlined wheels, not faired . . 8.50-10 wheels, faired . . . . . . 21-in. streamlined wheels, not faired . .	0.84 0.68 0.53
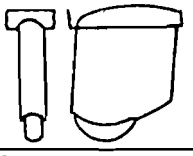	8.50-10 wheels	0.51
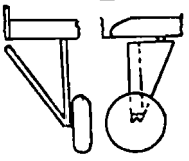	8.50-10 wheels, not faired . . . . . . 8.50-10 wheels, faired	1.52 1.02
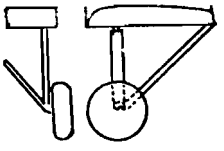	8.50-10 wheels, not faired	1.60
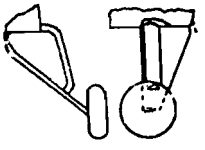	24-in. streamlined wheels, & intersections filleted . . . . . . 8.50-10 wheels, no fillets	0.86 1.13
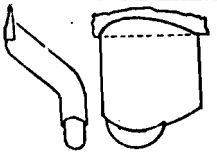	8.50-10 wheels	1.05
	Low pressure wheels, intersections filleted Low pressure wheels, no wheel fairing . . . Streamlined wheels, round strut, half fork no fairing	0.31 0.47 1.25
Nose Gear	For the nose gear $C_{D_{ng}} = .5 \rightarrow .8$ based on A_{ng} = (wheel diameter)(wheel width)	

TABLE A-4. AIRPLANE COMPONENTS

COMPONENTS	AREA FOR DRAG CALCULATION	C_{D_π}
Nacelles		
1. above wing, small airplane	Cross section area	.250
2. large leading edge nacelle, small airplane	Cross section area	.120
3. small leading edge nacelle, large airplane	Cross section area	.080
4. improved nacelle, no cooling flow	Cross section area	.050
5. improved nacelle, typical cooling air flow	Cross section area	.100
Wing Tanks		
1. centered on tip	Cross section area	.05-.07
2. below wing tip	Cross section area	.07-.10
3. inboard below wing	Cross section area	.15-.30
Wires and Struts		
1. smooth round wires and struts (per foot)	Frontal area	1.2-1.3
2. standard aircraft cable (per foot)	Frontal area	1.4-1.7
3. smooth elliptical wire (per foot)	Frontal area	
fineness ratio 2:1		0.6-0.4
fineness ratio 4:1		.35
fineness ratio 8:1		.3-.2
4. standard streamlined wire (per foot)	Frontal area	.45-.20
5. square wire (per foot)	Frontal area	.16-.20
6. streamlined struts (per foot)	Frontal area	.075-0.10

TABLE A-5. ATTENTUATION FACTORS ã

M \ Λ	0°	30°	35°	45°	AR
0.2	-0.96	----	-1.05	----	4.00
↓	-1.28	----	-1.55	----	6.00
↓	-1.40	----	-2.10	----	9.43
.4	-0.96	-1.00	-1.00	----	4.00
↓	-1.28	-1.35	-1.35	----	6.00
↓	-1.44	----	----	----	9.43
.9	-1.40	----	----	----	4.00
↓	-2.06	-2.06	-2.06	----	6.00
↓	-2.90	----	----	-2.1	9.43

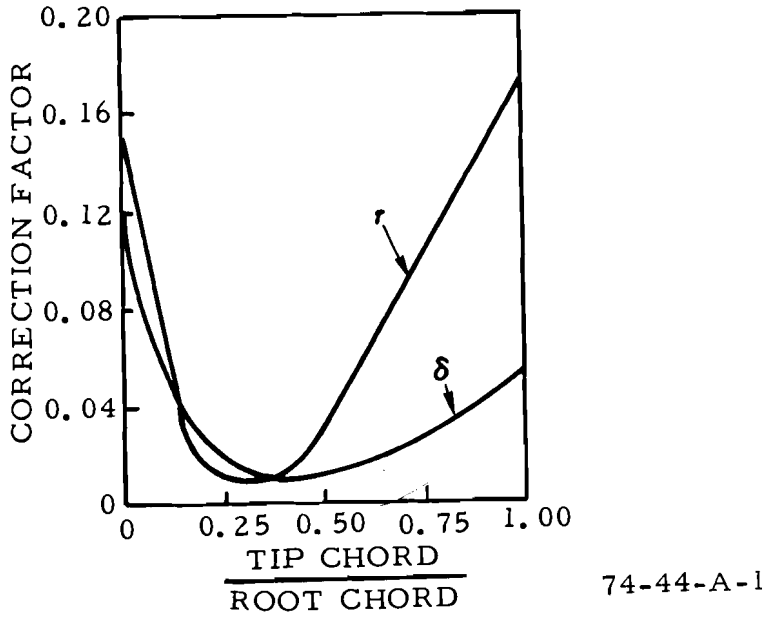

FIGURE A-1. VARIATION OF γ AND δ WITH TAPER RATIOS AT ASPECT RATIO OF 6.28

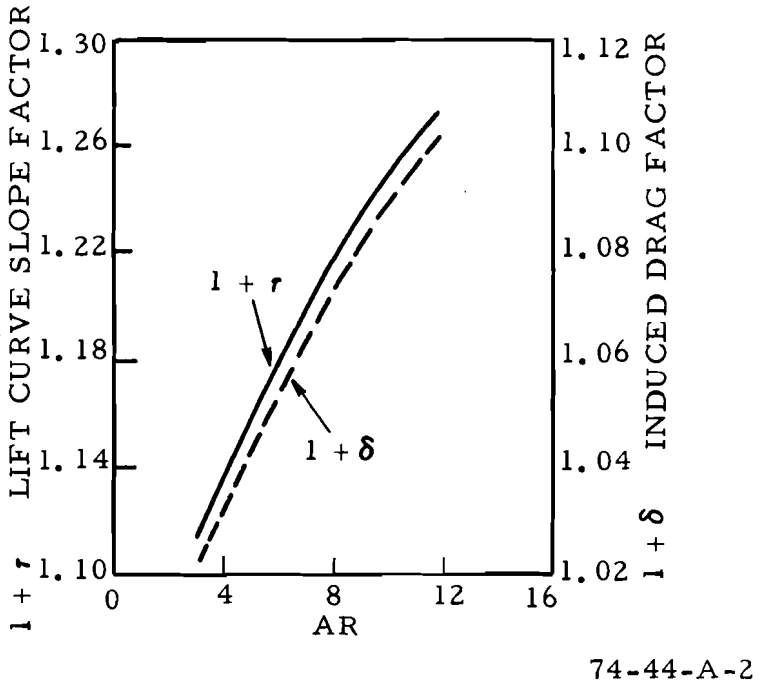

FIGURE A-2. VARIATION OF 1 + γ AND 1 + δ WITH ASPECT RATIOS AT TAPER RATIO OF 1.0

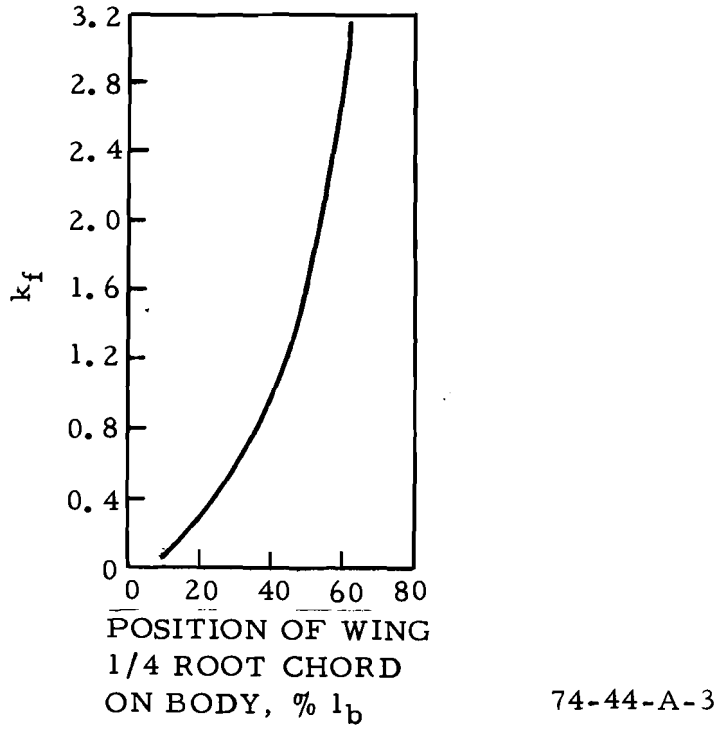

FIGURE A-3. EMPIRICAL FACTOR FOR FUSELAGE OR NACELLE CONTRIBUTION TO $C_{m_{\dot{\alpha}}}$

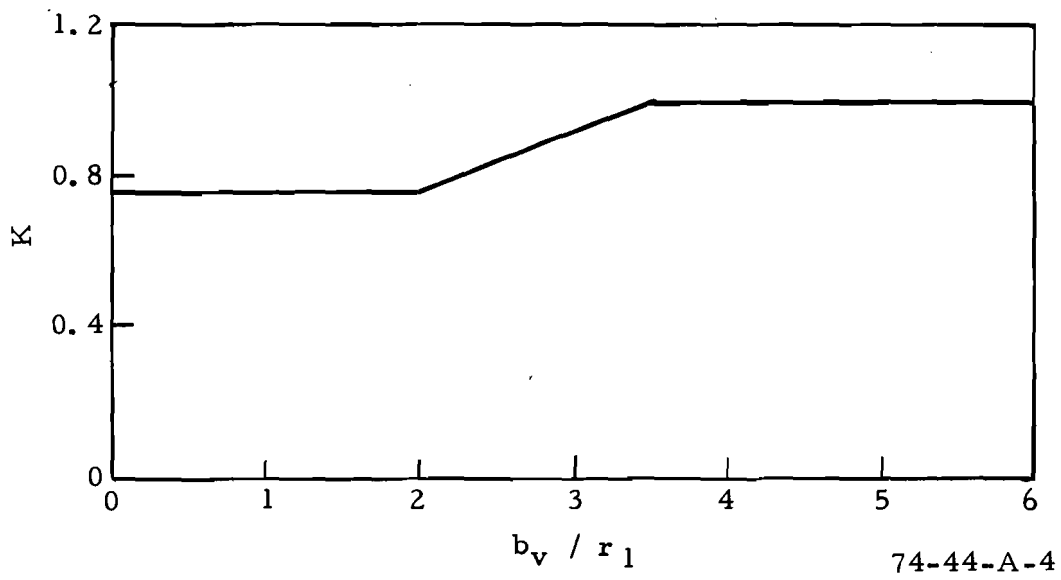

FIGURE A-4. VALUES FOR K AS A FUNCTION OF THE RATIO OF VERTICAL TAIL SPAN TO FUSELAGE DIAMETER IN THE TAIL REGION

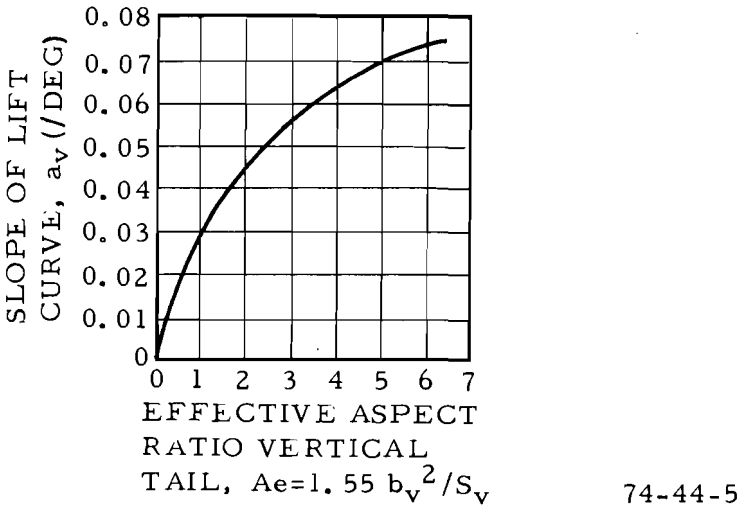

FIGURE A-5. VALUES OF a_v AS A FUNCTION OF VERTICAL TAIL ASPECT RATIO

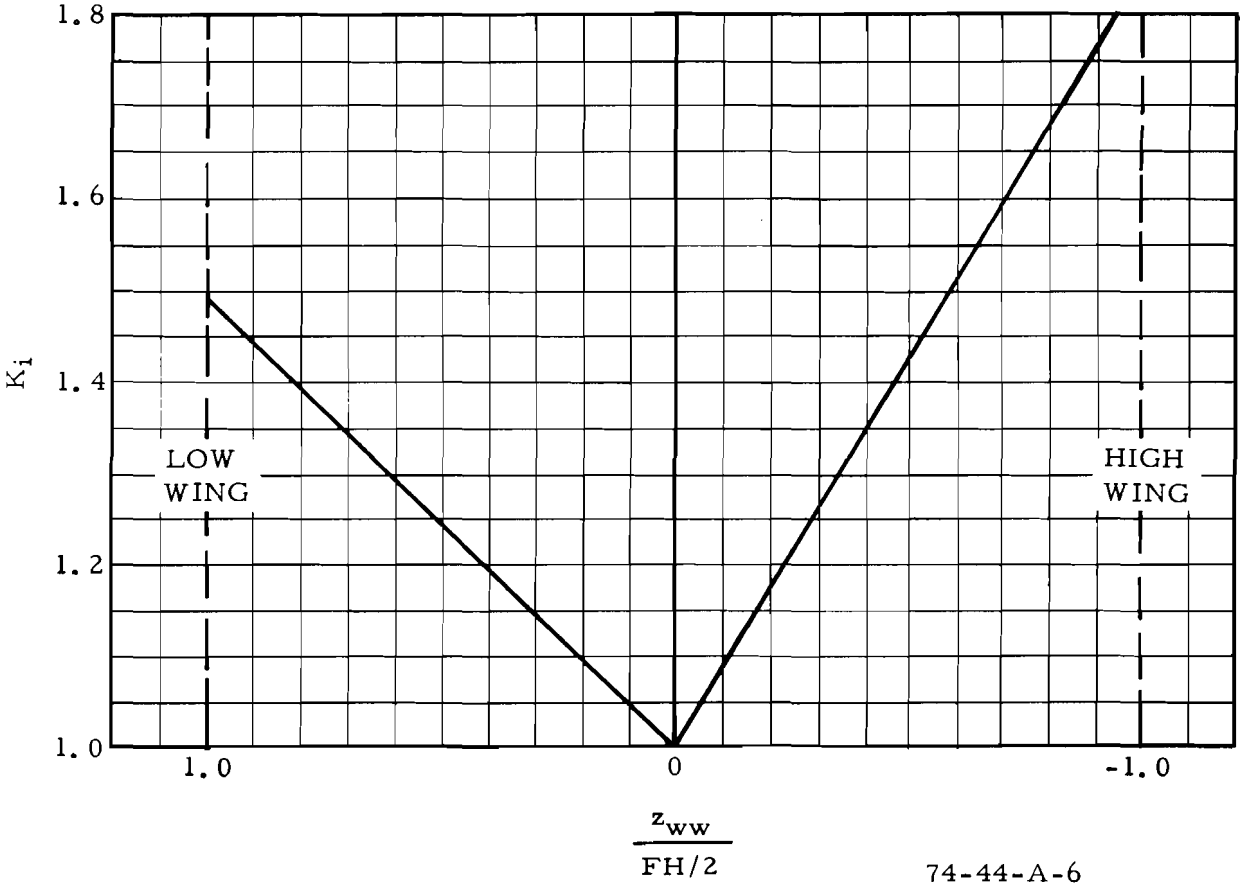

FIGURE A-6. VALUES FOR WING-FUSELAGE INTERFERENCE FACTOR

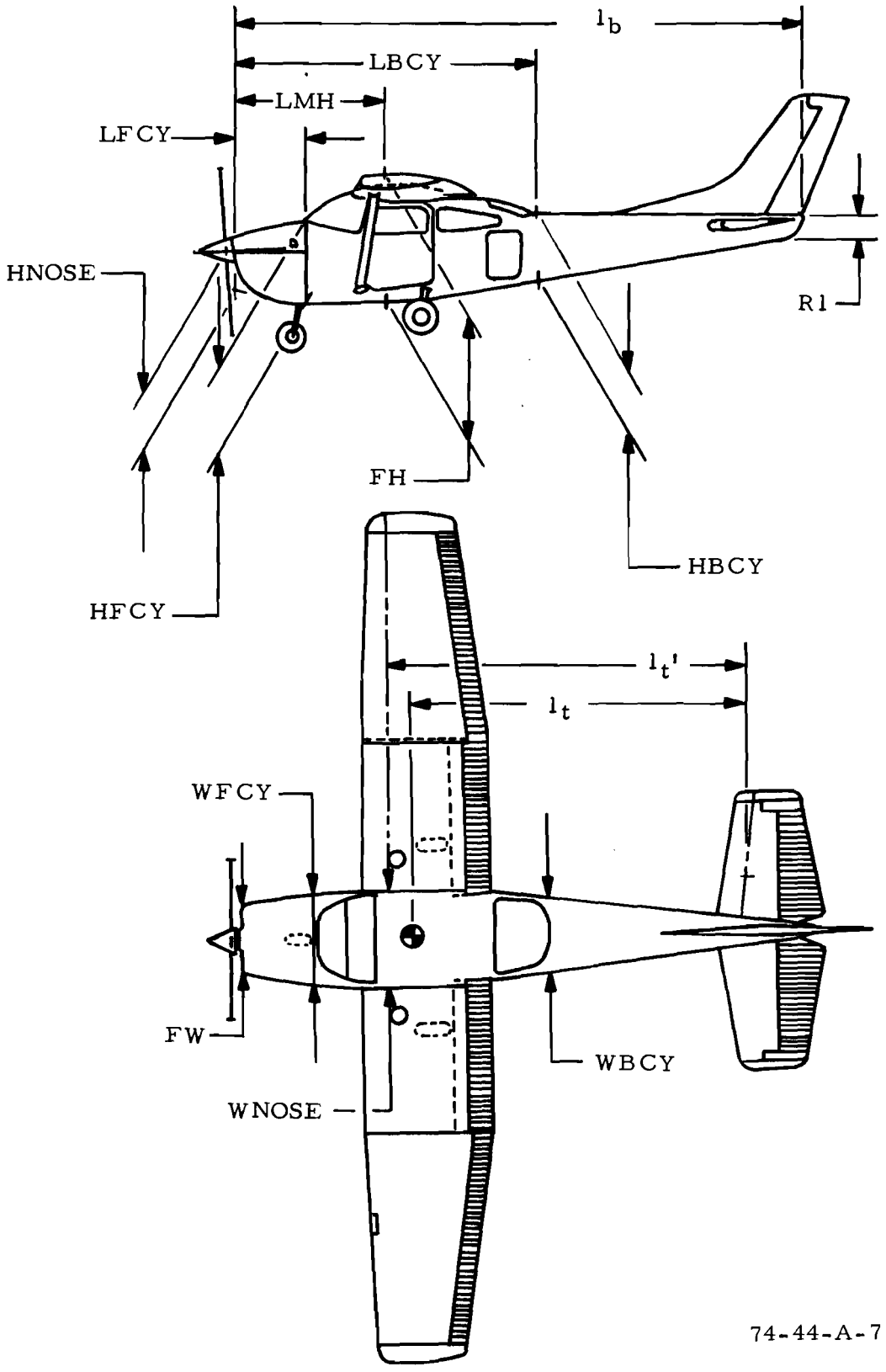

FIGURE A-7. DIMENSIONS REQUIRED TO ESTIMATE BODY SIDE AREA AND FUSELAGE VOLUME

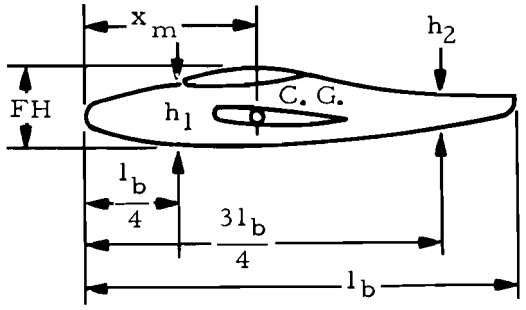

$$S_{b_s} = (HNOSE+HFCY)LFCY+(FH+HFCY)(LMH-LFCY)+(FH+HBCY)(LBCY-LMH)$$
$$+(HBCY+R1)(l_b-LBCY)/2$$

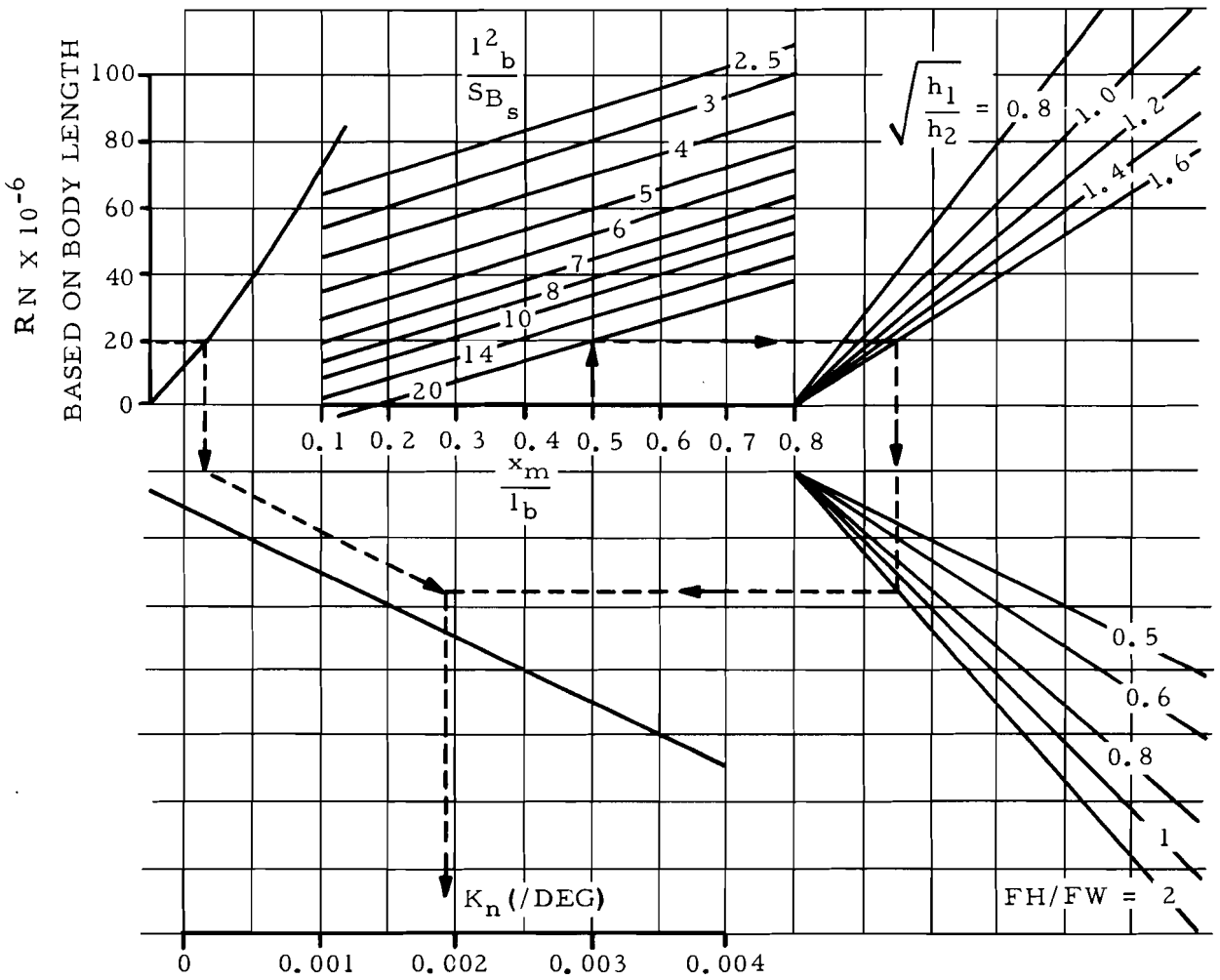

74-44-A-8

FIGURE A-8. EMPIRICAL INTERFERENCE FACTOR, K_n, AS A FUNCTION OF AIRCRAFT GEOMETRY AND REYNOLD'S NUMBER

APPENDIX B

COMPUTER PROGRAM USER'S GUIDE

APPENDIX B

COMPUTER PROGRAM USER'S GUIDE

PROGRAM ORGANIZATION.

This program is written in Control Data Corporation (CDC) time-sharing FORTRAN IV for the Control Data 6400 series computer. The use of FORTRAN language ensures reasonable compatibility with various other digital computer systems.

During development, the program was run on a CDC-6400 and CDC-6600 computer via CDC CYBERNET/KRONOS 2.1 time-sharing system. Any errors or complications encountered in using the program should be directed to Mr. John J. Petrakis. The program is structured such that input is in three basic blocks of data. The first block being general aircraft parameters which are used throughout the program. The second block provides for the direct input of known stability derivatives and also provides information for program branching to calculate derivatives which the user does not input. Stability derivatives are then computed, which could require additional inputs requiring a third block of data. These deviations make up the third block of data inputs. Power spectral density (PSD) responses and discrete gust loads are calculated and the results are put into a permanent file. The general flow of the program is illustrated in figure B-1.

Comment statements have been placed in the program to aid the user in program limitations and variable definitions.

INPUT VARIABLES.

The computer program is a conversational time-share program, that is to say that the user is prompted by computer-generated messages, questions, and instructions printed at the teletype station. The user, in turn, must make the proper response. Improper responses lead to erroneous results or possibly in aborting the program entirely. The inputs are all read into the computer through the teletype.

The unformatted "READ" statement is used to input data in the first two data blocks. This format can easily be modified to any other desired format.

The following input variables are listed in the order in which they are typed and read from the time-share teletype terminal:

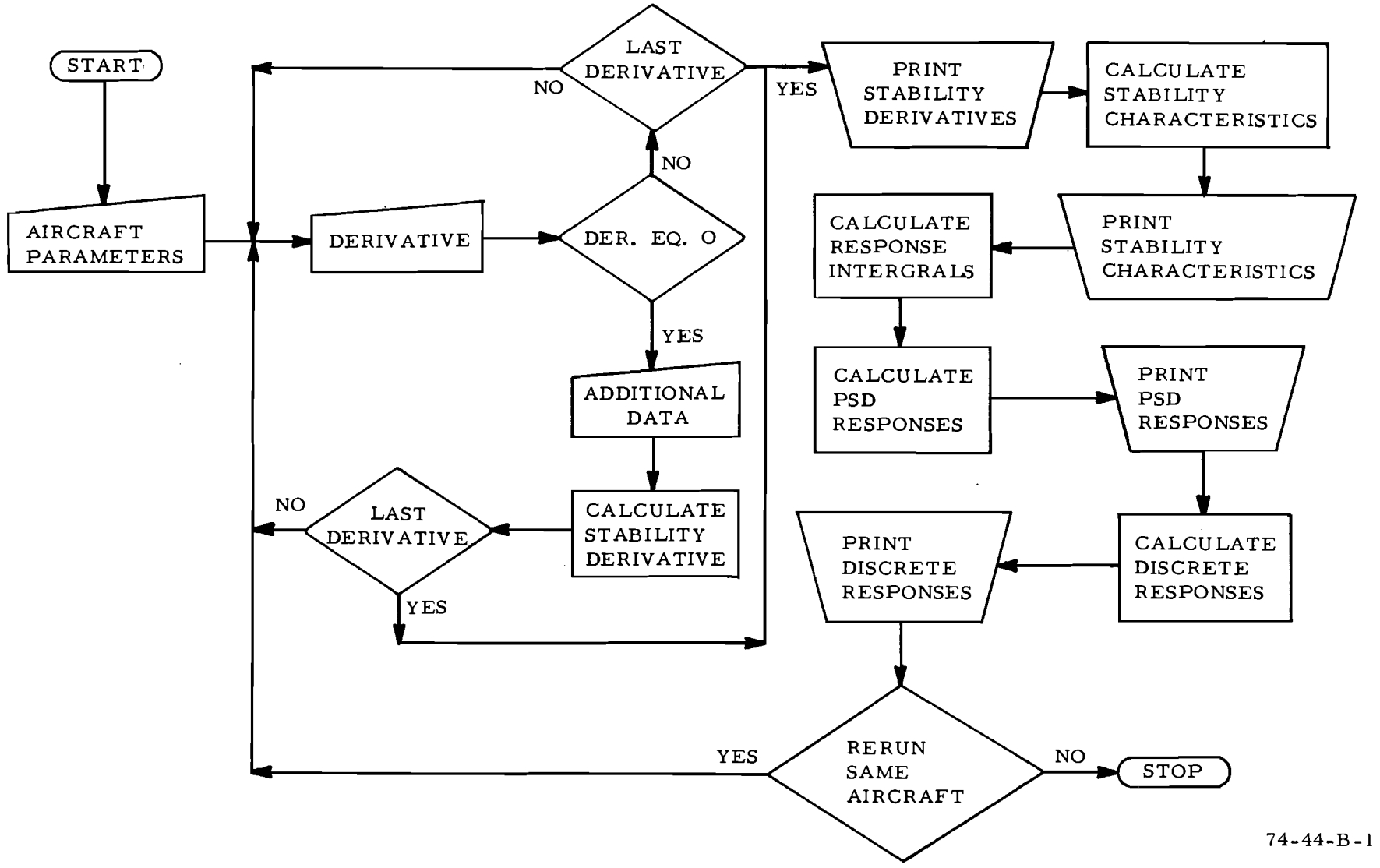

FIGURE B-1. PROGRAM FLOW CHART

MODEL	Airplane model.
S	Wing area, ft^2.
ST	Horizontal tail area, ft^2.
B	Wing span, ft.
BT	Horizontal tail span, ft.
W_{TO}	Airplane mass, lb_m.
CWTP	Wing tip chord, ft.
CWRT	Wing root chord, ft.
IYY	Mass moment of inertia about lateral axis.
IZZ	Mass moment of inertia about vertical axis.
XA	Distance parallel to relative wind from wing aerodynamic center (a.c.) to center of gravity (c.g.) (positive for a.c. ahead of the c.g.), ft.
ZAA	Vertical distance from wing a.c. to c.g. (positive a.c. above c.g.), ft.
LT	Length from c.g. to tail quarter chord, ft.
LB	Length of fuselage or body, ft.
LTP	Length from wing quarter chord to tail quarter chord, ft.
XP	Distance from c.g. to wing quarter chord (positive for c.g. ahead of quarter chord), ft.
ZWW	Distance from body centerline to quarter-chord point of exposed wing root chord (positive for quarter-chord point below the body centerline), ft.
SV	Vertical tail area, square ft.
BV	Vertical tail span, ft.
LV	Length from c.g. to vertical tail a.c., ft.
U	Airplane speed, fps.
WHT	Mass of the horizontal tail, lb_m.

ABA	Unsteady lift-force attenuation factor, longitudinal, use table A-5 in appendix A of this report.
ABB	Unsteady lift-force attenuation factor, lateral, use 0.8.
CMOWS	Wing section pitching moment coefficient at zero lift.
ALTC	Service ceiling, ft.
CLAP	Lift curve slope of plane, per rad, use zero to calculate or enter value.
CLAT	Lift curve slope of horizontal tail, per rad, use zero to calculate or enter value.
CLADT	$\partial C_{L_t}/\partial(\dot{\alpha}\bar{c}_w/2U)$ of horizontal tail, per rad, use zero to calculate or enter value.
CLADP	$\partial C_L/\partial(\dot{\alpha}\bar{c}_w/2U)$ of plane, per rad, use zero to calculate or enter value.
CLQT	$\partial C_{L_t}/(q\bar{c}_w/2U)$ of horizontal tail, per rad, use zero to calculate or enter value.
CLQP	$\partial C_L/(q\bar{c}_w/2U)$ of plane, per rad, use zero to calculate or enter value.
CMAP	Static stability of plane, per rad, use zero to calculate or enter value.
CMADP	Angle-of-attack damping derivative of plane, per rad, use zero to calculate or enter value.
CMQP	Pitch rate damping, per rad, use zero to calculate or enter value.
CYBT	Side-force derivative of horizontal tail, per rad, use zero to calculate or enter value.
CYBP	Side-force derivation of plane, per rad, use zero to calculate or enter value.
CYRVT	$\partial C_{Y_v}/\partial(rb_w/2U)$ of vertical tail, per rad, use zero to calculate or enter value.
CYRP	$\partial C_Y/\partial(rb_w/2U)$ of the plane, per rad, zero to calculate or enter value.

CNBP	Directional stability derivative of plane, per rad, use zero to calculate or enter value.
CNRP	Yaw damping derivative of plane, per rad, use zero to calculate or enter value.

The following input variable are formatted either F8.4 or F8.5. These variables are required if zero's are used in the second input data block. The variables are listed in the order they are most likely to appear if all derivatives are to be calculated.

T	Correction factor for induced angle, use figure A-1 or A-2 in appendix A of this report.
CLA2D	Section lift-curve slope of wing, per deg.
CLATD	Section lift-curve slope of horizontal tail, per deg.
TT	Elevator effectiveness factor, use figure A-1 or A-2.
NT	Efficiency factor for tail, use 0.85.
D	Correction factor for induced drag, use figure A-1 or A-2.
CLS	Section lift coefficient.
CDW	Wing drag coefficient.
CDF	Fuselage drag coefficient, see table A-1.
FH	Fuselage height, ft.
FW	Fuselage width, ft.
CDNG	Nose gear drag coefficient, see table A-3.
FCDMG	Main gear equivalent parasite area, ft^2, see table A-3.
WD	Nose wheel width, ft.
WH	Nose wheel height, ft.
CDE	Empennage drag coefficient, see table A-2.
CDNAC	Nacelle drag coefficient, see table A-4.
RNAC	Nacelle radius, ft.
CDTTK	Tip tank drag coefficient, see table A-4.

RTTK	Tip tank radius, ft.
IW	Wing incidence angle, deg.
KF	Emperical factor for fuselage nacelle contributions to Cm_{α}, see figure A-3.
K	Emperical factor, see figure A-4.
CLAV	Lift curve slope of vertical tail, per deg, use figure A-5.
L	Dihedral angle, deg.
KI	Wing-fuselage interference, see figure A-6.
CLAF	Lift curve slope of fuselage, per rad, use 0.1.
HNOSE	Fuselage height at nose, ft (see figure A-7).
HFCY	Fuselage height at front of canopy, ft (see figure A-7).
LFCY	Length from nose to front of canopy, ft (see figure A-7).
LMH	Length from nose to maximum fuselage height, ft (see figure A-7).
HBCY	Fuselage height at back of canopy, ft (see figure A-7).
LBCY	Length from nose to back of canopy, ft (see figure A-7).
WNOSE	Fuselage width at nose, ft (see figure A-7).
WFCY	Fuselage width at front of canopy, ft (see figure A-7).
WNCY	Fuselage width at back of canopy, ft (see figure A-7).
RI	Height of fuselage in area of the tail, ft (see figure A-7).
KN	Interference factor (see figure A-8).

SAMPLE INPUT.

The input for airplane III was accumulated from table E-3, figures A-1 through A-8, and tables A-1 through A-5. Stability derivatives from table 4 in the text portion of this report were used where required. Sample computer input data and responses for airplane III are shown in figure B-2. All of the formatted data is input in single entries from the teletype. The F8.5 or F8.4 format specification is overridden simply by placing a decimal point in its proper location. The critical thing to remember is not to exceed the field width of eight characters including decimal point when inputting data.

SAMPLE OUTPUT.

Most of the output variables are well documented in the following sample output. Additional definitions can be found in the glossary of terms. The example shown in figure B-3 is a partial output at sea level of airplane III using reference 7 estimated derivatives. The entire output includes results up to the service ceiling altitude of 25,000 feet at 5,000 foot intervals. Within each of these altitudes, results are given for two separate gust lengths of 750 and 2,500 feet, respectively.

A permanent file is created during the program run which contains all of the output data. This file labled power spectral density (PSD) is saved after every run and can be printed at the teletype terminal or at the high-speed printer, if available. The file PSD must be purged or the file name changed before another run is executed or the output data will not be recorded for the new run.

PROGRAM LISTING.

The complete FORTRAN program listing is presented in figure B-4.

```
    :0/02. 10.16.46.
AT ERN CLUSTER CTR/KRONOS 2.1.4.103.0-0 SYS B
USER NUMBER:  s7639cm,
TERMINAL:     61,TTY
RECOVER /SYSTEM:old,gust11
READY.

attl;0700

READY.

run,ma=77777

74/10/02. 10.17.47.
PROGRAM   GUSTII

RESPONSE OF RIGID LIGHTPLANES
TO CONTINUOUS TURBULENCE
J. PETRAKIS ARD 521
NUMBER OF AIRCRAFT RUNS ? 1.

INPUT THE FOLLOWING REQUIRED AIRCRAFT PARAMETERS

MODEL,S,ST,B,BT,WTO,CWTP,CWRT,IYY,
IZZ,ALT,XA,ZAA,LT,LB,LTP,XP,ZW,
SV,BV,LV,RHO,U,LGUST,WHT,ABA,ABB,CMOWS, ALTC

INPUT IN ORDER OUTLINED PLACING COMMAS OR BLANKS BETWEEN VARIABLES

? A/C-III   ,279.74,100.,45.88,22.38,10200.,3.5,8.635,719580.,
  1155097.,5000.,.8917,-.1925,21.186,43.66,22.013,-.827,.679,
  44.8[illegible],7.[illegible],17.625,.066,418.,2500.,197.,1.35,.8,-.005, 23000

THE REQUIRED STABILITY DERIVATIVES CAN BE CALCULATED OR
EXPERIMENTAL/WIND TUNNEL DERIVATIVES MAY BE INPUT DIRECTLY

WHEN A STABILITY DERIVATIVE IS REQUESTED, IF KNOWN, INPUT
QUANITY DIRECTLY, IF UNKNOWN, INPUT ZERO AND THE DERIVATIVE
WILL BE CALCULATED

ADDITIONAL DATA WILL BE REQUIRED IF THE STABILITY
DERIVATIVES ARE TO BE CALCULATED

INPUT THE FOLLOWING STABILITY DERIVATIVES

CLAP,CLAT,CLADT,CLADP,CLQT,CLQP,CMAP,CMADP,
CMQP,CYBT,CYBP,CYRVT,CYRP,CNBP,CNRP

? 5.2,0.,0.,2.7,0.,8.1,-1.719,-9.1,
? -34.0,0.,-.59,0.,.394,.082,-.194
    CLATD=? .074
    TT= ? .030
    NT= ? .85
    K=? ._1.0
    CLAV= ? .045
    FH= ? 5.91
RERUN SAME AIRCRAFT?? no                                    74-44-B-1
    STOP
```

FIGURE B-2. SAMPLE INPUT FOR AIRPLANE III

FIGURE B-3. SAMPLE OUTPUT FOR AIRPLANE III (2 Pages)

RESPONSE OF RIGID LIGHTPLANES
TO CONTINUOUS TURBULENCE
J. PETRAKIS ARO S21
AC-III

U=418.0000 FPS WTO=10200.00 LBS W/S= 36.4624 LBS/SQFT CW= 6.4297 FT TRW= .4053 ARW= 7.5248 ALT= 0. FT
S=279.7400 SQFT B= 45.8800 FT ST=100.0000 SQFT BT= 22.3800 FT SV= 44.8600 SQFT BV= 7.6000 FT LGUST= 750.00 FT

STABILITY DERIVATIVES ARE CALCULATED FROM NASA CR-1975
RIDING AND HANDLING QUALITIES OF LIGHT AIRCRAFT-A REVIEW AND ANALYSIS)

LONGITUDINAL

LIFT CURVE SLOPE
CLAP= 4.7438 /RAD

CHANGE IN LIFT COEFFICIENT DUE TO TIME RATE OF CHANGE IN ANGLE OF ATTACK
CLADP= 3.3578 /RAD

CHANGE IN LIFT COEFFICIENT DUE TO CHANGE IN PITCHING VELOCITY
CLQP= 5.4252 /RAD

CHANGE IN PITCHING MOMENT COEFFICIENT DUE TO CHANGE IN ANGLE OF ATTACK
CMAP= -.3862 /RAD

CHANGE IN PITCHING MOMENT COEFFICIENT DUE TO TIME RATE OF CHANGE IN ANGLE OF ATTACK
CMADP=-11.0640 /RAD

CHANGE IN PITCHING MOMENT COEFFICIENT DUE TO CHANGE IN PITCHING VELOCITY
CMQP= -21.7403 /RAD

LATERAL

CHANGE IN SIDE FORCE DUE TO CHANGE IN SIDESLIP ANGLE
CYBP= -.52327 /RAD

CHANGE IN SIDE FORCE DUE TO CHANGE IN YAWING VELOCITY
CYRP= .36525 /RAD

CHANGE IN YAWING MOMENT COEFFICIENT DUE TO CHANGE IN SIDESLIP ANGLE, WEATHERCOCK)
CNBP= .05903 /RAD

CHANGE IN YAWING MOMENT COEFFICIENT DUE TO CHANGE IN YAWING VELOCITY, YAW DAMPING DERIVATIVE)
CNRP= -.13932 /RAD

STABILITY CHARACTERISTICS

MASS PARAMETERS
KA= 124.852 KB= 158.619

UNDAMPED NATURAL FREQUENCY
KOA= .0270 KOB= .1167

DAMPING RATIO (SHORT PERIOD DUTCH ROLL)
ZA= .8991 ZB= .1878

DAMPING PARAMETER (SHORT PERIOD DUTCH ROLL)
GA= 3.0262 GB= 3.4745

GUST SCALE
SAGUST= 233.294 SBGUST= 32.694

RESPONSE INTEGRAL PARAMETERS
SKOA= 6.2891 SKOB= 3.8144
AKOA= .0364 AKOB= .0933

RESPONSE INTEGRALS

LONGITUDINAL
R0= .6839 R2= .0871 R4= .1449 R6= 3.9101

LATERAL
R0B= 1.3541 R2B= .6880 R4B= .7856 R6B= 4.1342

AIRPLANE RESPONSES ARE CALCULATED FROM NASA TN D-6273
=A METHOD FOR ESTIMATING SOME LONGITUDINAL AND LATERAL RIGID BODY RESPONSES OF AIRPLANES TO CONTINUOUS GUST TURBULENCE=

LONGITUDINAL

NORMAL-LOAD FACTOR RESPONSE
ADN= .0337 G/FT/SEC NODN= 2.1744 CRS/SEC

PITCH-ANGLE RATE RESPONSE
ATHD= .0007 RAD/SEC/FT/SEC NOTHD= .7194 CRS/SEC

PITCH-ANGLE ACCELERATION RESPONSE
ATDD= .0032 RAD/SEC2/FT/SEC NOTDD= 2.8980 CRS/SEC

HORIZONTAL TAIL LOAD
AZHT= 72.9726 LBS/FT/SEC NOHT= 2.2238 CRS/SEC

LATERAL

LATERAL-LOAD FACTOR RESPONSE
ADL= .0065 G/FT/SEC NODL= .7380 CRS/SEC

YAW ANGLE RESPONSE
ASI= .0027 RAD/FT/SEC NOSI= .2412 CRS/SEC

YAW-ANGLE RATE RESPONSE
ASID= .0041 RAD/SEC/FT/SEC NOSID= .3616 CRS/SEC

VERTICAL TAIL LOAD
AZVT= 55.9884 LBS/FT/SEC NOVT= .7677 CRS/SEC

AIRPLANE RESPONSES TO DICRETE GUST LOADS ARE DERIVED
FROM PROCEDURES OUTLINED IN FAR PART 23 AIRWORTHINESS STANDARDS NORMAL, UTILITY, AND ACROBATIC CATEGORY AIRPLANES

DISCRETE GUST LOAD FACTOR
N= 3.4321

DELTA LOAD ON HORIZONTAL TAIL DUE TO DISCRETE GUST
DLHT=3187.157 LBS

DELTA LOAD ON VERTICAL TAIL DUE TO DISCRETE GUST
DLVT=2438.681 LBS

HORIZONTAL TAIL LOAD(BALANCED FLIGHT)
HTL= 496.625 LBS

TOTAL HORIZONTAL TAIL LOAD
LHT=3683.782 LBS

TOTAL VERTICAL TAIL LOAD
LVT=2438.681 LBS

RMS GUST INTENSITY (ADN=N)
SIGWG= 72.202 FT/SEC

RATIO OF ADN/N (SIGWG=62 FT/SEC)
ADN/N= .900

74-44-3-A

AC-III

U=418.0000 FPS WTO=10200.00 LBS W/S= 36.4624 LBS/SQFT CW= 6.4297 FT TRW= .4053 ARW= 7.5248 ALT= 0. FT
S=279.7400 SQFT B= 45.8800 FT ST=100.0000 SQFT BT= 22.3800 FT SV= 44.8600 SQFT BV= 7.6000 FT LGUST= 2500.00 FT

GUST SCALE
SAGUST= 777.647 SBGUST= 108.980

RESPONSE INTEGRAL PARAMETERS
SKOA= 20.9635 SKOB= 12.7147
AKOA= .0364 AKOB= .0933

RESPONSE INTEGRALS

LONGITUDINAL
R0= .8501 R2= .0440 R4= .0657 R6= 1.7535

LATERAL
R0B= 1.1905 R2B= .3370 R4B= .3678 R6B= 1.8706

AIRPLANE RESPONSES ARE CALCULATED FROM NASA TN D-6273
=A METHOD FOR ESTIMATING SOME LONGITUDINAL AND LATERAL RIGID BODY RESPONSES OF AIRPLANES TO CONTINUOUS GUST TURBULENCE=

LONGITUDINAL

NORMAL-LOAD FACTOR RESPONSE
AON= .0233 G/FT/SEC NOON= 2.1085 CRS/SEC

PITCH-ANGLE RATE RESPONSE
ATHO= .0005 RAD/SEC/FT/SEC NOTHO= .6817 CRS/SEC

PITCH-ANGLE ACCELERATION RESPONSE
ATDD= .0021 RAD/SEC2/FT/SEC NOTDD= 2.8829 CRS/SEC

HORIZONTAL TAIL LOAD
AZHT= 50.3323 LBS/FT/SEC NOHT= 2.1596 CRS/SEC

LATERAL

LATERAL-LOAD FACTOR RESPONSE
ADL= .0045 G/FT/SEC NODL= .7444 CRS/SEC

YAW ANGLE RESPONSE
ASI= .0025 RAD/FT/SEC NOSI= .1800 CRS/SEC

YAW-ANGLE RATE RESPONSE
ASID= .0029 RAD/SEC/FT/SEC NOSID= .3535 CRS/SEC

VERTICAL TAIL LOAD
AYVT= 30.3312 LBS/FT/SEC NOVT= .7544 CRS/SEC

RMS GUST INTENSITY (ADN=N)
SIGWG= 104.523 FT/SEC

RATIO OF ADN/N (SIGWG=62 FT/SEC)
ADN/N= .712

AC-III

U=418.0000 FPS WTO=10200.00 LBS W/S= 36.4624 LBS/SQFT CW= 6.4297 FT TRW= .4053 ARW= 7.5248 ALT= 5000.00 FT
S=279.7400 SQFT B= 45.8800 FT ST=100.0000 SQFT BT= 22.3800 FT SV= 44.8600 SQFT BV= 7.6000 FT LGUST= 750.00 FT

STABILITY CHARACTERISTICS

MASS PARAMETERS
KA= 144.904 KB= 184.094

UNDAMPED NATURAL FREQUENCY
KOA= .0242 KOB= .1081

DAMPING RATIO (SHORT PERIOD OUTCH ROLL)
ZA= .8634 ZB= .1746

DAMPING PARAMETER (SHORT PERIOD OUTCH ROLL)
GA= 3.0262 GB= 3.4745

GUST SCALE
SAGUST= 233.294 SBGUST= 32.694

RESPONSE INTEGRAL PARAMETERS
SKOA= 5.6429 SKOB= 3.5336
AKOA= .0327 AKOB= .0865

RESPONSE INTEGRALS

LONGITUDINAL
R0= .6761 R2= .0971 R4= .1637 R6= 4.4067

LATERAL
R0B= 1.4335 R2B= .7796 R4B= .8910 R6B= 4.6481

AIRPLANE RESPONSES ARE CALCULATED FROM NASA TN D-6273
A METHOD FOR ESTIMATING SOME LONGITUDINAL AND LATERAL RIGID BODY RESPONSES OF AIRPLANES TO CONTINUOUS GUST TURBULENCE=

LONGITUDINAL

NORMAL-LOAD FACTOR RESPONSE
ADN= .0302 G/FT/SEC NODN= 1.9872 CRS/SEC

PITCH-ANGLE RATE RESPONSE
ATHO= .0008 RAD/SEC/FT/SEC NOTHO= .6499 CRS/SEC

PITCH-ANGLE ACCELERATION RESPONSE
ATDD= .0033 RAD/SEC2/FT/SEC NOTDD= 2.5972 CRS/SEC

HORIZONTAL TAIL LOAD
AZHT= 65.7309 LBS/FT/SEC NOHT= 2.0349 CRS/SEC

LATERAL

LATERAL-LOAD FACTOR RESPONSE
ADL= .0060 G/FT/SEC NODL= .7014 CRS/SEC

YAW ANGLE RESPONSE
ASI= .0028 RAD/FT/SEC NOSI= .2311 CRS/SEC

YAW-ANGLE RATE RESPONSE
ASID= .0041 RAD/SEC/FT/SEC NOSID= .3351 CRS/SEC

VERTICAL TAIL LOAD
AYVT= 51.2762 LBS/FT/SEC NOVT= .7092 CRS/SEC

AIRPLANE RESPONSES TO DICRETE GUST LOADS ARE DERIVED
FROM PROCEDURES OUTLINED IN FAR PART 23 AIRWORTHINESS STANDARDS NORMAL, UTILITY, AND ACROBATIC CATEGORY AIRPLANES

DISCRETE GUST LOAD FACTOR
N= 3.3039

DELTA LOAD ON HORIZONTAL TAIL DUE TO DISCRETE GUST
DLHT=3019.071 LBS

DELTA LOAD ON VERTICAL TAIL DUE TO DISCRETE GUST
DLVT=2274.979 LBS

HORIZONTAL TAIL LOAD(BALANCED FLIGHT)
HTL= 484.910 LBS

TOTAL HORIZONTAL TAIL LOAD
LHT=3503.981 LBS

TOTAL VERTICAL TAIL LOAD
LVT=2274.979 LBS

RMS GUST INTENSITY (ADN=N)
SIGWG= 76.308 FT/SEC

RATIO OF ADN/N (SIGWG=62 FT/SEC)
ADN/N= .869

74-44-3-B

FIGURE B-4. FORTRAN PROGRAM LISTING (16 Pages)

```
      PROGRAM GUSTV(INPUT,OUTPUT,TAPE7)
      EXTERNAL FUNC,FUNCB
      DIMENSION XINTS(4),TMPI(4),TXI1(4),TXI2(4),XINTSB(4),TMPIB(4)
     +,TXI1B(4),TXI2B(4)
      COMMON ABA,SAGUST,KOA,ZA,ABB,SBGUST,KOB,ZB
      REWIND 7
C
C     PROJECT NO. 184-520-04 POWER SPECTRAL DENSITY TECHNIQUE APPLIED TO
C     SMALL RIGID GENERAL AVIATION AIRCRAFT UTILIZING PROCEDURES OUTLINED
C     IN NASA TN D-6273 )A METHOD FOR ESTIMATING SOME LONGITUDINAL AND
C     LATERAL RIGID-BODY RESPONSES OF AIRPLANES TO CONTINUOUS ATMOSPHERIC
C     TURBULENCE).
C
      REAL IW,IXX,IYY,IZZ,MOM
      REAL NT,KF,LT,LTP,IVT,LGUST,LVT
      REAL L,KI,K,LB,LMH,LFCY,LBCY,LV,KN
      REAL N,M,MW,MQ,NV,NR,KA,KB,KOA,KOB,KG,KGT
      REAL LHT,NODN,NOTHD,NOTDD,NODL,NOSI,NOSID,NOHT,NOVT
C
      PRINT 1
    1 FORMAT(*RESPONSE OF RIGID LIGHTPLANES*/
     +*TO CONTINUOUS TURBULENCE*/*J. PETRAKIS ARD 521*)
      WRITE(7,2)
    2 FORMAT(*RESPONSE OF RIGID LIGHTPLANES*/
     +*TO CONTINUOUS TURBULENCE*/*J. PETRAKIS ARD 521*/)
      PRINT 5
    5 FORMAT(*NUMBER OF AIRCRAFT RUNS*,+ )
      READ 50,AC
C
C                          DEFINITIONS OF INPUT PARAMETERS
C
C     S=      WING AREA (SQ FT)                 ST=     HORIZONTAL TAIL AREA (SQ FT)
C     B=      WING SPAN (FT)                    BT=     HORIZONTAL TAIL SPAN (FT)
C     WTO=    AIRPLANE TAKE-OFF WT (LBS)        WLD=    LANDING WEIGHT (LBS)
C     CWTP=   WING CHORD TIP (FT)               CWRT=   WING CHORD ROOT (FT)
C     IYY=    MASS MOMENT OF INERTIA ABOUT      IZZ=    MASS MOMENT OF INERTIA ABOUT
C             PITCH AXIS (LBS- SQ FT)                   YAW AXIS (LBS-SQ FT)
C     XA=     WING AC TO CG (FT)                ZAA=    WING AC TO CG (FT)
C             (POS-AC AHEAD CG)                         (POS-AC ABOVE CG)
C     ALT=    ALTITUDE (FT)                     LT=     CG TO TAIL 1/4 CHORD (FT)
C     LB=     FUSELAGE LENGTH (FT)              LTP=    WING 1/4 CHORD TO TAIL
C     XP=     CG TO WING 1/4 CHORD (FT)                 1/4 CHORD (FT)
C             (POS-CG AHEAD 1/4)                LV=     CG TO VERTICAL TAIL AC (FT)
C     ZWW=    BODY CL TO 1/4 CHORD EXPOSED      SV=     VERTICAL TAIL AREA (SQ FT)
C             W CHORD (FT)(POS-1/4 BELOW CL)    BV=     VERTICAL TAIL SPAN (FT)
C     RHO=    DENSITY ALTITUDE (LBS/CU FT)      U=      AIRSPEED (FT/SEC)
C     LGUST=GUST LENGTH                         WHT=    HORIZONTAL TAIL WEIGHT (LBS)
C     ABA=    UNSTEADY LIFT FORCE               ABB=    UNSTEADY LIFT FORCE
C             ATTENTUATION FACTOR (LONG.)               ATTENTUATION FACTOR (LAT.)
C     CMONS=  WING SECT PITCHING MOMENT         ALTC=   SERVICE CEILING (FT)
C             COEFFICIENT AT ZERO LIFT
C
C     T=      WING EFFICIENCY FACTOR            CLA2D=  W 2D LIFT CURVE SLOPE (/DEG)
C     CLATD=  TAIL 2D LIFT CURVE SLOPE (/DEG)   TT=     ELEVATOR EFFECTIVENESS FACTO
C
C     NT=     TAIL EFFICIENCY FACTOR            CLAV=   VVERTICAL TAIL LIFT CURVE
C                                                       SLOPE (/DEG)
```

```
00580C
00590C      IW=     WING INCIDENCE (DEG)              CLS=    WING SECT LIFT COEFFICIENT
00600C      D=      CORRECTION FACTOR INDUCED DRAG    CDW=    WING DRAG COEFFICIENT
00610C      CDF=    FUSELAGE DRAG COEFFICIENT         FH=     FUSELAGE HEIGHT (FT)
00620C      FW=     FUSELAGE WIDTH (FT)               CDNG=   NOSE GEAR DRAG COEFFICIENT
00630C      FCDMG=  MAIN GEAR EQUIVALENT              WD=     NOSE WHEEL DEPTH (FT)
00640C              PARASITE AREA (SQ FT)             WH=     NOSE WHEEL HEIGHT (FT)
00650C      CDE=    EMPENNAGE DRAG COEFFICIENT        RNAC=   NACELLE RADIUS (FT)
00660C      KF=     EMPERICAL FACTOR FUSELAGE OR      CDTTK=  TIP TANK DRAG COEFFICIENT
00670C              NAC CONTRIBUTIONS TO CMAD         RTTK=   TTIP TANK RADIUS (FT)
00680C                                                CDNAC=  NACELLE DRAG COEFFICIENT
00690C
00700C      L=      DEHEDRAL ANGLE (DEG)              KI=     WING-FUSE INTERFERENCE FACTO
00710C      CLAF=   FUSELAGE LIFT CURVE               K=      EMPERICAL FACTOR
00720C              SLOPE (/RAD)                      HNOSE=  FUSE HEIGHT NOSE SECT (FT)
00730C      WNOSE=  FUSELAGE WIDTH NOSE               HFCY=   FUSELAGE HEIGHT FRONT
00740C              SECTION (FT)                              CANOPY (FT)
00750C      WFCY=   FUSELAGE WIDTH FRONT              LFCY=   LENGTH NOSE TO FRONT
00760C              CANOPY (FT)                               CANOPY (FT)
00770C      LMH=    LENGTH NOSE TO MAXIMUM            HBCY=   FUSELAGE HEIGHT BACK
00780C              FUSELAGE HEIGHT (FT)                      CANOPY (FT)
00790C      WBCY=   FUSELAGE WIDTH BACK               LBCY=   LENGTH NOSE TO BACK
00800C              CANOPY (FT)                               CANOPY (FT)
00810C      KN=     INTERFERENCE FACTOR (/DEG)        R1=     DIA OF EMPENNAGE (FT)
00820C
00830C      AIRCRAFT PARAMETERS
00840C
00850    10 PRINT 15
00860    15 FORMAT(/*INPUT THE FOLLOWING REQUIRED AIRCRAFT PARAMETERS*//*MODEL,*
00870+      *S,ST,B,BT,WTO,CWTP,CWRT,IYY,*/*IZZ,XA,ZAA,LT,LB,LTP,XP,ZWW,*/
00880+      *SV,BV,LV,U,WHT,ABA,ABB,CMOWS,ALTC*//*INPUT IN ORDER OUTLINED*
00890+      * PLACING COMMAS OR BLANKS BETWEEN VARIABLES*/)
00900       READ,MODEL,S,ST,B,BT,WTO,CWTP,CWRT,IYY
00910       READ,IZZ,XA,ZAA,LT,LB,LTP,XP,ZWW
00920       READ,SV,BV,LV,U,WHT,ABA,ABB,CMOWS,ALTC
00930    30 FORMAT(F8.4,↑ )
00940    50 FORMAT(F8.4)
00950   110 FORMAT(F8.5,↑ )
00960       RHOO=.0766
00970       PRINT 20
00980    20 FORMAT(/*THE REQUIRED STABILITY DERIVATIVES CAN BE CALCULATED OR*/
00990+      *EXPERIMENTAL/WIND TUNNEL DERIVATIVES MAY BE INPUT DIRECTLY*//
01000+      *WHEN A STABILITY DERIVATIVE IS REQUESTED, IF KNOWN, INPUT*/
01010+      *QUANTITY DIRECTLY, IF UNKNOWN, INPUT ZERO AND THE DERIVATIVE*/
01020+      *WILL BE CALCULATED*//
01030+      *ADDITTIONAL DATA WILL BE REQUIRED IF THE STABILITY*
01040+      /*DERIVATIVES ARE TO BE CALCULATED*/)
01050    22 PRINT 40
01060    40 FORMAT(/*DO YOU WANT ALL DERIVATIVES CALCULATED*,↑)
01070       READ 413,DC
01080       IF(DC.EQ.3HYES)70,55
01090    55 IF(DC.EQ.2HNO)35,60
01100    60 PRINT 65
01110    65 FORMAT(*YES OR NO ANSWERE. TRY AGAIN.*)
01120       GO TO 22
01130    70 CLAP=CLAT=CLADT=CLADP=CLQT=CLQP=CMAP=CMADP=0.
01140       CMQP=CYBT=CYBP=CYRVT=CYRP=CNBP=CNRP=0.
01150       GO TO 80
```

```
   35 PRINT 45
   45 FORMAT(/*SOURCE OF INPUT DERIVATIVES≥*,+ )
      READ 90,PA,PB,PC,PD,PE,PF,PG,PH
   90 FORMAT(8A10)
      PRINT 25
   25 FORMAT(*INPUT THE FOLLOWING STABILITY DERIVATIVES*//
      *CLAP,CLAT,CLADT,CLADP,CLQT,CLQP,CMAP,CMADP,*/
      *CMQP,CYBT,CYBP,CYRVT,CYRP,CNBP,CNRP*/)
      READ,CLAP,CLAT,CLADT,CLADP,CLQT,CLQP,CMAP,CMADP
      READ,CMQP,CYBT,CYBP,CYRVT,CYRP,CNBP,CNRP
   80 LGUST=750.
      ALT=0.0
      RHO=RHOO
C
C     LONGITUDINAL AND LATERAL STABILITY DERIVATIVES ARE CALCULATED FROM
C     NASA CR-1975 [RIDING AND HANDLING QUALITIES OF LIGHT AIRCRAFT-
C     A REVIEW AND ANALYSIS].
C
C                 AIRCRAFT LIMITATIONS
C
C     1. RIGID STRUCTURE WITH LITTLE OR NO WING SWEEP.
C     2. MAX. GROSS WEIGHT            10,000 LBS.
C     3. MAX. WING LOADING            40 LBS/SQFT
C     4. MAX. INDICATED AIRSPEED      300 MPH(441 FPS)
C     5. MAX. MACH NUMBER             .4
C     6. MIN. ASPECT RATIO            5.0
C
C     LONGITUDINAL STABILITY DERIVATIVES
C
      WS=WTO/S
      ARW=(B*B)/S
      CT=ST/BT
      ART=(BT*BT)/ST
      TRW=CWTP/CWRT
      CW=(2./3.)*CWRT*((1.+TRW+(TRW**2.))/(1.+TRW))
      IF(CLAP.EQ.0)225,240
  225 IF(T.EQ.0)226,236
  226 PRINT 230
  230 FORMAT(4X,2HT=,+ )
      READ 30,T
      PRINT 235
  235 FORMAT(4X,6HCLA2D=,+ )
      READ 50,CLA2D
  236 E1=1./(1.+T)
      CLAW=(CLA2D/(1.+((CLA2D*57.3)/(3.1416*E1*ARW))))*(180./3.1416)
      CLAP=CLAW
  240 CLAW=CLAP
      DEDA=(20.*CLAW*(3.1416/180.))*(((1./TRW)**.3)/(ARW**.725))*(((3.*
     +CW)/LTP)**.25)
      IF(CLAT.EQ.0)250,275
  250 IF(CLATD.EQ.0)251,266
  251 PRINT 255
  255 FORMAT(4X,6HCLATD=,+ )
      READ 30,CLATD
      PRINT 260
```

```
260 FORMAT(4X,3HTT=,+ )
    READ 265,TT
265 FORMAT(F8.5)
    E2=1./(1.+TT)
266 CLAT=(CLATD/(1.+((CLATD*57.3)/(3.1416*E2*ART))))*(180./3.1416)
275 IF(CLADT.EQ.0)290,300
290 IF(NT.EQ.0)291,296
291 PRINT 295
295 FORMAT(4X,3HNT=,+ )
    READ 265,NT
296 CLADT=2.*CLAT*DEDA*(LTP/CW)*(ST/S)*NT
300 IF(CLADP.EQ.0)310,315
310 CLADP=CLADT
315 IF(CLQT.EQ.0)325,345
325 IF(NT.EQ.0)330,340
330 PRINT 335
335 FORMAT(4X,3HNT=,+ )
    READ 265,NT
340 CLQT=(2.*(LT/CW)*CLAT*(ST/S)*NT)
345 IF(CLQP.EQ.0)355,360
355 CLQW=(2.*(XP/CW)*CLAP)
    CLQP=CLQW+CLQT
360 IF(CMAP.EQ.0)370,485
370 IF(D.EQ.0)371,376
371 PRINT 375
375 FORMAT(4X,2HD=,+ )
    READ 110,D
376 IF(CLS.EQ.0)377,390
377 PRINT 385
385 FORMAT(4X,4HCLS=,+ )
    READ 110,CLS
390 IF(CDW.EQ.0)391,401
391 PRINT 395
395 FORMAT(4X,4HCDW=,+ )
    READ 110, CDW
    PRINT 400
400 FORMAT(4X,4HCDF=,+ )
    READ 265,CDF
401 IF(FH.EQ.0)404,406
404 PRINT 405
405 FORMAT(4X,3HFH=,+ )
    READ 30,FH
406 IF(FW.EQ.0)407,411
407 PRINT 410
410 FORMAT(4X,3HFW=,+ )
    READ 30,FW
411 PRINT 412
412 FORMAT(4X,*RETRACTABLE GEAR*,+ )
    READ 413,RG
413 FORMAT(A10)
    IF(RG.EQ.3HYES)431,414
414 IF(RG.EQ.2HNO)418,416
416 PRINT 417
417 FORMAT(*YES OR NO ANSWERE. TRY AGAIN.*)
```

```
      GO TO 411
  418 IF(CDNG.EQ.0)419,456
  419 PRINT 415
  415 FORMAT(4X,5HCDNG=,↑ )
      READ 30,CDNG
      PRINT 420
  420 FORMAT(4X,6HFCDMG=,↑ )
      READ 30,FCDMG
      PRINT 425
  425 FORMAT(4X,3HWD=,↑ )
      READ 30,WD
      PRINT 430
  430 FORMAT(4X,3HWH=,↑ )
      READ 50,WH
  431 IF(CDE.EQ.0)432,456
  432 PRINT 435
  435 FORMAT(4X,4HCDE=,↑ )
      READ 30,CDE
      PRINT 440
  440 FORMAT(4X,6HCDNAC=,↑ )
      READ 30,CDNAC
      PRINT 445
  445 FORMAT(4X,5HRNAC=,↑ )
      READ 30,RNAC
      PRINT 450
  450 FORMAT(4X,6HCDTTK=,↑ )
      READ 30,CDTTK
      PRINT 455
  455 FORMAT(4X,5HRTTK=,↑ )
      READ 30,RTTK
  456 IF(IW.EQ.0)457,461
  457 PRINT 460
  460 FORMAT(4X,3HIW=,↑ )
      READ 50,IW
  461 IF(NT.EQ.0)465,475
  465 PRINT 470
  470 FORMAT(4X,3HNT=,↑ )
      READ 110,NT
  475 IF(KF.EQ.0)476,481
  476 PRINT 480
  480 FORMAT(4X,3HKF=,↑ )
      READ 50,KF
  481 A=IW
      E=1./(1.+D)
      CLW=CLS/(1.+(2./ARW))
      CLT=CLW*(XA/LT)*(S/ST)*(1./NT)
      CLP=CLW+(CLT*(ST/S)*NT)
      CDFP=(((CDW*S)+(1.2*CDF*FH*FW)+FCDMG+(CDNG*WD*WH)+(CDE*ST)+CDNAC*
     3.1416*RNAC*RNAC+CDTTK*3.1416*RTTK*RTTK)*1.15)/S
      CDP=CDFP+((CLW*CLW)/(3.1416*E*ARW))
      CMAW=(((1.+(((2.*CLP)/(3.1416*E*ARW))*((A-IW)/57.3))+(CDP/CLAP))
     *(XA/CW))+((((2.*CLP)/(3.1416*E*ARW))-((A-IW)/57.3)
     -(CLP/CLAP))*(ZAA/CW)))*CLAP
      CMAT=CLAT*(1.-DEDA)*(ST/S)*(LT/CW)*NT
      CMAF=(KF*(FW**2.)*LB)/(S*CW)
      CMAP=CMAW-CMAT+CMAF
```

```
485 IF(CMADP.EQ.0)495,515
495 IF(NT.EQ.0)500,510
500 PRINT 505
505 FORMAT(4X,3HNT=,↑ )
    READ 265,NT
510 CMADP=(-2.*CLAT*DEDA)*(LT/CW)*(LTP/CW)*(ST/S)*NT
515 IF(CMQP.EQ.0)525,545
525 IF(NT.EQ.0)530,540
530 PRINT 535
535 FORMAT(4X,3HNT=,↑ )
    READ 265,NT
540 CMQP=(((-2.*XP)/(CW**2.))*ABS(XP)*CLAP)-(2.*((LT**2.)/(CW**2.))*
+   CLAT*(ST/S)*NT)
545 CONTINUE
*
*   LATERAL STABILITY DERIVATIVES
*
    ARV=(BV*BV)/SV
    IF(CYBT.EQ.0)590,620
590 IF(K.EQ.0)591,604
591 PRINT 600
600 FORMAT(4X,2HK=,↑ )
    READ 30,K
    PRINT 603
603 FORMAT(4X,*CLAV=*,↑ )
    READ 30,CLAV
604 IF(FH.EQ.0)605,615
605 PRINT 610
610 FORMAT(4X,3HFH=,↑ )
    READ 265,FH
615 SWDPR=.724+(1.53*(SV/S))+(.4*(ZWW/FH))+(.009*ARW)
    CYBT=-K*CLAV*SWDPR*(SV/S)*57.3
620 IF(CYBP.EQ.0)630,702
630 IF(L.EQ.0)631,646
631 PRINT 635
635 FORMAT(4X,2HL=,↑ )
    READ 30,L
    PRINT 640
640 FORMAT(4X,3HKI=,↑ )
    READ 30,KI
    PRINT 645
645 FORMAT(4X,5HCLAF=,↑ )
    READ 30,CLAF
646 IF(HNOSE.EQ.0)647,651
647 PRINT 650
650 FORMAT(4X,6HHNOSE=,↑ )
    READ 30,HNOSE
    PRINT 660
660 FORMAT(4X,5HHFCY=,↑ )
    READ 50,HFCY
    PRINT 670
670 FORMAT(4X,5HLFCY=,↑ )
    READ 30,LFCY
    PRINT 675
675 FORMAT(4X,4HLMH=,↑ )
```

```
      READ 30,LMH
      PRINT 680
  680 FORMAT(4X,5HHBCY=,↑ )
      READ 30,HBCY
      PRINT 690
  690 FORMAT(4X,5HLBCY=,↑ )
      READ 30,LBCY
      PRINT 695
  695 FORMAT(4X,3HR1=,↑ )
      READ 50,R1
  651 IF(WNOSE.EQ.0)664,694
  664 PRINT 655
  655 FORMAT(4X,6HWNOSE=,↑ )
      READ 30,WNOSE
      PRINT 665
  665 FORMAT(4X,5HWFCY=,↑ )
      READ 30,WFCY
      PRINT 685
  685 FORMAT(4X,5HWBCY=,↑ )
      READ 30,WBCY
  694 IF(FH.EQ.0)696,698
  696 PRINT 697
  697 FORMAT(4X,3HFH=,↑ )
      READ 30,FH
  698 IF(FW.EQ.0)699,701
  699 PRINT 700
  700 FORMAT(4X,3HFW=,↑ )
      READ 30,FW
  701 V1=LFCY*(2.*(HNOSE*WNOSE+HFCY*WFCY)+(HFCY*WNOSE)+(HNOSE*WFCY))
      V2=(LMH-LFCY)*(2.*(HFCY*WFCY+FH*FW)+FH*WFCY+HFCY*FW)
      V3=(LBCY-LMH)*(2.*(HBCY*WBCY+FH*FW)+FH*WBCY+FW*HBCY)
      V4=(LB-LBCY)*(2.*(HBCY*WBCY+(R1**2.))+HBCY*R1+WBCY*R1)
      FUSV=(V1+V2+V3+V4)/6.
      BRA=FUSV**(2./3.)
      CYBF=-KI*CLAF*(BRA/S)
      CYBW=-.0001*ABS(L)*(180./3.1416)
      CYBP=CYBW+CYBF+CYBT
  702 IF(CYRVT.EQ.0)710,715
  710 CYRVT=-2.*(LV/B)*CYBT
  715 IF(CYRP.EQ.0)725,755
  725 IF(CLW.EQ.0)730,750
  730 IF(CLS.EQ.0)735,745
  735 PRINT 740
  740 FORMAT(4X,4HCLS=,↑ )
      READ 110,CLS
  745 CLW=CLS/(1.+(2./ARW))
  750 CYRW=(.143*CLW)-.05
      CYRP=CYRW+CYRVT
  755 IF(CNBP.EQ.0)765,786
  765 IF(HNOSE.EQ.0)766,774
  766 PRINT 767
  767 FORMAT(4X,6HHNOSE=,↑ )
      READ 30,HNOSE
      PRINT 768
  768 FORMAT(4X,5HHFCY=,↑ )
      READ 50,HFCY
```

```
      PRINT 769
  769 FORMAT(4X,5HLFCY=,↑ )
      READ 30,LFCY
      PRINT 770
  770 FORMAT(4X,4HLMH=,↑ )
      READ 30,LMH
      PRINT 771
  771 FORMAT(4X,5HHBCY=,↑ )
      READ 30,HBCY
      PRINT 772
  772 FORMAT(4X,5HLBCY=,↑ )
      READ 30,LBCY
      PRINT 773
  773 FORMAT(4X,3HR1=,↑ )
      READ 50,R1
  774 IF(KN.EQ.0)781,782
  781 PRINT 775
  775 FORMAT(4X,3HKN=,↑ )
      READ 50,KN
  782 IF(FH.EQ.0)776,785
  776 PRINT 780
  780 FORMAT(4X,3HFH=,↑ )
      READ 265,FH
  785 BODSA=(((HNOSE+HFCY)*LFCY)+((FH+HFCY)*(LMH-LFCY))+((FH+HBCY)
     *(LBCY-LMH))+((HBCY+R1)*(LB-LBCY)))/2.
      CNBP=-(KN*57.3*(BODSA/S)*(LB/B))-((CYBT)*(LV/B))
  786 CDO=CDFP
      IF(CNRP.EQ.0)805,850
  805 IF(CLW.EQ.0)810,830
  810 IF(CLS.EQ.0)815,825
  815 PRINT 820
  820 FORMAT(5X,4HCLS=,↑ )
      READ 110,CLS
  825 CLW=CLS/(1.+(2./ARW))
  830 IF(NT.EQ.0)835,841
  835 PRINT 840
  840 FORMAT(4X,3HNT=,↑ )
      READ 110,NT
  841 IF(CDO.EQ.0)787,845
  787 IF(CDW.EQ.0)842,843
  842 PRINT 788
  788 FORMAT(4X,4HCDW=,↑ )
      READ 110, CDW
      PRINT 789
  789 FORMAT(4X,4HCDF=,↑ )
      READ 265,CDF
  843 IF(FH.EQ.0)801,802
  801 PRINT 790
  790 FORMAT(4X,3HFH=,↑ )
      READ 30,FH
  802 IF(FW.EQ.0)803,804
  803 PRINT 791
  791 FORMAT(4X,3HFW=,↑ )
      READ 30,FW
  804 IF(RG.EQ.3HYES)811,806
  806 PRINT 807
  807 FORMAT(4X,*RETRACTABLE GEAR*,↑ )
```

```
      READ 413,RG
      IF(RG.EQ.3HYES)811,808
  808 IF(RG.EQ.2HNO)809,812
  812 PRINT 813
  813 FORMAT(*YES OR NO ANSWERE. TRY AGAIN.*)
      GO TO 806
  809 IF(CDNG.EQ.0)844,846
  844 PRINT 792
  792 FORMAT(4X,5HCDNG=,↑ )
      READ 30,CDNG
      PRINT 793
  793 FORMAT(4X,6HFCDMG=,↑ )
      READ 30,FCDMG
      PRINT 794
  794 FORMAT(4X,3HWD=,↑ )
      READ 30,WD
      PRINT 795
  795 FORMAT(4X,3HWH=,↑ )
      READ 50,WH
  811 PRINT 796
  796 FORMAT(4X,4HCDE=,↑ )
      READ 30,CDE
      PRINT 797
  797 FORMAT(4X,6HCDNAC=,↑ )
      READ 30,CDNAC
      PRINT 798
  798 FORMAT(4X,5HRNAC=,↑ )
      READ 30,RNAC
      PRINT 799
  799 FORMAT(4X,6HCDTTK=,↑ )
      READ 30,CDTTK
      PRINT 800
  800 FORMAT(4X,5HRTTK=,↑ )
      READ 30,RTTK
  846 CDFP=(((CDW*S)+(1.2*CDF*FH*FW)+FCDMG+(CDNG*WD*WH)+(CDE*ST)+CDNAC*
     +3.1416*RNAC*RNAC+CDTTK*3.1416*RTTK)*1.15)/S
      CDO=CDFP
  845 CNRW=-(.33*((1.+(3.*TRW))/(2.+(2.+TRW)))*CDO)-(.02*(1.-((ARW-6.)/
     +13.)-((1.-TRW)/2.5))*(CLW**2.))
      CNRT=2.*((LV/B)**2.)*CYBT
      CNRP=CNRW+CNRT
  850 CONTINUE
      WRITE(7,851)MODEL,U,WTO,WS,CW,TRW,ARW,ALT,S,B,ST,BT,SV,BV,LGUST
  851 FORMAT(A10//*U=*,F8.4,1X,*FPS*,5X,*WTO=*,F8.2,1X,*LBS*,5X,*W/S=*,
     +F8.4,1X,*LBS/SQFT*,5X,*CW=*,F8.4,1X,*FT*,5X,*TRW=*,F8.4,5X,*ARW=*,
     +F8.4,5X,*ALT=*,F8.2,1X,*FT*/*S=*,F8.4,1X,*SQFT*,4X,*B=*,F8.4,1X,
     +*FT*,8X,*ST=*,F8.4,1X,*SQFT*,10X,*BT=*,F8.4,1X,*FT*,5X,*SV=*,
     +F8.4,1X,*SQFT*,1X,*BV=*,F8.4,1X,*FT*,3X,*LGUST=*,F8.2,1X,*FT*/)
      IF(LGUST.EQ.2500)900,847
  847 IF(ALT.EQ.0)852,879
  852 CONTINUE
      IF(PA.EQ.0)854,853
  853 WRITE(7,856)PA,PB,PC,PD,PE,PF,PG,PH
  856 FORMAT(/*STABILITY DERIVATIVES ARE CALCULATED FROM *
     +*NASA CR-1975*/*AND INPUT FROM *,8A10/)
      GO TO 857
```

```
      854 WRITE(7,855)
      855 FORMAT(/*STABILITY DERIVATIVES ARE CALCULATED FROM NASA CR-1975*
     +    /*RIDING AND HANDLING QUALITIES OF LIGHT AIRCRAFT*
     +    *-A REVIEW AND ANALYSIS*//*LONGITUDINAL*,43X,*LATERAL*/)
      857 WRITE(7,860)CLAP,CYBP
      860 FORMAT(5X,*LIFT CURVE SLOPE*,39X,*CHANGE IN SIDE FORCE DUE TO*
     +    * CHANGE IN SIDESLIP ANGLE*/9X,*CLAP=*,F8.4,1X,*/RAD*,37X,*CYBP=*
     +    ,F8.5,1X,*/RAD*/)
          WRITE(7,865)CLADP,CYRP
      865 FORMAT(5X,*CHANGE IN LIFT COEFFICIENT DUE TO TIME*,17X,*CHANGE IN*
     +    * SIDE FORCE DUE TO CHANGE IN YAWING VELOCITY*/5X,*RATE OF CHANGE*
     +    * IN ANGLE OF ATTACK*/9X,*CLADP=*,F8.4,1X,*/RAD*,36X,*CYRP=*
     +    ,F8.5,1X,*/RAD*/)
          WRITE(7,870)CLQP,CNBP
      870 FORMAT(5X,*CHANGE IN LIFT COEFFICIENT DUE TO*,22X,*CHANGE IN*
     +    * YAWING MOMENT COEFFICIENT DUE TO CHANGE*/5X,*CHANGE IN PITCHING*
     +    * VELOCITY*,28X,*IN SIDESLIP ANGLE, WEATHERCOCK]*/9X,*CLQP=*,
     +    F8.4,1X,*/RAD*,37X,*CNBP=*,F8.5,1X,*/RAD*/)
          WRITE(7,875)CMAP,CNRP
      875 FORMAT(5X,*CHANGE IN PITCHING MOMENT COEFFICIENT*,18X,*CHANGE IN*
     +    * YAWING MOMENT COEFFICIENT DUE TO CHANGE*/5X,*DUE TO CHANGE IN*
     +    * ANGLE OF ATTACK*,23X,*IN YAWING VELOCITY, YAW DAMPING*
     +    * DERIVATIVE]*/9X,*CMAP=*,F8.4,1X,*/RAD*,37X,*CNRP=*,F8.5,1X,
     +    */RAD*/)
          WRITE(7,876)CMADP
      876 FORMAT(5X,*CHANGE IN PITCHING MOMENT COEFFICIENT DUE TO*/5X,
     +    *TIME RATE OF CHANGE IN ANGLE OF ATTACK*/9X,*CMADP=*,F8.4,1X,
     +    */RAD*/)
          WRITE(7,878)CMQP
      878 FORMAT(5X,*CHANGE IN PITCHING MOMENT COEFFICIENT DUE*/5X,*TO*
     +    * CHANGE IN PITCHING VELOCITY*/9X,*CMQP=*,1X,F8.4,1X,*/RAD*/)
      879 CONTINUE
C
C     STABILITY CHARACTERISTICS
C
          WRITE(7,880)
      880 FORMAT(25HSTABILITY CHARACTERISTICS//)
          RX=(IYY/WTO)**.5
          RY=(IZZ/WTO)**.5
          KA=(8.*WTO)/(RHO*S*CW*CLAP)
          KB=-(8.*WTO)/(RHO*S*B*CYBP)
          KOA=(CW/RX)*(((-1./(KA*CLAP))*(((2./KA)*CMQP)+CMAP))**.5)
          KOB=(B/RY)*(((1./(KB*CYBP))*(((2./KB)*CNRP)-CNBP))**.5)
          ZA=(1./(KA*KOA))*(1.-(((CW/RX)**2.)*((CMQP+CMADP)/(2.*CLAP))))
          ZB=(1./(KB*KOB))*(1.+(((B/RY)**2.)*(CNRP/(2.*CYBP))))
          GA=ZA*KA*KOA
          GB=ZB*KB*KOB
          WRITE(7,885)KA,KB,ZA,ZB
      885 FORMAT(5X,*MASS PARAMETERS*,40X,*DAMPING RATIO (SHORT PERIOD*
     +    *   DUTCH ROLL)*/9X,*KA=*,F8.3,5X,*KB=*,F8.3,28X,*ZA=*,F8.4,
     +    5X,*ZB=*,F8.4/)
          WRITE(7,890)KOA,KOB,GA,GB
      890 FORMAT(5X,*UNDAMPED NATURAL FREQUENCY*,29X,*DAMPING PARAMETER*
     +    * (SHORT PERIOD   DUTCH ROLL)*/9X,*KOA=*,F8.4,4X,*KOB=*,
     +    F8.4,27X,*GA=*,F8.4,5X,*GB=*,F8.4/)
      900 CONTINUE
          SAGUST=(2.*LGUST)/CW
```

```
      SBGUST=(2.*LGUST)/B
      WRITE(7,910)SAGUST,SBGUST
  910 FORMAT(*GUST SCALE*/5X,*SAGUST=*,F8.3,1X,*SBGUST=*,F8.3/)
      S1=SAGUST*KOA
      S2=SBGUST*KOB
      A1=ABA*KOA
      A2=ABB*KOB
      WRITE(7,915)S1,S2,A1,A2
  915 FORMAT(28HRESPONSE INTEGRAL PARAMETERS/5X,5HSKOA=,F8.4,
     +3X,5HSKOB=,F8.4/5X,5HAKOA=,F8.4,3X,5HAKOB=,F8.4//)
C
C     RESPONSE INTEGRALS
C
      WRITE(7,920)
  920 FORMAT(*RESPONSE INTEGRALS*/)
      CALL TRAPI(.00001,.001,200,XINTS,FUNC,TMPI,4)
      CALL SIMPI(.001,2.,2000,TXI1,FUNC,TMPI,4)
      CALL TRAPI(2.,20.,200,TXI2,FUNC,TMPI,4)
      DO 925 I=1,4
  925 XINTS(I)=((SAGUST*KOA)/3.1416)*(XINTS(I)+TXI1(I)+TXI2(I))
      R0=XINTS(1)
      R2=XINTS(2)
      R4=XINTS(3)
      R6=XINTS(4)
      CALL TRAPI(.00001,.001,200,XINTSB,FUNCB,TMPIB,4)
      CALL SIMPI(.001,2.,2000,TXI1B,FUNCB,TMPIB,4)
      CALL TRAPI(2.,20.,200,TXI2B,FUNCB,TMPIB,4)
      DO 935 I=1,4
  935 XINTSB(I)=((SBGUST*KOB)/3.1416)*(XINTSB(I)+TXI1B(I)+TXI2B(I))
      R0B=XINTSB(1)
      R2B=XINTSB(2)
      R4B=XINTSB(3)
      R6B=XINTSB(4)
      WRITE(7,930)(XINTS(I),I=1,4),(XINTSB(I),I=1,4)
  930 FORMAT(5X,*LONGITUDINAL*,43X,*LATERAL*/9X,*R0=*,F7.4,1X,*R2=*,
     +F7.4,1X,*R4=*,F7.4,1X,*R6=*,F7.4,15X,*R0B=*,F7.4,1X,*R2B=*,F7.4,
     +1X,*R4B=*,F7.4,1X,*R6B=*,F7.4/)
C
C     RESPONSES ARE CALCULATED FROM NASA TN D-6273 =A METHOD FOR
C     ESTIMATING SOME LONGITUDINAL AND LATERAL RIGID BODY RESPONSES
C     OF AIRPLANES TO CONTINUOUS ATMOSPERIC TURBULENCE=
C
C     AIRPANE RESPONSES
C
  940 WRITE(7,945)
  945 FORMAT(*AIRPLANE RESPONSES ARE CALCULATED FROM NASA TN D-6273*
     +/*=A METHOD FOR ESTIMATING SOME LONGITUDINAL AND LATERAL RIGID*
     +* BODY RESPONSES OF AIRPLANES TO CONTINUOUS GUST TURBULENCE=*//
     +*LONGITUDINAL*,43X,*LATERAL*/)
      ZW=-((RHO*U*S)/(2.*WTO))*CLAP
      MW=((RHO*U*S*CW)/(2.*IYY))*CMAP
      MQ=((RHO*U*S*CW**2.)/(4.*IYY))*CMQP
      WOA=(ZW*MQ-U*MW)**.5
      YV=((RHO*U*S)/(2.*WTO))*CYBP
      NV=((RHO*U*S*B)/(2.*IZZ))*CNBP
      NR=((RHO*U*S*B**2.)/(4.*IZZ))*CNRP
      WOB=(NR*YV+U*NV)**.5
      ADN=((2.*ZA*WOA)/(32.2*GA))*(R4+((4.*ZA**2.)*((1.-(1./GA))**2.)*R2)
```

```
06200+      )**.5
06210       NODN=(WO[illegible](2.[illegible].1416))*((R6+((4.*ZA**2.)*((1.-(1./GA))**2.)*R4))/(R4
06220+      +((4.*ZA**2.)*((1.-(1./GA))**2.)*R2)))**.5
06230       ATHD=(WOA/U)*ABS((4.*((ZA**2.)/GA)*(1.-(1./GA)))-1.)*R2**.5
06240       NOTHD=(WOA/(2.*3.1416))*(R4/R2)**.5
06250       ATDD=((WOA**2.)/U)*ABS((4.*((ZA**2.)/GA)*(1.-(1./GA)))-1.)*R4**.5
06260       NOTDD=(WOA/(2.*3.1416))*(R6/R4)**.5
06270       ADL=((2.*ZB*WOB)/(32.2*GB))*(R4B+(4.*(ZB**2.)*((1.-(1./GB))**2.)
06280+      *R2B))**.5
06290       NODL=(WOB/(2.*3.1416))*((R6B+(4.*(ZB**2.)*((1.-(1./GB))**2.)*R4B))/
06300+      (R4B+(4.*(ZB**2.)*((1.-(1./GB))**2.)*R2B)))**.5
06310       ASI=(1./U)*ABS((4.*((ZB**2.)/GB)*(1.-(1./GB)))-1.)*(R0B**.5)
06320       NOSI=(WOB/(2.*3.1416))*((R2B/R0B)**.5)
06330       ASID=(WOB/U)*ABS((4.*((ZB**2.)/GB)*(1.-(1./GB)))-1.)*(R2B**.5)
06340       NOSID=(WOB/(2.*3.1416))*((R4B/R2B)**.5)
06350       Q=((.5)*RHO*(U**2.))/32.2
06360       SR=ST/S
06370       C1=-SR+(2.*(CLADT/CLAT)*((KOA*ZA)/GA))+(((4.*U*U*KOA*WHT)/(32.2*
06380+      Q*S*CW*CLAT))*((ZA/GA)-(((KOA*LT)/CW)*((4.*((ZA*ZA)/GA)*(1.-(1./
06390+      GA)))-1.))))
06400       C2=(2.*ZA*SR*(1.-(1./GA)))-((CLADT/CLAT)*KOA)+((CLQT/CLAT)*KOA*((4.
06410+      *((ZA*ZA)/GA)*(1.-(1./GA)))-1.))-(((2.*U*U*KOA*WHT)/(Q*S*CW*CLAT
06420+      *32.2))*(((4.*ZA*ZA)/GA)*(1.-(1./GA))))
06430       AZHT=ABS((Q*S*CLAT)/U)*(C1*C1*R4+C2*C2*R2)**.5
06440       NOHT=(WOA/(2.*3.1416))*((C1*C1*R6+C2*C2*R4)/(C1*C1*R4+C2*C2*R2))**.5
06450       C3=1.
06460       C4=-2.*ZB*(1.-(1./GB))+KOB*(CYRVT/CYBT)*(((4.*ZB*ZB)/GB)*(1.-
06470+      (1./GB))-1.)
06480       AYVT=ABS((Q*S*CYBT)/U)*(C3*C3*R4B+C4*C4*R2B)**.5
06490       NOVT=(WOB/(2.*3.1416))*((C3*C3*R6B+C4*C4*R4B)
06500+      /(C3*C3*R4B+C4*C4*R2B))**.5
06510       WRITE(7,1000)ADN,NODN,ADL,NODL
06520 1000  FORMAT(5X,*NORMAL-LOAD FACTOR RESPONSE*,28X,*LATERAL-LOAD FACTOR*
06530+      * RESPONSE*/9X,*ADN=*,1X,F6.4,1X,*G/FT/SEC*,8X,*NODN=*,1X,F8.4,1X
06540+      ,*CRS/SEC*,5X,*ADL=*,1X,F6.4,1X,*G/FT/SEC*,7X,*NODL=*,1X,F8.4,
06550+      1X,*CRS/SEC*/)
06560       WRITE(7,1005)ATHD,NOTHD,ASI,NOSI
06570 1005  FORMAT(5X,*PITCH-ANGLE RATE RESPONSE*,30X,*YAW ANGLE RESPONSE*
06580+      /9X,*ATHD=*,F6.4,1X,*RAD/SEC/FT/SEC*,2X,*NOTHD=*,F8.4,1X,
06590+      *CRS/SEC*,5X
06600+      ,*ASI=*,1X,F6.4,1X,*RAD/FT/SEC*,5X,*NOSI=*,1X,F8.4,1X,*CRS/SEC*/)
06610       WRITE(7,1010)ATDD,NOTDD,ASID,NOSID
06620 1010  FORMAT(5X,*PITCH-ANGLE ACCELERATION RESPONSE*,22X,*YAW-ANGLE*
06630+      * RATE RESPONSE*/9X,*ATDD=*,F6.4,1X,*RAD/SEC2/FT/SEC*,1X,*NOTDD=*,
06640+      F8.4,1X,
06650+      *CRS/SEC*,5X,*ASID=*,F6.4,1X,*RAD/SEC/FT/SEC*,1X,*NOSID=*,F8.4,1X,
06660+      *CRS/SEC*/)
06670       WRITE(7,1015)AZHT,NOHT,AYVT,NOVT
06680 1015  FORMAT(5X,*HORIZONTAL TAIL LOAD*,35X,*VERTICAL TAIL LOAD*/9X,
06690+      *AZHT=*,F8.4,1X,*LBS/FT/SEC*,4X,*NOHT=*,1X,F8.4,1X,*CRS/SEC*,5X,
06700+      *AYVT=*,F8.4,1X,*LBS/FT/SEC*,3X,*NOVT=*,1X,F8.4,1X,*CRS/SEC*/)
06710C
06720C      DISCRETE GUST LOADS AND LOAD FACTORS ARE DERIVED FROM PROCEDURES
06730C      OUTLINED IN FAR PART 23
06740C
```

```
06750C      DISCRETE GUST LOADS
06760C
06770       IF(LGUST.EQ.2500.)GO TO 1070
06780       WRITE(7,1040)
06790 1040  FORMAT(*AIRPLANE RESPONSES TO DICRETE GUST LOADS ARE DERIVED*/
06800+      *FROM PROCEDURES OUTLINED IN FAR PART 23  AIRWORTHINESS STANDARDS*
06810+      * NORMAL, UTILITY, AND ACROBATIC CATEGORY AIRPLANES */)
06820       UG=(2.*(WTO/S))/(RHO*CW*CLAW)
06830       KG=(.88*UG)/(5.3+UG)
06840       VKTS=U*(1./1.6888)*(RHO/RHOO)**.5
06850       IF(ALT.GE.20000.)1043,1042
06860 1042  UDE=50.
06870       GO TO 1044
06880 1043  UDE=(ALT-80000.)/(-1200.)
06890 1044  N=1.+(KG*UDE*VKTS*CLAW)/(498.*(WTO/S))
06900       WRITE(7,1045)N
06910 1045  FORMAT(5X,25HDISCRETE GUST LOAD FACTOR/9X,2HN=,F8.4,/)
06920       DLHT=((KG*UDE*VKTS*CLAT*ST)/498.)*(1.-DEDA)
06930       CV=SV/BV
06940       UGT=((2.*WTO)/(RHO*CV*CLAV*SV*57.3))*(RY/LV)**2.
06950       KGT=(.88*UGT)/(5.3+UGT)
06960       DLVT=(KGT*UDE*VKTS*CLAV*SV*57.3 )/498.
06970       WRITE(7,1050)DLHT,DLVT
06980 1050  FORMAT(5X,*DELTA LOAD ON HORIZONTAL TAIL DUE TO DISCRETE GUST*,
06990+      5X,*DELTA LOAD ON VERTICAL TAIL DUE TO DISCRETE GUST*/9X,
07000+      *DLHT=*,F8.3,1X,*LBS*,38X,*DLVT=*,F8.3,1X,*LBS*/)
07010       MOM=Q*S*CW*CMOWS
07020       IF(XA.LT.0)1056,1058
07030 1056  HTL=((-XA*WTO)+MOM)/(LT+XA)
07040 1058  HTL=((XA*WTO)-MOM)/(XA+LT)
07050       LHT=DLHT+HTL
07060       LVT=DLVT
07070       WRITE(7,1060)HTL
07080 1060  FORMAT(5X,37HHORIZONTAL TAIL LOAD(BALANCED FLIGHT)/9X,4HHTL=,F8.3,
07090+      1X,3HLBS/)
07100       WRITE(7,1065)LHT,LVT
07110 1065  FORMAT(5X,*TOTAL HORIZONTAL TAIL LOAD*,29X,*TOTAL VERTICAL*
07120+      * TAIL LOAD*/9X,*LHT=*,F8.3,1X,*LBS*,39X,*LVT=*,F8.3,1X,*LBS*/)
07130 1070  CONTINUE
07140       SIGWG=(N-1.)/ADN
07150       ADN1=(ADN*62.)+1.
07160       RATIO=ADN1/N
07170       WRITE(7,1080)SIGWG,RATIO
07180 1080  FORMAT(*RMS GUST INTENSITY (ADN=N)*,29X,*RATIO OF ADN/N *
07190+      *(SIGWG=62 FT/SEC)*//5X,*SIGWG=*,F8.3,1X,*FT/SEC*,34X,
07200+      *ADN/N=*,F8.3////)
07210       IF(LGUST.EQ.2500.)GO TO 1095
07220       IF(LGUST.EQ.750.)LGUST=2500.
07230       GO TO 850
07240 1095  CONTINUE
07250       IF(ALT.GE.5000.)1083,1082
07260 1082  ALT=5000.
07270       RHO=.066
07280       LGUST=750.
07290       GO TO 850
07300 1083  IF(ALT.GE.15000.)1068,1081
```

```
1081 ALT=ALT+5000.
     RHO=RHO-.009
     LGUST=750.
     GO TO 850
1068 IF(ALT.GE.ALTC)1085,1071
1071 IF(ALT.GE.25000.)1059,1072
1072 ALT=ALT+5000.
     RHO=RHO-.007
     LGUST=750.
     GO TO 850
1059 IF(ALT.GE.ALTC)1085,1061
1061 IF(ALT.GE.40000.)1057,1062
1062 ALT=ALT+5000.
     RHO=RHO-.005
     LGUST=750.
     GO TO 850
1057 IF(ALT.GE.ALTC)1085,1063
1063 IF(ALT.GE.45000.)1085,1064
1064 ALT=ALT+5000.
     RHO=RHO-.004
     LGUST=750.
     GO TO 850
1085 CONTINUE
1100 PRINT 1110
1110 FORMAT(*RERUN SAME AIRCRAFT>*,+ )
     READ 413,RSA
     IF(RSA.EQ.3HYES)22,1130
1130 IF(RSA.EQ.2HNO)1160,1140
1140 PRINT 1150
1150 FORMAT(*YES OR NO ANSWERE. TRY AGAIN.*)
     GO TO 1100
1160 AC=AC-1.
     IF(AC.EQ.0)1090,1100
1090 CONTINUE
     END FILE 7
     REWIND 7
     CALL SAVE(5HTAPE7,3HPSD,0,0,0)
     STOP
     END
C
     SUBROUTINE FUNC(BETA,RJ)
     DIMENSION RJ(4)
     COMMON ABA,SAGUST,KOA,ZA,ABB,SBGUST,KOB,ZB
     REAL KOA
     J=0
     DO 10 I=1,4
     Z1=BETA**J
     Z2=2.71828**(-1.*ABA*KOA*BETA)
     SKOA=SAGUST*KOA
     Z3=1.+((8./3.)*1.339*1.339*SKOA*SKOA*BETA*BETA)
     Z4=1.-BETA*BETA
     Z5=Z4*Z4
     Z6=4.*ZA*ZA*BETA*BETA
     Z7=(1.+(1.339*1.339*SKOA*SKOA*BETA*BETA))**(11./6.)
     RJ(I)=(Z1*Z2*Z3)/((Z5+Z6)*Z7)
  10 J=J+2
     RETURN
     END
C
```

```
      SUBROUTINE SIMPI(A,B,N,ANS,FUNC,TEMP,NI)
      DIMENSION ANS(NI),TEMP(NI)
      DO 4 I=1,NI
    4 ANS(I)=0.
      IF(B-A)1,2,3
    2 RETURN
    1 X=A
      A=B
      B=X
    3 H=(B-A)/N
      NM1=N-1
      CALL FUNC(A,TEMP)
      DO 5 I=1,NI
    5 ANS(I)=ANS(I)+TEMP(I)
      CALL FUNC(B,TEMP)
      DO 6 I=1,NI
    6 ANS(I)=ANS(I)+TEMP(I)
      K=2
      DO 7 J=1,NM1
      CALL FUNC(A+J*H,TEMP)
      IF(K-2) 8,9,8
    8 K=2
      GO TO 10
    9 K=4
   10 DO 7 I=1,NI
    7 ANS(I)=ANS(I)+K*TEMP(I)
      DO 11 I=1,NI
   11 ANS(I)=ANS(I)*H/3
      RETURN
      END
C
      SUBROUTINE TRAPI(A,B,N,ANS,FUNC,TEMP,NI)
      DIMENSION ANS(NI),TEMP(NI)
      DO 4 I=1,NI
    4 ANS(I)=0.
      IF(B-A) 1,2,3
    2 RETURN
    1 X=A
      A=B
      B=X
    3 H=(B-A)/N
      NM1=N-1
      CALL FUNC(A,TEMP)
      DO 5 I=1,NI
    5 ANS(I)=ANS(I)+TEMP(I)/2
      CALL FUNC(B,TEMP)
      DO 6 I=1,NI
    6 ANS(I)=ANS(I)+TEMP(I)/2
      DO 7 J=1,NM1
      CALL FUNC(A+J*H,TEMP)
      DO 7 I=1,NI
    7 ANS(I)=ANS(I)+TEMP(I)
      DO 8 I=1,NI
    8 ANS(I)=ANS(I)*H
      RETURN
      END
```

```
C
      SUBROUTINE FUNCB(BETA,RJB)
      DIMENSION RJB(4)
      COMMON ABA,SAGUST,KOA,ZA,ABB,SBGUST,KOB,ZB
      REAL KOB
      J=0
      DO 10 I=1,4
      Z1=BETA**J
      Z2=2.71828**(-1.*ABB*KOB*BETA)
      SKOB=SBGUST*KOB
      Z3=1.+((8./3.)*1.339*1.339*SKOB*SKOB*BETA*BETA)
      Z4=1.-BETA*BETA
      Z5=Z4*Z4
      Z6=4.*ZB*ZB*BETA*BETA
      Z7=(1.+(1.339*1.339*SKOB*SKOB*BETA*BETA))**(11./6.)
      RJB(I)=(Z1*Z2*Z3)/((Z5+Z6)*Z7)
   10 J=J+2
      RETURN
      END
```

APPENDIX C

AIRCRAFT RESPONSE TO CONTINUOUS ATMOSPHERIC TURBULENCE

MOTION OF CENTER OF GRAVITY

A simplified method for estimating longitudinal and lateral responses, applicable to general aviation aircraft, to random atmospheric turbulence is presented here. The following equations were adopted from a NASA Technical Note, "A Method for Estimating Some Longitudinal and Lateral Rigid-Body Responses of Airplanes to Continuous Atmospheric Turbulence" (reference 2).

Stability Characteristics

Undamped Natural Reduced Frequency - K_O

$$K_{O_\alpha} = \frac{\bar{c}_w}{R_x}\left[-\frac{1}{K_\alpha C_{L_\alpha}}\left(\frac{2}{K_\alpha}C_{M_q} + C_{M_\alpha}\right)\right]^{1/2} \qquad \text{(C-1)}$$

$$K_{O_\beta} = \frac{b_w}{R_Y}\left[\frac{1}{K_\beta C_{Y_\beta}}\left(\frac{2}{K_\beta}C_{N_r} - C_{N_\beta}\right)\right]^{1/2} \qquad \text{(C-2)}$$

Damping Ratio - ζ

$$\zeta_\alpha = \frac{1}{K_\alpha K_{O_\alpha}}\left[1 - \left(\frac{\bar{c}_w}{R_x}\right)^2 \frac{C_{m_q} + C_{m_{\dot{\alpha}}}}{2C_{L_{\alpha_\ell}}}\right] \qquad \text{(C-3)}$$

$$\zeta_\beta = \frac{1}{K_\beta K_{O_\beta}}\left[1 + \left(\frac{b_w}{R_Y}\right)^2 \frac{C_{n_r}}{2C_{Y_\beta}}\right] \qquad \text{(C-4)}$$

Mass Parameter - K

$$K_\alpha = \frac{8W_{TO}}{\rho S_w \bar{c}_w C_{L_\alpha}} \qquad \text{(C-5)} \qquad\qquad K_\beta = \frac{-8W_{TO}}{\rho S_w b_w C_{Y_\beta}} \qquad \text{(C-6)}$$

Damping Parameter - γ

$$\gamma_\alpha = \zeta_\alpha K_\alpha K_{O_\alpha} \qquad \text{(C-7)} \qquad\qquad \gamma_\beta = \zeta_\beta K_\beta K_{O_\beta} \qquad \text{(C-8)}$$

Stability Derivatives

$$Z_W = -\frac{\rho U S_w C_{L_\alpha}}{2W_{TO}} \tag{C-9}$$

$$M_W = \frac{\rho U S_w \bar{c}_w C_{m_\alpha}}{2I_{YY}} \tag{C-10}$$

$$Mq = \frac{\rho U S_w \bar{c}_w^2 C_{m_q}}{4I_{YY}} \tag{C-11}$$

$$Y_V = \frac{\rho U S_w C_{Y_\beta}}{2W_{TO}} \tag{C-12}$$

$$N_V = \frac{\rho U S_w b_w C_{n_\beta}}{2I_{ZZ}} \tag{C-13}$$

$$N_r = \frac{\rho U S_w b_w^2 C_{n_r}}{4I_{ZZ}} \tag{C-14}$$

Undamped Natural Circular Frequency - ω_o

$$\omega_{o_\alpha} = (Z_w M_q - U M_w)^{1/2} \tag{C-15}$$

$$\omega_{o_\beta} = (N_r Y_v + U N_v)^{1/2} \tag{C-16}$$

<u>Response Formulas</u>

Normal Load Factor

$$\bar{A}_{\Delta n} = \frac{2\zeta_\alpha \omega_{o\alpha}}{g\gamma_\alpha}\left[R_4 + 4\zeta_\alpha^2(1 - 1/\gamma_\alpha)^2 R_2\right]^{1/2} \tag{C-17}$$

$$N_o(\Delta n) = \frac{\omega_{o\alpha}}{2\pi}\left[\frac{R_6 + 4\zeta_\alpha^2(1 - 1/\gamma_\alpha)^2 R_4}{R_4 + 4\zeta_\alpha^2(1 - 1/\gamma_\alpha)^2 R_2}\right]^{1/2} \tag{C-18}$$

Pitch - Angle Rate

$$\bar{A}_{\dot{\theta}} = \frac{\omega_{o\alpha}}{U}\left|\frac{4\zeta_\alpha^2}{\gamma_\alpha}(1 - 1/\gamma_\alpha) - 1\right| R_2^{1/2} \tag{C-19}$$

$$N_o(\dot{\theta}) = \frac{\omega_{o\alpha}}{2\pi}\left(\frac{R_4}{R_2}\right)^{1/2} \tag{C-20}$$

Pitch - Angle Acceleration

$$\bar{A}_{\ddot{\theta}} = \frac{\omega_{o_\alpha}^2}{U}\left|4\frac{\zeta_\alpha^2}{\gamma_\alpha}(1-1/\gamma_\alpha)-1\right| R_4^{1/2} \tag{C-21}$$

$$N_o(\ddot{\theta}) = \frac{\omega_{o_\alpha}}{2\pi}\left(\frac{R_6}{R_4}\right)^{1/2} \tag{C-22}$$

Lateral - Load Factor

$$\bar{A}_{\ddot{y}/g} = \frac{2\zeta_\beta \omega_{o_\beta}}{g\gamma_\beta}\left[R_{4_\beta}+4\zeta_\beta^2(1-1/\gamma_\beta)^2 R_{2_\beta}\right]^{1/2} \tag{C-23}$$

$$N_o(\ddot{y}/g) = \frac{\omega_{o_\beta}}{2\pi}\left[\frac{R_{6_\beta}+4\zeta_\beta^2(1-1/\gamma_\beta)^2 R_{4_\beta}}{R_{4_\beta}+4\zeta_\beta^2(1-1/\gamma_\beta)^2 R_{2_\beta}}\right]^{1/2} \tag{C-24}$$

Yaw Angle

$$\bar{A}_\psi = \frac{1}{U}\left|4\frac{\zeta_\beta^2}{\gamma_\beta}(1-1/\gamma_\beta)-1\right| R_{o_\beta}^{1/2} \tag{C-25}$$

$$N_o(\psi) = \frac{\omega_{o_\beta}}{2\pi}\left(\frac{R_{2_\beta}}{R_{o_\beta}}\right)^{1/2} \tag{C-26}$$

Yaw-Angle Rate

$$\bar{A}_{\dot{\psi}} = \frac{\omega_{o_\beta}}{U}\left|4\frac{\zeta_\beta^2}{\gamma_\beta}(1-1/\gamma_\beta)-1\right| R_{2_\beta}^{1/2} \tag{C-27}$$

$$N_o(\dot{\psi}) = \frac{\omega_{o_\beta}}{2\pi}\left(\frac{R_{4_\beta}}{R_{2_\beta}}\right)^{1/2} \tag{C-28}$$

Response Integrals Longitudinal - Rj_k

$$Rj = \frac{s_\alpha K_{o_\alpha}}{\pi}\int_0^\infty \frac{\bar{\beta}_\alpha^{\,j}\, e^{-\tilde{a}K_{o_\alpha}\bar{\beta}_\alpha}\left[1+8/3(1.339\, s_\alpha K_{o_\alpha}\bar{\beta}_\alpha)^2\right]}{\left[(1-\bar{\beta}_\alpha^2)^2+4\zeta_\alpha^2\bar{\beta}_\alpha^2\right]\left[1+(1.339 s_\alpha K_{o_\alpha}\bar{\beta}_\alpha)^2\right]^{11/6}}\, d\bar{\beta}_\alpha \tag{C-29}$$

Where;

$j=0,2,4,6 \quad \bar{\beta}_\alpha = \omega/\omega_{o_\alpha} \quad \bar{\beta}_\beta = \omega/\omega_{o_\beta}$

Response Integrals Lateral - Rj_β

$$Rj_\beta = \frac{s_\beta K_{o_\beta}}{\pi}\int_0^\infty \frac{\bar{\beta}_\beta^{\,j}\, e^{-\tilde{a}_\beta K_{o_\beta}\bar{\beta}_\beta}\left[1+8/3(1.339\, s_\beta K_{o_\beta}\bar{\beta}_\beta)^2\right]}{\left[(1-\bar{\beta}_\beta^2)^2+4\zeta_\beta^2\bar{\beta}_\beta^2\right]\left[1+(1.339 s_\beta K_{o_\beta}\bar{\beta}_\beta)^2\right]^{11/6}}\, d\bar{\beta}_\beta \tag{C-30}$$

HORIZONTAL TAIL LOAD

Gust forces along with aerodynamic forces created by airplane motion counteract the inertial force of the tail surface and the force due to fuselage restraint. The total vertical force which acts on the horizontal tail is as follows,

$$Z_t = W_t(\dot{w} - U\dot{\theta}) + qS_tC_{L_{\alpha_t}}\left(\frac{w}{U}\right) + qS_tC_{L_{\alpha_t}}\left(\frac{w_g}{U}\right) + W_t l_t\ddot{\theta} + qS_wC_{L_{q_t}}\frac{\bar{c}_w}{2U}\dot{\theta} + qS_wC_{L_{\dot{\alpha}_t}}\left(\frac{\dot{w}}{U}\right)\frac{\bar{c}_w}{2U} \tag{C-31}$$

In the frequency domain the equation takes the form

$$Z_t(\omega) = i\omega W_t w(\omega) + i\omega U W_t \theta(\omega) + qS_tC_{L_{\alpha_t}}\left(\frac{w(\omega)}{U}\right) + qS_tC_{L_{\alpha_t}}\left(\frac{w_g(\omega)}{U}\right)\phi(\omega) - \omega^2 W_t l_t \theta(\omega) + iqS_w\frac{\bar{c}_w}{2U}C_{L_{q_t}}\omega\theta(\omega) + iqS_wC_{L_{\dot{\alpha}_t}}\left(\frac{w(\omega)}{U}\right)\frac{\bar{c}_w}{2U}\omega$$

Then the frequency response function is

$$\frac{Z_t(\omega)}{w_g(\omega)} = i\omega W_t\left(\frac{w(\omega)}{w_g(\omega)}\right) - i\omega U^2 W_t\left(\frac{\theta(\omega)}{w_g(\omega)}\right) + \frac{qS_t}{U}C_{L_{\alpha_t}}\left(\frac{w(\omega)}{w_g(\omega)}\right) + q\frac{S_t}{U}C_{L_{\alpha_t}}\phi(\omega) - \omega^2 W_t l_t\left(\frac{\theta(\omega)}{w_g(\omega)}\right) + i\omega qS_w\frac{\bar{c}_w}{2U}C_{L_{q_t}}\left(\frac{\theta(\omega)}{w_g(\omega)}\right) + q\frac{\bar{c}_w S_w}{2U^2}C_{L_{\dot{\alpha}_t}}i\omega\left(\frac{w(\omega)}{w_g(\omega)}\right) \tag{C-32}$$

Normalizing the tail load equation by

$$Z_s = \frac{qS_wC_{L_{\alpha_t}}}{U}$$

The equation then becomes

$$\frac{Z_t(\omega)}{Z_s} = \frac{i\omega W_t U}{qS_wC_{L_{\alpha_t}}}\left(\frac{w(\omega)}{w_g(\omega)}\right) - \frac{i\omega U^2 W_t}{qS_wC_{L_{\alpha_t}}}\left(\frac{\theta(\omega)}{w_g(\omega)}\right) + \left(\frac{w(\omega)}{w_g(\omega)}\right)\frac{S_t}{S_w} + \phi(\omega)\frac{S_t}{S_w} - \frac{\omega^2 W_t l_t U}{qS_wC_{L_{\alpha_t}}}\left(\frac{\theta(\omega)}{w_g(\omega)}\right) + i\omega\frac{\bar{c}_w}{2}\frac{C_{L_{q_t}}}{C_{L_{\alpha_t}}}\left(\frac{\theta(\omega)}{w_g(\omega)}\right) + i\omega\frac{\bar{c}}{2U}\frac{C_{L_{\dot{\alpha}_t}}}{C_{L_{\alpha_t}}}\left(\frac{w(\omega)}{w_g(\omega)}\right) \tag{C-33}$$

By definition

$$\bar{\beta}_\alpha = \frac{\omega}{\omega_{o_\alpha}} \quad \text{and} \quad K_{o_\alpha} = \frac{\omega_{o_\alpha}\bar{c}_w}{2U}$$

Therefore the substitution of $i\omega = i\frac{\bar{\beta}_\alpha 2UK_{o_\alpha}}{\bar{c}_w}$ can be made and grouping terms yields.

$$\frac{Z_t(K_{o_\alpha}\bar{\beta}_\alpha)}{Z_s} = \left\{\frac{S_t}{S_w} + \frac{i2UK_{o_\alpha}\bar{\beta}_\alpha}{\bar{c}_w}\left[\frac{\bar{c}_w}{2U}\frac{C_{L_{\dot{\alpha}_t}}}{C_{L_{\alpha_t}}} + \frac{W_tU}{qS_wC_{L_{\alpha_t}}}\right]\right\}\frac{w(K_{o_\alpha}\bar{\beta}_\alpha)}{w_g} + \left\{\frac{i2UK_{o_\alpha}\bar{\beta}_\alpha}{\bar{c}_w}\left[W_tl_t\frac{i2U^2K_{o_\alpha}\bar{\beta}_\alpha}{qS_wC_{L_{\alpha_t}}\bar{c}_w} + \frac{\bar{c}_w}{2}\frac{C_{L_{q_t}}}{C_{L_{\alpha_t}}} - \frac{W_tU^2}{qS_wC_{L_{\alpha_t}}}\right]\right\}\frac{\theta(K_{o_\alpha}\bar{\beta}_\alpha)}{w_g} + \phi(K_{o_\alpha}\bar{\beta}_\alpha)\frac{S_t}{S_w} \tag{C-34}$$

Airplane responses as developed in reference 2 are obtained by solving two degrees-of-freedom equations of motion for independently applied gust forces of unit sinusoidal vertical and lateral gust velocities.

$$H_w^{w_g}(K_{o_\alpha}\bar{\beta}_\alpha) = \frac{w(K_{o_\alpha}\bar{\beta}_\alpha)}{w_g} = -\frac{(1+i2\zeta_\alpha\bar{\beta}_\alpha/\gamma_\alpha)}{1-\bar{\beta}_\alpha^2+i2\zeta_\alpha\bar{\beta}_\alpha}\,\phi(K_{o_\alpha}\bar{\beta}_\alpha) \tag{C-35}$$

$$H_\theta^{w_g}(K_{o_\alpha}\bar{\beta}_\alpha) = \frac{\theta(K_{o_\alpha}\bar{\beta}_\alpha)}{w_g} = \frac{1/U\left[4\zeta_\alpha^2/\gamma_\alpha(1-1/\gamma_\alpha)-1\right]}{1-\bar{\beta}_\alpha^2+i2\zeta_\alpha\bar{\beta}_\alpha}\,\phi(K_{o_\alpha}\bar{\beta}_\alpha) \tag{C-36}$$

Substitution yields the frequency response function

$$H_{\ddot{z}_t}^{w_g}(K_{o_\alpha}\bar{\beta}_\alpha) = \frac{Z_t}{Z_s}(K_{o_\alpha}\bar{\beta}_\alpha) = \frac{\phi(K_{o_\alpha}\bar{\beta}_\alpha)(\bar{\beta}_\alpha^2 C_1 + i\bar{\beta}_\alpha C_2)}{1-\bar{\beta}_\alpha^2+i2\zeta_\alpha\bar{\beta}_\alpha} \tag{C-37}$$

$$\left|H_{\ddot{z}_t}^{w_g}\right|^2 = \frac{|\phi(K_{o_\alpha}\bar{\beta}_\alpha)|^2(\bar{\beta}_\alpha^4 C_1^2+\bar{\beta}_\alpha^2 C_2^2)}{\left[(1-\bar{\beta}_\alpha^2)^2+4\zeta_\alpha^2\bar{\beta}_\alpha^2\right]}$$

Where

$$C_1 = -\frac{S_t}{S_w} + \frac{2C_{L_{\dot{\alpha}_t}}K_{o_\alpha}\zeta_\alpha}{C_{L_{\alpha_t}}\gamma_\alpha} + \frac{4U^2K_{o_\alpha}W_t}{qS_w\bar{c}_wC_{L_{\alpha_t}}}\left(\frac{\zeta_\alpha}{\gamma_\alpha} - \frac{K_{o_\alpha}l_t}{\bar{c}_w}\left[4\frac{\zeta_\alpha^2}{\gamma_\alpha}\left(1-\frac{1}{\gamma_\alpha}\right)-1\right]\right)$$

$$C_2 = 2\frac{\zeta_\alpha S_t}{S_w}\left(1-\frac{1}{\gamma_\alpha}\right) - K_{o_\alpha}\frac{C_{L_{\dot{\alpha}_t}}}{C_{L_{\alpha_t}}} + K_{o_\alpha}\frac{C_{L_{q_t}}}{C_{L_{\alpha_t}}}\left(4\frac{\zeta_\alpha^2}{\gamma_\alpha}\left(1-\frac{1}{\gamma_\alpha}\right)-1\right)$$
$$- \frac{2K_{o_\alpha}W_tU^2}{\bar{c}_wqS_wC_{L_{\alpha_t}}}\left(4\frac{\zeta_\alpha^2}{\gamma_\alpha}\left(1-\frac{1}{\gamma_\alpha}\right)\right)$$

The ratio of the root mean square output and input yields the horizontal tail load response parameter of equation (C-38)

$$\bar{A}_{z_t}^2 = \frac{\sigma_{\ddot{z}_t}^2}{\sigma_{w_g}^2} = \int_0^\infty \frac{\Phi_{w_g}(\omega_\alpha)\left|H_{\ddot{z}_t}^{w_g}(\omega_\alpha)\right|^2 d\omega_\alpha}{\sigma_{w_g}^2} \tag{C-38}$$

Where $\Phi_{w_g}(\omega)$, the Von Karman spectrum is

$$\Phi_{w_g}(\omega) = \sigma_{w_g}^2\frac{L}{\pi U}\,\frac{1+8/3(1.339L\omega/U)^2}{\left[1+(1.339L\omega/U)^2\right]^{11/6}}$$

Assuming unsteady lift-function approximation

$$|\phi(K_{o_\alpha}\bar{\beta}_\alpha)|^2 \approx e^{-\tilde{a}K_{o_\alpha}\bar{\beta}_\alpha}$$

Then $$\bar{A}^2_{Z_t} = \int_0^\infty \frac{(\bar{\beta}_\alpha^4 C_1^2 + \bar{\beta}_\alpha^2 C_2^2)\, e^{-\tilde{a}K_{o_\alpha}\bar{\beta}_\alpha}}{[(1-\bar{\beta}_\alpha^2)^2 + 4\zeta_\alpha^2\bar{\beta}_\alpha^2]} \left(\frac{S_\alpha K_{o_\alpha}}{\pi} \frac{[1 + 8/3(1.339 S_\alpha K_{o_\alpha}\bar{\beta}_\alpha)^2]}{[1+(1.339 S_\alpha K_{o_\alpha}\bar{\beta}_\alpha)^2]^{11/6}} \right) d\bar{\beta}_\alpha$$

Therefore it follows that the rms value for the horizontal tail load can be put in the response integral format utilizing equation (C-29) and

$$\bar{A}_{Z_t} = |Z_s| [C_1^2 R_4 + C_2^2 R_2]^{1/2} \tag{C-39}$$

The average number of response zero crossings with positive slope is given by the following

$$N_o(Z_t) = \frac{1}{2\pi\sigma_{\ddot{Z}_t}} \left[\int_0^\infty \omega_\alpha^2 \Phi_{w_g}(\omega_\alpha) |H^{w_g}_{\ddot{Z}_t}(\omega_\alpha)|^2 d\omega_\alpha \right]^{1/2} \tag{C-40}$$

Substitution of equation (C-38) yields

$$N_o(Z_t) = \frac{1}{2\pi\bar{A}_{Z_t}\sigma_{w_g}} [\bar{\beta}_\alpha^2 \omega_{o_\alpha}^2 \bar{A}_{Z_t}^2 \sigma_{w_g}^2]^{1/2}$$

Then,

$$N_o(Z_t) = \frac{\omega_{o_\alpha}}{2\pi} \left[\frac{C_1^2 R_6 + C_2^2 R_4}{C_1^2 R_4 + C_2^2 R_2} \right]^{1/2} \tag{C-41}$$

VERTICAL TAIL LOAD

Neglecting the inertial loads the forces acting on the vertical tail surface are

$$Y_v(\omega) = \frac{qS_w}{U} C_{Y_{\beta_v}} v(\omega) + \frac{qS_w}{2U} C_{Y_{r_v}} b_w \dot{\psi}(\omega) - \frac{qS_w}{U} C_{Y_{\beta_v}} v_g(\omega) \Psi(\omega) \tag{C-42}$$

The frequency response function is obtained in the same manner as described in the previous section for the horizontal tail. Normalizing this function with

$$Y_s = \frac{qS_w}{U} C_{Y_{\beta_v}}$$

and

$$\frac{Y_v(\omega)}{v_g(\omega)} = \frac{v(\omega)}{v_g(\omega)} + i\omega \frac{b_w}{2} \frac{C_{Y_{r_v}}}{C_{Y_{\beta_v}}} \frac{\psi(\omega)}{v_g(\omega)} - \Psi(\omega) \tag{C-43}$$

The airplane lateral responses as developed in reference 2 are again obtained by solving the two degree of freedom equations of lateral motion and are as follows.

$$H_v^{v_g}(\bar{\beta}_\beta) = \frac{v(\bar{\beta}_\beta)}{v_g} = \frac{(1 + i2\zeta_\beta \bar{\beta}_\beta/\gamma_\beta)}{1 - \bar{\beta}_\beta^2 + i2\zeta_\beta \bar{\beta}_\beta} \Psi(\omega_{o_\beta} \bar{\beta}_\beta) \tag{C-44}$$

$$H_\psi^{v_g}(\bar{\beta}_\beta) = \frac{\psi(\bar{\beta}_\beta)}{v_g} = \frac{\frac{1}{U}\left[4\frac{\zeta_\beta^2}{\gamma_\beta}\left(1 - \frac{1}{\gamma_\beta}\right) - 1\right]}{1 - \bar{\beta}_\beta^2 + i2\zeta_\beta \bar{\beta}_\beta} \Psi(\omega_{o_\beta} \bar{\beta}_\beta) \tag{C-45}$$

Substitution yields the frequency response function

$$|H_{\ddot{Y}}^{v_g}|^2 = \frac{|\Psi(K_{o_\beta} \bar{\beta}_\beta)|^2 (\bar{\beta}_\beta^4 C_3^2 + \bar{\beta}_\beta^2 C_4^2)}{[(1 - \bar{\beta}_\beta^2)^2 + 4\zeta_\beta^2 \bar{\beta}_\beta^2]} \tag{C-46}$$

Where

$$C_3 = 1$$

$$C_4 = -2\zeta_\beta\left(1 - \frac{1}{\gamma_\beta}\right) + K_{o_\beta} \frac{C_{Y_{r_v}}}{C_{Y_{\beta_v}}} \left[4\frac{\zeta_\beta^2}{\gamma_\beta}\left(1 - \frac{1}{\gamma_\beta}\right) - 1\right]$$

The rms value for the vertical tail load in response integral format is

$$\bar{A}_{Y_v} = |Y_s| [C_3^2 R_{4\beta} + C_4^2 R_{2\beta}] \tag{C-47}$$

and number of zero crossings is as follows

$$N_0(Y_v) = \frac{\omega_{0\beta}}{2\pi}\left[\frac{C_3^2 R_{6\beta} + C_4^2 R_{4\beta}}{C_3^2 R_{4\beta} + C_4^2 R_{2\beta}}\right]^{1/2} \tag{C-48}$$

APPENDIX D

FEDERAL AVIATION REGULATIONS, PART 23 AND 25

The discrete-gust analysis equations for the determination of gust load factors and tail loads were taken directly from Federal Aviation Regulations (FAR), Part 23. The same equations apply for FAR, Part 25.

23.341 Gust Load Factor

In the absence of a more rational analysis, the gust load factor must be computed as follows:

$$n = 1 + \frac{K_g U_{de} V_e a_w}{498\, W_{TO}/S_w} \qquad \text{(D-1)}$$

Where,

Gust alleviation factor,

$$K_g = \frac{.88\mu_g}{5.3+\mu_g}$$

Airplane mass ratio,

$$\mu_g = \frac{2\, W_{TO}/S_w}{\rho \bar{c}_w a_w}$$

Derived gust velocities,

U_{de} = 50 ft/s at V_C between altitudes at sea level and 20,000 feet

Airplane equivalent airspeed (knots),

$$V_e = .592\left(\frac{\rho}{\rho_0}\right)^{1/2} U$$

a_w = wing lift curve slope (1/RAD)

23.425 Gust Loads, Horizontal Tail Surfaces

When determining the total load on the horizontal tail, due to gusts, the initial balancing tail loads for steady unaccelerated flight at the pertinent speed must first be determined. The incremental tail load resulting from the gusts must be added to the initial balancing tail load to obtain the total tail load.

In the absence of a more rational analysis, the incremental tail load due to the gust must be computed as follows:

$$\Delta L_t = K_g U_{de} V_e a_t S_t (1 - \delta\epsilon/\delta\alpha) \qquad \text{(D-2)}$$

a_t = Horizontal tail lift curve slope (/RAD)

Tail load for balanced flight[1]

$$L_t = \frac{x_a W_{TO} + qS_w \bar{c}_w C_{m_{0_{WS}}}}{x_a + l_t} \qquad \text{(AFT c.g.)} \qquad \text{(D-3)}$$

$$L_t = \frac{x_a W_{TO} - qS_w \bar{c}_w C_{m_{0_{WS}}}}{l_t - x_a} \qquad \text{(Forward c.g.)} \qquad \text{(D-4)}$$

23.443 Gust loads, vertical tail surfaces

In absence of a more rational analysis, the gust load must be computed as follows:

$$L_v = K_{g_t} U_{de} V_e a_v S_v / 498 \qquad \text{(D-5)}$$

Where ,

Gust allevation Factors

$$K_{g_t} = \frac{.88 \mu_{g_t}}{5.3 + \mu_{g_t}}$$

Lateral mass ratio

$$\mu_{g_t} = \frac{2W_{TO}}{\rho \bar{c}_v \; a_v S_v} \left(\frac{R_Y}{l_v}\right)^2$$

Derived gust velocities

U_{de} = 50 ft/s at V_C between altitudes at sea level and 20,000 feet

a_v = Vertical tail lift curve slope (1 / RAD)

NOTE:

1. Tail load equations (D-3) and (D-4) are not part of FAR but are used here to determine total load on horizontal tail surface.

APPENDIX E

GENERAL AVIATION AIRPLANE DESCRIPTION AND CHARACTERISTICS

LIST OF TABLES

Table		Page
E-1	Airplane I--Four-Seat Single-Engine High Wing With Fixed Gear	E-1
E-2	Airplane II--Four-Seat Twin-Engine Low Wing	E-2
E-3	Airplane III--Light-Passenger Twin-Turboprop Transport Low Wing	E-3
E-4	Airplane IV--Light-Passenger Twin-Turboprop Transport High Wing	E-4
E-5	Airplane V--Twenty-Passenger Twin-Turboprop Commuter Low Wing	E-5
E-6	Airplane VI--Twin-Jet Light Executive Transport Low Wing	E-6

TABLE E-1. AIRPLANE I -- FOUR-SEAT SINGLE-ENGINE HIGH WING WITH FIXED GEAR

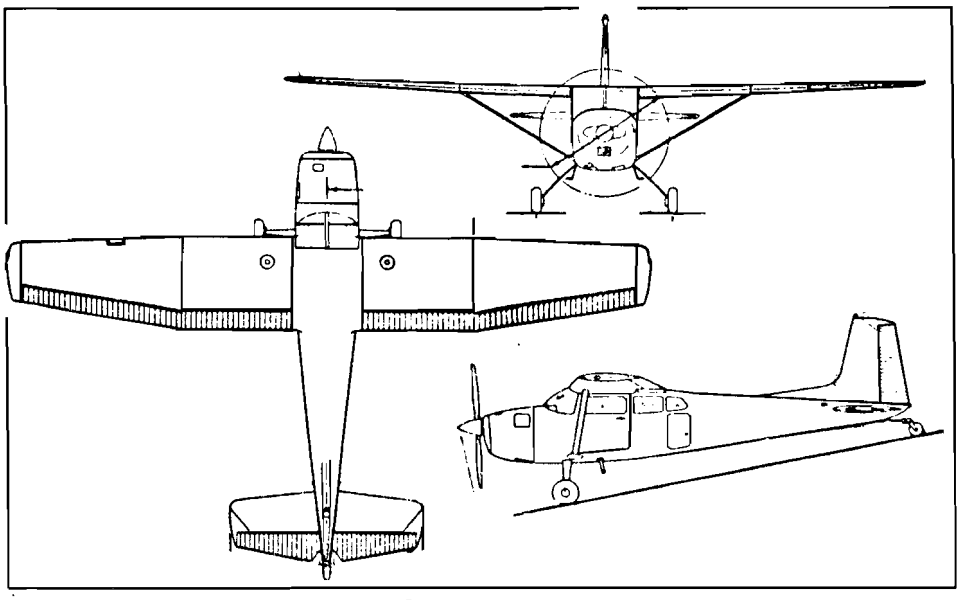

	WING	HORIZONTAL TAIL
AREA	174.00 FT^2	38.71 FT^2
SPAN	35.88 FT	11.54 FT
ASPECT RATIO	7.40	3.44
TAPER RATIO	.69	.65
MAC	4.57 FT	3.35 FT
SWEEP	0.00^o	7.64^o
DIHEDRAL	1.73^o	0.00^o
INCIDENCE	1.50^o ,- 1.50^o(TIP)	3.25^o
AIRFOIL SECT.	NACA 2412(ROOT)	NACA 0009(ROOT) NACA 0006(TIP)

VERTICAL TAIL		POWER PLANT	
AREA	18.57 FT^2	ENGINE	CONTINENTAL 0-470-R
SPAN	5.75 FT	HP RATING	230 HP @ 2600 RPM
FIN OFF-SET	0.00^o		
AIRFOIL SECT.	NACA 0009.5 (ROOT) NACA 0008 (TIP)		

MASS & INERTIA CHARACTERISTICS

GROSS WEIGHT	2,950 lb.
WEIGHT FOR GUST ANALYSIS	2,950 lb.
CENTER OF GRAVITY	26.4% MAC
PITCHING MOMENT OF INERTIA	43,341 lb. - FT^2
YAWING MOMENT OF INERTIA	63,337 lb. - FT^2

FLIGHT CHARACTERISTICS

CRUISE VELOCITY	219 FT/SEC.

TABLE E-2. AIRPLANE II -- FOUR-SEAT TWIN-ENGINE LOW WING

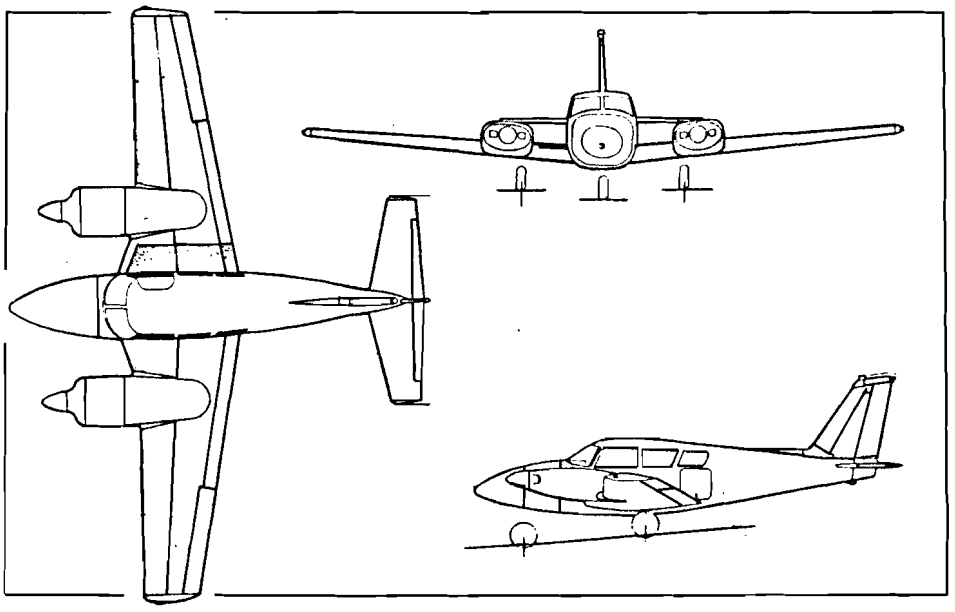

	WING	HORIZONTAL TAIL
AREA	178.00 FT^2	32.50 FT^2
SPAN	36.00 FT	12.50 FT
ASPECT RATIO	7.28	4.61
TAPER RATIO	.51	.52
MAC	4.98 FT	2.71 FT
SWEEP	0.00^o	12.28^o
DIHEDRAL	5.00^o	0.00^o
INCIDENCE	2.00^o	0.00^o
AIRFOIL SECT.	NACA 64_2A215	NACA 0008

VERTICAL TAIL	
AREA	14.90 FT^2
SPAN	4.66 FT
FIN OFF-SET	0.00^o

POWER PLANT	
ENGINE	2- LYCOMING IO-320-B
HP RATING	160 HP

MASS & INERTIA CHARACTERISTICS

GROSS WEIGHT	3,600 lb.
WEIGHT FOR GUST ANALYSIS	3,600 lb.
CENTER OF GRAVITY	19.58% MAC
PITCHING MOMENT OF INERTIA	61,180 lb-FT^2
YAWING MOMENT OF INERTIA	144,900 lb - FT^2

FLIGHT CHARACTERISTICS

CRUISE VELOCITY	285 FT/SEC.

TABLE E-3. AIRPLANE III -- LIGHT-PASSENGER TWIN-TURBOPROP TRANSPORT LOW WING

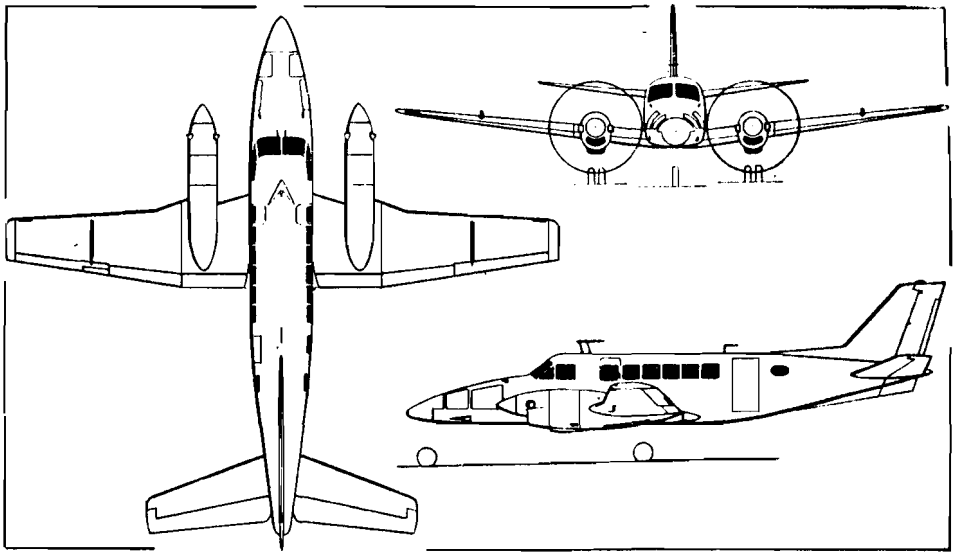

	WING	HORIZONTAL TAIL
AREA	279.74 FT^2	100.00 FT^2
SPAN	45.88 FT	22.38 FT
ASPECT RATIO	7.52	5.00
TAPER RATIO	.41	.50
MAC	6.43 FT	4.47 FT
SWEEP	0.00^{o}	20.00^{o}
DIHEDRAL	7.00^{o}	7.00^{o}
INCIDENCE	4.85^{o}, 0.00^{o}(TIP)	$+6.1^{o}$ TO -3.25^{o}(TIP)
AIRFOIL SECT.	NACA 23018(ROOT) NACA 23012(TIP)	NACA 0012-64(ROOT) NACA 0008-64(TIP)

VERTICAL TAIL		POWER PLANT	
AREA	44.86 FT^2	ENGINE	2- PRATT & WHITNEY PT6A-20
SPAN	7.60 FT	HP RATING	550 HP
FIN OFF-SET	0.00^{o}		
AIRFOIL SECT.	NACA 0008 (ROOT)		

MASS & INERTIA CHARACTERISTICS

GROSS WEIGHT	10,400 lb.
WEIGHT FOR GUST ANALYSIS	10,200 lb.
CENTER OF GRAVITY	37.86% MAC
PITCHING MOMENT OF INERTIA	719,580 lb-FT^2
YAWING MOMENT OF INERTIA	1,155,097 lb.FT^2

FLIGHT CHARACTERISTICS

CRUISE VELOCITY	418 FT/SEC

TABLE E-4. AIRPLANE IV -- LIGHT-PASSENGER TWIN-TURBOPROP TRANSPORT HIGH WING

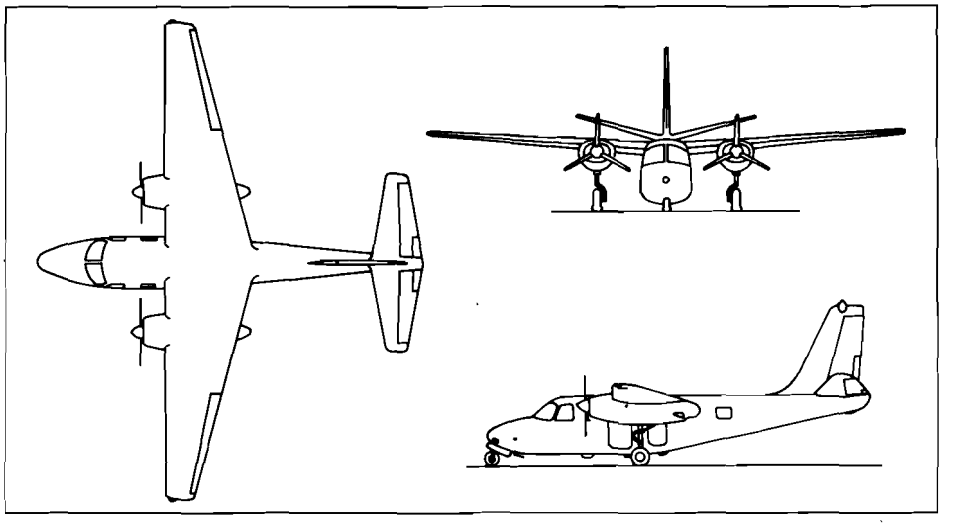

	WING	HORIZONTAL TAIL
AREA	266.00 FT^2	58.37 FT^2
SPAN	46.55 FT	19.75 FT
ASPECT RATIO	8.15	6.67
TAPER RATIO	.32	.21
MAC	6.21 FT	2.96 FT
SWEEP	0.00 ^{o}	25.00^o
DIHEDRAL	4.00^o	10.00^o
INCIDENCE	3.00^o,-1.00^o(TIP)	-.75°
AIRFOIL SECT.	NACA 23012	NACA 0010

VERTICAL TAIL		POWER PLANT	
AREA	44.27 FT^2	ENGINE	2-AIRESEARCH TPE 331-5-251
SPAN	8.95 FT	HP RATING	700 HP
FIN OFF-SET	0.00^o		
AIRFOIL SECT.	NACA 0009		

MASS & INERTIA CHARACTERISTICS

GROSS WEIGHT	10,300 lb.
WEIGHT FOR GUST ANALYSIS	10,250 lb.
CENTER OF GRAVITY	21.13% MAC
PITCHING MOMENT OF INERTIA	427,358 lb. - FT^2
YAWING MOMENT OF INERTIA	646,479 lb. - FT^2

FLIGHT CHARACTERISTICS

CRUISE VELOCITY 408 FT./SEC.

TABLE E-5. AIRPLANE V -- TWENTY-PASSENGER TWIN-TURBOPROP COMMUTER LOW WING

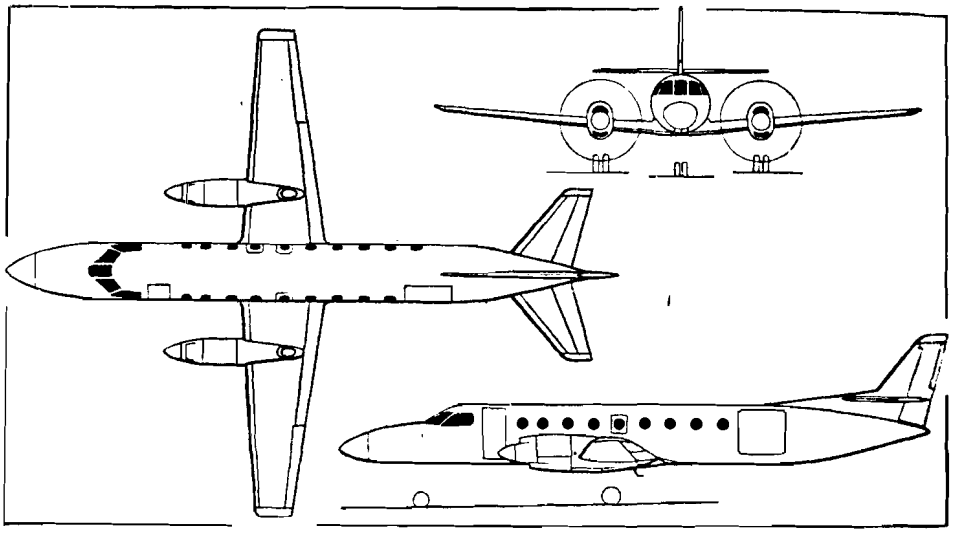

	WING	HORIZONTAL TAIL
AREA	277.50 FT^2	75.97 FT^2
SPAN	46.25 FT	15.96 FT
ASPECT RATIO	7.71	3.08
TAPER RATIO	.40	.39
MAC	6.37 FT	5.17 FT
SWEEP	4.00^o	40.00^o
DIHEDRAL	5.00^o	0.00^o
INCIDENCE	1.00^o,-1.00^o(TIP)	VARIABLE
AIRFOIL SECT.	NACA 65_2A215(ROOT) NACA 64_2A415(TIP)	NACA 66A009 (ROOT) NACA 63A009(TIP)

VERTICAL TAIL		POWER PLANT	
AREA	56.00 FT^2	ENGINE	2-AIRESEARCH TPE 331-3U-303
SPAN	10.12 FT	HP RATING	840 HP
FIN OFF-SET	$.33^o$		

NACA 66A009 (ROOT)
NACA 63A009 (TIP)

MASS & INERTIA CHARACTERISTICS

GROSS WEIGHT	12,560 lb.
WEIGHT FOR GUST ANALYSIS	12,500 lb.
CENTER OF GRAVITY	10% MAC
PITCHING MOMENT OF INERTIA	942,576 lb.-FT^2
YAWING MOMENT OF INERTIA	1,643,450 lb. FT^2

FLIGHT CHARACTERISTICS

CRUISE VELOCITY 372 FT./SEC.

TABLE E-6. AIRPLANE VI -- TWIN-JET LIGHT EXECUTIVE TRANSPORT LOW WING

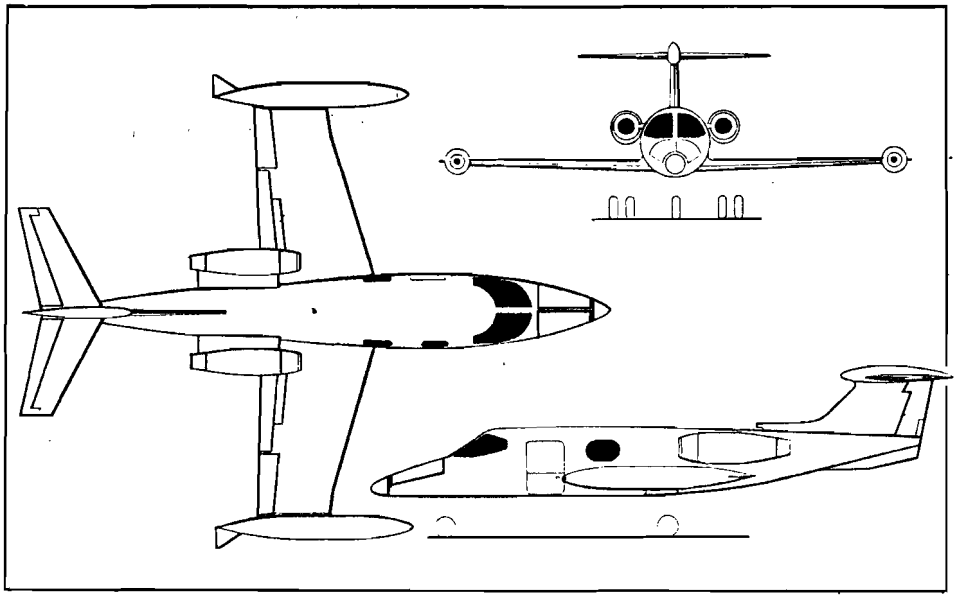

	WING	HORIZONTAL TAIL
AREA	231.80 FT^2	54.00 FT^2
SPAN	34.12 FT	14.70 FT
ASPECT RATIO	5.02	3.97
TAPER RATIO	.51	.47
MAC	7.04 FT	3.70 FT
SWEEP	16.00°	29.00°
DIHEDRAL	2.50°	0.00°
INCIDENCE	1.00°	-7.00° to -.50° (TIP)
AIRFOIL SECT.	NACA 64A109	

VERTICAL TAIL		POWER PLANT	
AREA	40.75 FT^2	ENGINE	2-GENERAL ELECTRIC CJ610-6
SPAN	5.81 FT	RATING	2,950 lb.
FIN OFF-SET	0.00°		

MASS & INERTIA CHARACTERISTICS

GROSS WEIGHT	12,800 lb.
WEIGHT FOR GUST ANALYSIS	9,000 lb.
CENTER OF GRAVITY	20.9% MAC
PITCHING MOMENT OF INERTIA	528,000 lb.-FT^2
YAWING MOMENT OF INERTIA	681,000 lb. - FT^2

FLIGHT CHARACTERISTICS

CRUISE VELOCITY 878 FT./SEC.

TABLE E-7. AIRPLANE VII -- TWIN-JET BUSINESS TRANSPORT LOW WING

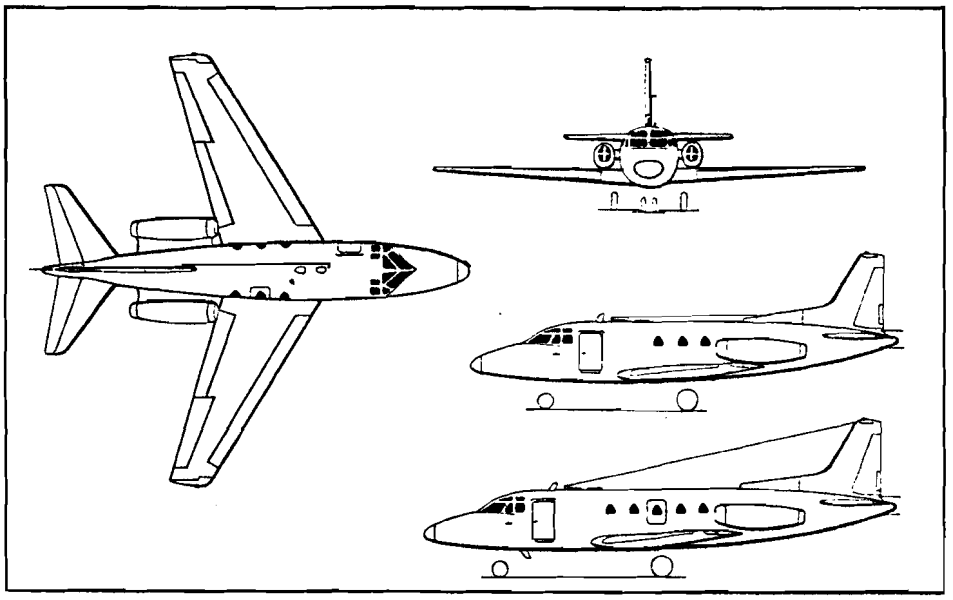

	WING	HORIZONTAL TAIL
AREA	342.05 FT^2	77.00 FT^2
SPAN	44.43 FT	17.55 FT
ASPECT RATIO	5.77	3.00
TAPER RATIO	.32	.30
MAC	8.38 FT	4.39 FT
SWEEP	32.00°	35.00°
DIHEDRAL	3.14°	0.00°
INCIDENCE	-.005°, 2.90°(TIP)	-6.00° to 0.00°(TIP)
AIRFOIL SECT.	NACA 64A SERIES	NACA 64A010

	VERTICAL TAIL		POWER PLANT
AREA	41.58 FT^2	ENGINE	2- PRATT & WHITNEY JT12A-8
SPAN	7.66 FT	RATING	3,300 lb.
FIN OFF-SET	0.00°		
AIRFOIL SECT.	NACA 63A010		

MASS & INERTIA CHARACTERISTICS

GROSS WEIGHT	18,650 lb.
WEIGHT FOR GUST ANALYSIS	17,375 lb.
CENTER OF GRAVITY	27.2% MAC
PITCHING MOMENT OF INERTIA	978,880 lb. FT^2
YAWING MOMENT OF INERTIA	1,655,080 lb. - FT^2

FLIGHT CHARACTERISTICS

CRUISE VELOCITY	932 FT./SEC.